

# **ICUS/INCEDE REPORT 2002-01**



**INTERNATIONAL CENTER FOR  
URBAN SAFETY ENGINEERING**

---

**INSTITUTE OF INDUSTRIAL SCIENCE  
THE UNIVERSITY OF TOKYO**

## **URBAN SAFETY ENGINEERING 2001**

**- Proceedings of the Joint Workshop -**

**Editors**

**Dushmanta Dutta and Taketo Uomoto  
ICUS/INCEDE, IIS, The University of Tokyo, Japan**

*Proceedings of the Joint Workshop on*  
***Urban Safety Engineering 2001***

**September 21-22, 2001  
AIT, Thailand**

**Editors**

**Dushmanta Dutta and Taketo Uomoto  
ICUS/INCEDE, IIS,  
The University of Tokyo, Japan**

*Organized by*

**International Center for Urban Safety Engineering (ICUS/INCEDE), Japan  
Asian Institute of Technology (AIT), Thailand**





# **Proceedings of the Joint Workshop on Urban Safety Engineering 2001**

Editors

Dushmanta Dutta and Taketo Uomoto  
ICUS/INCEDE, IIS,  
The University of Tokyo

**ICUS/INCEDE Report No. 1, October 2002**

## **Executive Summary**

This volume of the ICUS/INCEDE Report contains the proceedings of the *Joint Workshop on Urban Safety Engineering 2001* organized at the Asian Institute of Technology (AIT), Thailand by ICUS/INCEDE and AIT during September 21-22, 2001. This report provides a wealth of information on development and application of various advanced technologies for tackling some of the most pressing issues towards urban safety.

With the rapid economic development in the last few decades, there has been a phenomenal growth of high-rise buildings and other infrastructure. However, this growth of infrastructure is not adequately balanced by the appropriate measures for their maintenance and management and that has led to a deterioration of urban infrastructures and resulted in urban disasters in many cities. Although, such problems are mounting with the expansion of urban areas, there is lack of awareness of the issues relating to urban safety in most of the Asian countries. As a center dedicated for research and development for urban safety, ICUS/INCEDE organized this workshop in Thailand to share its experience and expertise with the Thai researchers.

This report contains a total of 13 technical papers covering a wide range of topics in the areas of urban safety engineering including modeling, monitoring and maintenance of urban structures; prediction, assessment and control of natural and artificial disasters; and application of remote sensing, GIS and information technology tools for urban safety. Many of these papers present comprehensive reviews of the problems and applications of various advanced tools and techniques to problems related to urban safety.

**International Center for Urban Safety Engineering**





*Participants pose for a group photograph at the end of the 1<sup>st</sup> day of the workshop*

# CONTENTS

PENNING WARNITCHAI, C. SANGARAYAKUL and S. A. ASHFOR	
- Seismic Hazard in Bangkok due to Long-Distance Earthquakes.....	1
KIMIRO MEGURO	
- Applied Element Method: A New Efficient Tool for Design of Structure Considering Its Failure Behavior.....	13
RYOZO OOKA	
- Urban Warming and Its Control Techniques.....	31
WORSAK KANOK-NUKULCHAI	
- The Changing Role of Civil Engineers in Urban Safety.....	43
TAKETO UOMOTO	
- Application of Non-destructive Inspection to Concrete Structures.....	49
SOMNUK TANGTERMSIRIKUL	
- Durability Problems of Concrete Structures in Thailand and their Solutions.....	61
FUMIO YAMAZAKI	
- Applications of Remote Sensing and GIS for Damage Assessment.....	69
THANYAWAT POTHISIRI and BOONCHAI STITMANNAITHUM	
- Overview of Research Activities Related to Urban Safety at the Department of Civil Engineering, Chulalongkorn University.....	85
YOSHIFUMI YASUOKA	
- Assessment of Urban Safety and Environment by Use of Remote Sensing.....	91
T.THUY VU and MITSUHARU TOKUNAGA	
- Wavelet and Scale-Space Theory in Segmentation of Airborne Laser Scanner Data.....	97
KIYOSHI HONDA	
- Remote Sensing and GIS Activities in Asian Institute of Technology: Education, Training and Research.....	105
TAWATCHAI TINGSANCHALI and TUANTAN KITPAISALSAKUL	
- Optimal Capacity of River Flood Control System of Bangkok based on Flood Risk and Economic Analysis.....	117

DUSHMANTA DUTTA, SRIKANTHA HERATH and KATUMI MUSIAKE	
- Direct Flood Damage Modeling Towards Urban Flood Risk Management.....	127
APPENDIX I	
- Workshop Program.....	145
APPENDIX II	
- Workshop Resolutions.....	147



# **SEISMIC HAZARD IN BANGKOK DUE TO DISTANT EARTHQUAKES**

P. WARNITCHAI, C. SANGARAYAKUL  
School of Civil Engineering, Asian Institute of Technology,  
Thailand

S. A. ASHFORD  
Department of Structural Engineering, University of California, San Diego,  
USA

## **ABSTRACT**

*A seismic hazard assessment of Bangkok is conducted. The results are presented in the form of predicted peak ground accelerations for various levels of probability of exceedance in a 50-year period and the corresponding elastic response spectra. The results indicate that Bangkok, though located at a remote distance from seismic sources, is still at risk of damaging earthquake ground motions similar to those found in Mexico City during the 1985 Michoacan earthquake. The risk is essentially caused by three factors. First, several regional seismic sources that may contribute significantly to the seismic hazard of Bangkok are capable of generating large earthquakes. Second, the attenuation rate of ground motions in this region appears to be rather low and well represented by attenuation models of Central and Eastern North America. Third, the surficial deposits in Bangkok have the ability to amplify earthquake ground motions about 3 to 4 times.*

*Keywords: Probabilistic seismic hazard analysis, Attenuation model, Cornell's method, Dynamic properties of soils, Site response analysis, Acceleration response spectrum, Michoacan earthquake, Bangkok.*

## **1. INTRODUCTION**

It has been recently recognized that urban areas located at rather remote distances from earthquake sources may, under some special conditions, possess a danger of earthquake disaster. A well-known example is the 1985 Michoacan earthquake, in which a large earthquake ( $M_s = 8.1$ ) on the coastal Mexico caused considerable destruction and loss of life in Mexico City, 350 km from the epicentral location. Much of the destruction was due to significant amplification of earthquake ground motions by thick surficial deposits in the downtown area of Mexico City [Seed et al., 1987]. Despite our improved understanding of seismic hazard potential from distant earthquakes, several cities around the world that possess such potential are still being considered by most people as being free from seismic risk. Bangkok, the capital city of Thailand, with a population of over eight million, seems to be one of these cities. The nearest zone of

active faults is located only about 120 to 300 km from the city, but their rate of seismic activity is rather low. More active seismic sources are between 400 km and 1000 km from Bangkok. The surficial geologic setting at Bangkok also appears qualitatively similar to the setting of Mexico City, and hence Bangkok, by analogy, appears to be susceptible to the same type of soil amplification of ground motions.

In this paper, a seismic hazard assessment of Bangkok is presented. It is intended to provide the 'best estimate' of Bangkok's earthquake ground motion parameters based on currently available information, so that engineers can use them for improved building design and construction. The assessment results are presented in the form of predicted peak ground accelerations for various levels of probability of exceedance in a 50-year exposure period and the corresponding elastic response spectra. The results indicate that there is a possibility of an earthquake disaster in Bangkok similar to the Mexico City event, and that there is an urgent need to upgrade the existing building design code by incorporating some necessary seismic design requirements.

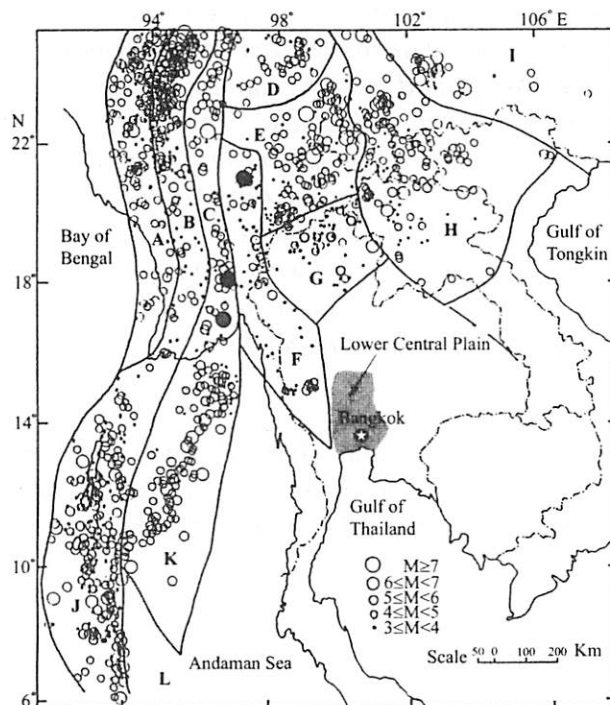


Figure 1: Twelve regional seismic source zones (A-L) and epicenters of earthquakes during 1910 - present

## 2. MODELLING OF REGIONAL SEISMIC SOURCES

Based on seismotectonic features of the Burma-Thailand-Indochina region and the spatial distribution of earthquake epicenters, twelve seismic source zones in this region were identified by Nutalaya et al. (1985). They are named zones A to L as shown in Fig. 1. An earthquake catalogue containing instrumental data of earthquakes occurring in this region from 1910 to 1983 was also compiled by Nutalaya et al. (1985) using data

collected from USGS, ISC (U.K.), the Thai Meteorological Department (TMD), and several other agencies. Note that most of the data before 1970s were recorded by global networks of seismograph stations outside Thailand. Due to the sparsity of the stations a large number of small and moderate earthquakes in this region were neither detected nor recorded, i.e. data incompleteness. After a TMD network of seismograph stations inside Thailand was established and began to operate in the late 1970s, the capability to detect small regional earthquakes has been significantly improved. As TMD has continued to improve its network by installing new stations, the TMD's instrumental data of regional earthquakes after 1982 were found to be as complete as or even more complete than the data from the global networks. Therefore, we combined the Nutalaya's data (1910-1983) with the TMD's data from 1984 to 1989 to form an 80-year instrumental database for our probabilistic seismic hazard assessment of Bangkok.

In order to make the database suitable for an unbiased estimate of earthquake recurrence, some corrections of the database were carried out. First, all dependent events, either foreshocks, aftershocks or smaller events within an earthquake swarm were identified and deleted from the database, so the remaining data show only independent events (mainshocks). The spatial distribution of epicenters of these independent earthquake events are presented in Fig. 1. Second, a statistical analysis of data was conducted in order to identify the time periods of complete data. The time periods represent the time span over which earthquakes of a given magnitude range are completely recorded. The reliable average rate of earthquake occurrence for each magnitude range for each source zone was then estimated from the corresponding complete data.

For each source zone, an exponential magnitude-recurrence relationship was fitted to the estimated occurrence rates by a least-square technique. A smooth truncation was also imposed on the relationship such that the occurrence rate starts to deviate from its exponential relation at the magnitude  $M_0$  and drops to nearly zero at approximately  $M_0 + 0.5$ . In most seismic source zones,  $M_0$  was set to the largest recorded earthquake magnitude in the zone. For zones F and G, however, there is new information regarding the expected maximum earthquake magnitude from two site-specific seismic hazard assessments conducted recently by Woodward-Clyde Federal Services (WWC)—one for a large irrigation dam to be constructed in northern Thailand [DMR, 1996] and another one for two existing large dams in western Thailand [EGAT, 1998]. As a principal part of each assessment, WWC conducted a preliminary paleoseismic investigation over a region within approximately a 200-km radius from the site. The investigation results indicated that there are at least seven active faults in northern Thailand (zone G) and five active faults in western Thailand (the lower portion of zone F). Although these active faults exhibited low levels of seismicity, it was estimated from their expected rupture dimensions that a maximum earthquake of magnitude ( $M_w$ )  $6.8$  to  $7.2 \pm 0.3$  and  $7.3$  to  $7.5 \pm 0.3$  could be generated in northern and western Thailand, respectively, by these active faults. Based on these paleoseismic



investigation results, we decided to set  $M_0$  for zones G and F to 7.0 and 7.4, respectively.

### 3. ATTENUATION MODELS FOR DISTANT LARGE EARTHQUAKES

Traditionally an attenuation model for a specific region is empirically developed from statistical regression analyses of hundreds of earthquake ground motion records. For this region, however, a very limited number of strong motion records are available, and most of them were recorded during small to moderate earthquake events in 1983-85 in western Thailand with source-to-station distances of less than 60 km. One solution to this data limitation is to assume that some existing attenuation models developed for other regions with similar seismotectonic characteristics can adequately represent ground motion attenuation in this region. With this in mind, Nutalaya and Shrestha (1990) compared the recorded peak ground acceleration (PGA) values in western Thailand with those predicted by several existing attenuation models, and they found that the Esteva model [Esteva and Villaverde, 1973] gives the best fit. So they suggested that the model could be used for seismic hazard assessments in this region.

In this assessment, in addition to the Esteva model, many new attenuation models for shallow crustal earthquakes are considered in order to improve assessment reliability. Attenuation models for subduction zone earthquakes are not included because our instrumental and seismotectonic data indicate that most earthquakes within approximately a 600-km radius from Bangkok belong to the shallow crustal type. The first group of new models to be considered are four empirical models developed for Western North America (WNA) by Boore et al. in 1997, Abrahamson and Silva in 1997, Campbell and Bozorgnia in 1994, Sadigh et al. in 1993. The second group are two new empirical models for Europe (EU) developed from regression analyses of European and Italy strong-motion data by Ambraseys and Bommer in 1992 and Sabetta and Pugliese in 1987, respectively. These two groups represent the attenuation characteristics of shallow crustal earthquakes in active tectonic regions. The third group are three new models for Central and Eastern North America (CENA) developed by Toro and McGuire in 1987, Atkinson and Boore in 1995, and Hwang and Huo in 1997. These three models are for shallow crustal earthquakes in a stable continental region. Further details of attenuation models in all groups can be found in SSA (1997).

A rough estimate using these attenuation models indicates that a destructive ground motion in Bangkok can only be induced by a large earthquake of magnitude ( $M_w$ ) 6.5 to 8 at a source-to-site distance of 120 to 300 km. Therefore, the peak rock outcrop acceleration (PRA) attenuation curves computed from these models for earthquakes of magnitude ( $M_w$ ) 7.2 and 8 are compared in Fig. 2. It can be observed that all WNA and EU models, which are developed for active tectonic regions, yield very similar PRA curves for rupture distances less than about 100 km. Beyond this

distance range, the PRA curves diverge from each other. This is also beyond the prediction limits of these models; they are not intended to be used for such long rupture distances. CENA models, on the other hand, have much higher distance limits—up to 200 to 300 km or more. Their PRA curves lie very close to each other over a wide rupture distance range, up to several hundreds kilometers. Compared with WNA and EU models, CENA models predict higher PRA values for rupture distances between 10 and 200 km due to the lower attenuation rate in stable continental region. Another point worth noting is that the PRA curves of the Esteva model match surprisingly well with those of CENA models. The question then arises: “Between WNA/EU models and CENA/Esteva models, which group is a better representation of the attenuation characteristics of this region?”

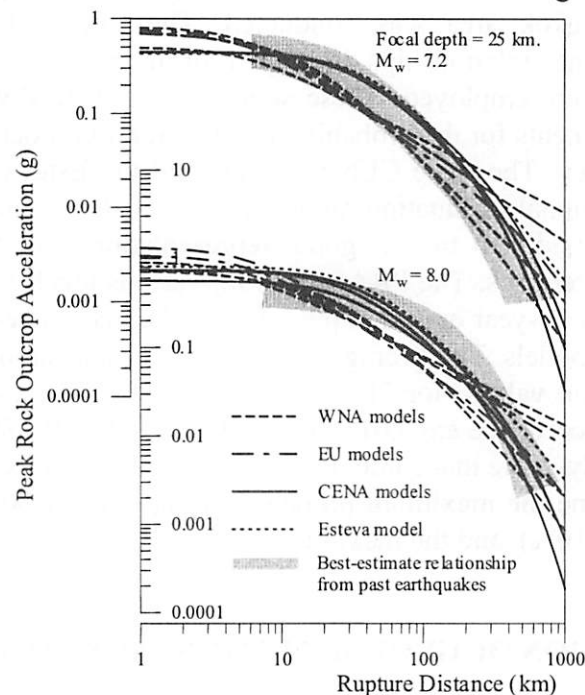


Figure 2: Comparison of attenuation relationships

To answer this question, we searched through past earthquake records and reports for more information on the ground motion attenuation of large earthquakes in this region. The best available information is from isoseismal maps of the Mandalay earthquake ( $M_s = 8$ ) of 23 May 1912; the Pegu earthquake ( $M_s = 7.2$ ) of 5 May 1930; and the Pyu earthquake ( $M_s = 7.2$ ) of 3 December 1930 [Natalaya, 1985]. The epicenters of these Burmese earthquakes are shown by shaded circles in Fig. 1. The isoseismal maps show contour lines of ground shaking intensity in the Rossi-Forel scale over the whole country of Burma and some portion of Thailand. We first converted the intensities into those in the Modified Mercalli (MM) scale, and then computed equivalent PGA values by using an empirical relationship proposed by Trifunac and Brady (1975). We assumed that each MM intensity value contains an error of  $\pm 0.3$  scale; this is to account for possible errors in the transformation process. The PGA values were further scaled into the corresponding PRA values by assuming that typical surficial deposits are stiff soils. For this scaling, the ratio of PGA at a stiff soil site to PRA was assumed to be 1.0, 1.3, 1.5, 1.8, and 2.0 for PRA values of 600,

250, 130, 30, and 5 cm/sec<sup>2</sup>, respectively. From the results obtained, two bands of best-estimate regional PRA attenuation relationship were constructed as shown in Fig. 2. The attenuation characteristic of these bands looks more like those of CENA and Esteva models than WNA and EU models. Although a definite conclusion can not be drawn from these limited results, we tend to believe that the group of CENA and Esteva models is a better representation of the regional attenuation characteristics.

#### **4. PROBABILISTIC SEISMIC HAZARD ANALYSIS**

Using the well-known Cornell method, a probabilistic prediction of PRA in the Bangkok area was conducted. The truncated exponential magnitude-recurrence relationships developed for the eleven regional source zones (A to K) were employed. These source zones were divided into as many as 9890 segments for the probabilistic integration in order to achieve a reasonable accuracy. The three CENA models and the Esteva model were adopted as the regional attenuation models for the analysis since these four models were considered to be good representations of the regional attenuation characteristics. The PRA values for various levels of probability of exceedance in a 50-year exposure period were then computed for each of these attenuation models. The average PRA values, which can be considered as the best-estimate values, for 70%, 50%, 10%, 5%, 2%, 1%, and 0.5% probabilities of exceedance are 0.015, 0.019, 0.043, 0.056, 0.075, 0.088, and 0.10 g, respectively. Note that some of these probabilities of exceedance are often used to define the maximum probable earthquake (50%), the design-basis earthquake (10%), and the maximum capable earthquake (2%).

#### **5. AMPLIFICATION OF GROUND MOTIONS IN BANGKOK**

The city of Bangkok is situated on a large and extremely flat plain, commonly known as the “lower Central plain” of Thailand. The length from north to south of the plain is about 250 km and the average width is approximately 200 km (see Fig. 1). The lower Central plain consists of a broad deep basin filled with alluvial and deltaic sediments with occasional shallow sea sedimentation, forming alternate layers of sand, gravel and clay. The depth of bedrock surface is estimated to be between 550 and 2000 m. The uppermost soil layer is a “soft” silty marine clay, usually referred to as “soft Bangkok clay”. Throughout this large area of the lower Central plain, the composition and thickness of the clay are remarkably consistent with gradual coarsening and thinning towards the margin of the plain. The clay is about 10 to 18 m thick in the Bangkok metropolitan area. The soft Bangkok clay was deposited during the latest transgression of the sea over the plain, which began about 10,000 years ago [AIT, 1980]. After the sea withdrew at about 2,700 years ago, the soft clay was exposed and the uppermost 1 to 2 m has been weathered. Since its sedimentation, the clay has never been subjected to mechanical over-consolidation due to over-stressing. Hence, it is highly compressible and its shear strength is extremely low. The soft clay is underlain by a layer of “stiff” silty clay known as the first stiff clay layer.



Similar to the soft clay layer, the thickness of the stiff clay is rather uniform, varying between 5 to 10 m in the Bangkok area. The stiff clay, however, is significantly older than the soft clay and is clearly separated from it by a pronounced disconformity. The shear strength of the stiff clay is much greater than that of the soft clay, and the compressibility is much less. The deeper strata consist of alternate layers of sand deposits and stiff clay with high strength and low compressibility extending horizontally over a large area.

Since the soil deposits underlying the whole Bangkok and its surrounding areas consist of nearly uniform and horizontal layers of clay and sand, the response of these deposits to bedrock motions can be reasonably evaluated by a one-dimensional wave propagation analysis. Thus, the method of one-dimensional site response analysis using the computer program SHAKE91 [Idriss and Sun, 1992] is adopted in this study. To conduct site response analyses for the Bangkok area using this method, a generalized soil profile must be developed with corresponding dynamic soil properties necessary for the analyses. These properties are: shear wave velocity (or low-strain dynamic shear modulus), mass density, and relationships for variation of dynamic shear modulus and damping ratio as a function of strain.

From a comprehensive investigation of soil characteristics at 9 different sites around the Bangkok metropolitan area, Ashford et al. (1996) developed a generalized soil profile and a corresponding generalized shear wave velocity profile of Bangkok as shown in Fig. 3. They first estimated shear wave velocity (denoted by  $V_s$ ) from specific field and laboratory soil data of the 9 sites using several published empirical correlations, and then confirmed such estimates with actual insitu  $V_s$  measurements at another 4 sites around Bangkok using a downhole method. Excellent agreement was found between the estimated and measured  $V_s$  profiles. The obtained generalized  $V_s$  profile shows extremely low  $V_s$  in soft Bangkok clay (about 60 to 100 m/s). This is comparable to Mexico City clay. The velocity increases sharply and considerably to about 200 to 250 m/s in the first stiff clay, and it continues to increase at a slower rate in the deeper strata.

The high contrast in  $V_s$  between the uppermost soft clay layer and the underlying layer in the Bangkok area is similar to that in Mexico City as shown in Fig. 3. In Mexico City, the  $V_s$  discontinuity interface allows the upward propagating shear waves to easily propagate through, but it acts more like a reflector to the downward propagating shear waves coming from the reflection at the ground surface. Hence, a major portion of shear waves is trapped within the soft clay layer. During the 1985 earthquake, this created a wave resonance when the trapped waves interacted constructively with the continual upward propagating waves from the bedrock, and resulted in a significant amplification of motions in the soft clay layer. Therefore, the discontinuity of the  $V_s$  profile in Bangkok, though not as sharp as in Mexico City, suggests that a similar amplification mechanism may occur in this area.

Additional important information on dynamic soil properties was obtained from a series of comprehensive insitu and laboratory tests of soils at a site in central Bangkok area conducted by Shibuya and Tamrakar (1999). These tests include an insitu seismic cone (SC) test at the site and a laboratory undrained cyclic torsional shear (CTS) test of several hollow cylindrical clay specimens taken from the site at depths of 4, 8, and 12 meters. In the CTS test, each specimen was isotropically consolidated to its insitu effective overburden pressure, and then subjected to a multi-stage undrained cyclic shear at the frequency of 0.1 Hz. The test results are presented by plotting the ratio of  $G/G_{max}$  (i.e. the ratio of shear modulus at a given strain,  $G$ , over the low-strain shear modulus,  $G_{max}$ ) and the damping ratio versus shear strain. The results are found to be in excellent agreement with the Vucetic-Dobry relation for clay with plasticity index (PI) of 50. Note that PI of soft Bangkok clay varies between 30 to 70 with an average value of about 50. This excellent agreement indicates that the Vucetic-Dobry empirical relationships can be reasonably used for Bangkok clays. In the SC test, the shear wave was generated on the ground surface by plank hammering, and a cone with two receivers at 1 m apart was used for the insitu  $V_s$  measurement. The measured results are also in good agreement with the generalized  $V_s$  profile as shown in Fig. 3.

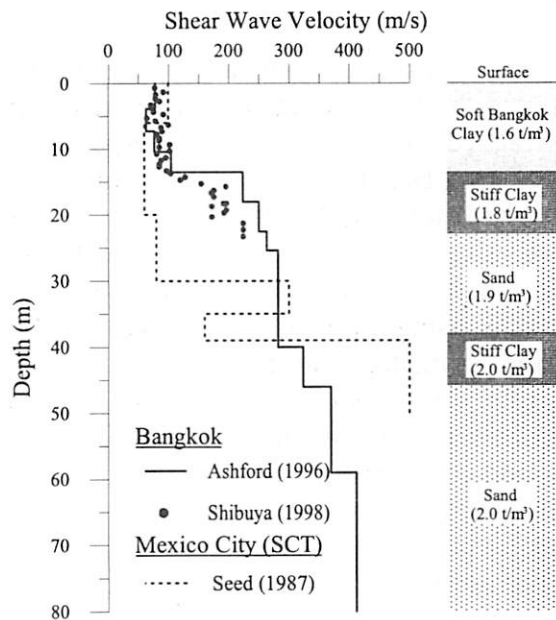


Figure 3: Generalized Bangkok soil and shear wave velocity profiles

In this study, the generalized soil and  $V_s$  profiles of Bangkok proposed by Ashford et al. (1996) and the relationships for strain-dependent modulus and damping of clay by Vucetic and Dobry (1991) and sand by Seed et al. (1984) were employed for Bangkok’s site response analyses. Below the depth of 80 m, no data was available to make a reasonable estimate of the  $V_s$  profile, so it was assumed that rock-like material exists below this depth with a  $V_s$  of 900 m/s. Seven different accelerograms were employed to represent rock outcrop motions in the Bangkok area. These accelerograms were selected from actual acceleration records at rock sites generated by

magnitude 7 to 8 earthquakes at source-to-site distances from 80 to 350 km. The peak acceleration values of these selected records vary from 0.005 g to 0.09 g, and the predominant periods from 0.5 sec to 2 sec. These records were scaled to various peak acceleration values between 0.002 g and 0.075 g and used as input rock outcrop motions. All together, about 90 individual site response analyses were conducted using these input motions. In each analysis, the amplification factor (i.e. the ratio of PGA to input PRA) was computed, and in some selected cases the elastic response spectrum of the computed ground motion was also evaluated in order to examine its frequency content and damage potential on buildings and structures.

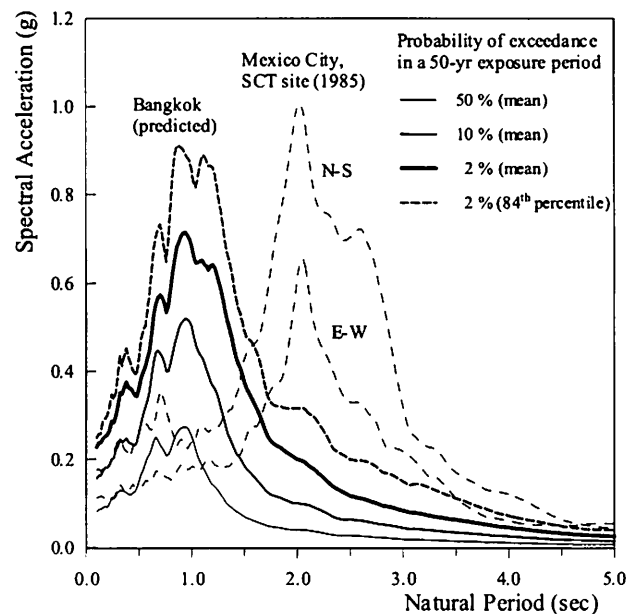


Figure 4: Comparison between the elastic response spectra of predicted ground motions in Bangkok and the spectra of the damaging ground motions in Mexico City

The computed results clearly show that the soil profile underlying Bangkok has the ability to amplify earthquake ground motions about 3 to 6 times in terms of peak acceleration for extremely low intensity input motions (PRA from 0.002 to 0.01g) and about 3 to 4 times for relatively stronger input motions (PRA from 0.02 to 0.075g). This range of amplification factors is comparable to those found in Mexico City. The mean PGA values for input PRA values of 0.015, 0.019, 0.043, 0.056, 0.075, 0.088, and 0.10 g are 0.056, 0.072, 0.14, 0.18, 0.22, 0.24, and 0.26 g, respectively. These are the best-estimate PGA values for Bangkok that have, respectively, 70%, 50%, 10%, 5%, 2%, 1%, and 0.5% probabilities of exceedance ( $P_e$ ) in a 50-year exposure period. The amplified ground motions can be described as narrowband random motions with a relatively long predominant period of about 1 second. This is clearly illustrated by the mean elastic response spectra (5% damping) for computed ground motions of 50%, 10%, and 2%  $P_e$  as shown in Fig. 4. Each spectrum shows a high spectral amplification in a narrow range of periods centered at about 1 second. The mean and 84<sup>th</sup> percentile spectra for ground motions of 2%  $P_e$ , which characterize the maximum capable earthquake ground motion in the

Bangkok area, are comparable in peak spectral acceleration to those of the damaging ground motions in Mexico City during the 1985 earthquake event. Based on these results, it is reasonable to infer that the maximum capable ground motion, if it occurred, would most likely cause severe damage or even complete collapse to structures with fundamental periods ranging from about 0.5 sec to 1.5 seconds as well as to short-period structures that do not have sufficient lateral strength.

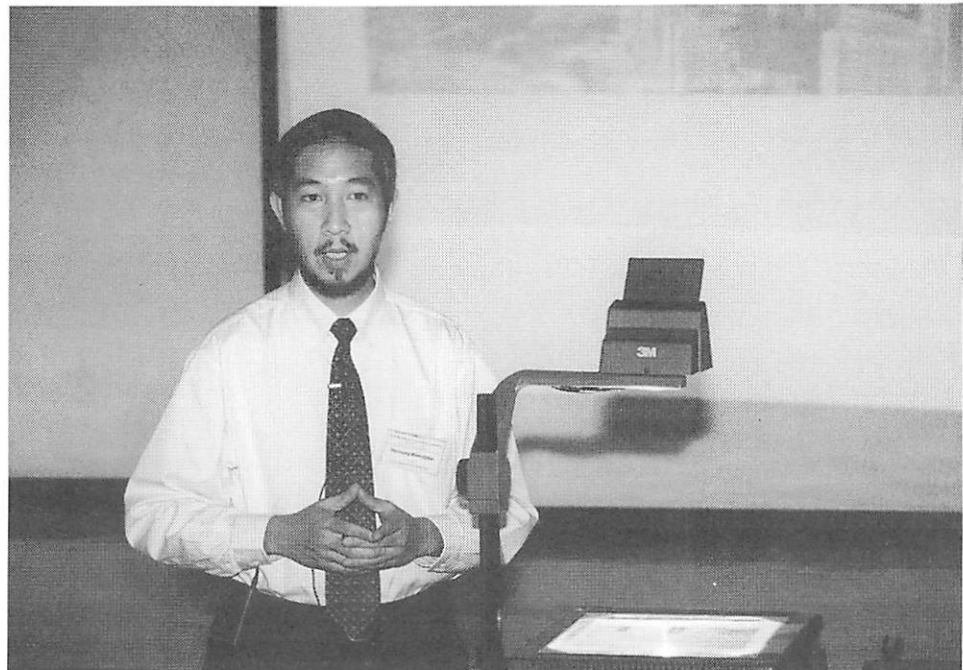
## 6. CONCLUDING REMARKS

The seismic hazard assessment presented in this paper indicates that Bangkok, though located at a remote distance from seismic sources, is still at risk of strong earthquake ground motions. The risk is essentially caused by three major factors: the ability of regional seismic sources to generate large earthquakes, the low attenuation rate of ground motions in this region, and the ability of thick unconsolidated surficial deposits in Bangkok to considerably amplify earthquake ground motions. The predicted strong earthquake ground motions could cause extensive building destruction and considerable loss of life in Bangkok. To avoid such unacceptable economic and social consequences, the existing building design code must be improved by incorporating necessary seismic design requirements, and the safety of existing important buildings and hazardous facilities must be critically reviewed. The predicted earthquake ground motion parameters from this assessment can be directly used for these purposes.

## REFERENCES

- AIT (1980): Asian Institute of Technology. Investigation of Land Subsidence Caused by Deep Well Pumping in the Bangkok Area, Phase II, AIT research report submitted to the National Environmental Board, Thailand.
- Ashford, S.A., Jakrapiyanun, W. and Lukkanaprasit, P. (1996): Amplification of Earthquake Ground Motions in Bangkok, AIT research report submitted to the Public Works Department, Thailand.
- DMR (1996): Department of Mineral Resources. Environmental Impact Assessment: Geological Aspect, Kaeng Sua Ten Dam Project, Changwat Phrae, Main Report No. 3, Ministry of Industry, Thailand.
- EGAT (1998): Electricity Generating Authority of Thailand. Preliminary Seismic Hazard Evaluation of Khao Laem and Srinagarind Dams, Thailand, Thailand.
- Esteva, L. and Villaverde, R. (1973): Seismic risk, design spectra and structural reliability. Proc. 5<sup>th</sup> World Conf. on Earthq. Eng., Rome 2, 2586-2596.
- Idriss, I.M. and Sun, J.I. (1992): User Manual for SHAKE91, Center for Geotechnical Modeling, Dept. of Civil & Environ. Eng., Univ. of California, Davis, California.
- Nutalaya, P. and Shrestha (1990): Earthquake ground motions and seismic risk in Thailand. Proc. 1990 Annual Conf., Engineering Institute of Thailand, Bangkok, 55-77.

- Nutalaya, P., Sodsri, S., and Arnold, E.P. (1985): Southeast Asia Association of Seismology and Earthquake Engineering: Series on Seismology Volume II-Thailand, Bangkok.
- Seed, H.B., Romo, M.P., Sun, J.P., Jaime, A., and Lysmer, J. (1987): Relationships between Soil Conditions and Earthquake Ground Motions in Mexico City in the Earthquake of Sept. 19, 1985, UCB/EERC-87/15, Univ. of California, Berkeley, California.
- Seed, H.B., Wong, R.T., Idriss, I.M., and Tokimatsu, K. (1984): Moduli and Damping Factors for Dynamic Response Analysis, UCB/EERC-84/14, Univ. of California, Berkeley, California.
- Shibuya, S. and Tamrakar, S.B. (1999): In-situ and laboratory investigations into engineering properties of Bangkok clay. Proc. of Intl. Symp. Characterization of Soft Marine Clays-Bothkennar, Drammen, Quebec and Ariake Clays, Balkema.
- SSA (1997): Seismological Society of America. Seismological Research Letters 68:1, 255 pages.
- Trifunac, M. D. and Brady, A. G. (1975): On the correlation of seismoscope response with earthquake magnitude and Modified Mercalli intensity. Bull. Seism. Soc. Am. 65:2, 307-321.
- Vucetic, M. and Dorby, R. (1991): Effect of soil plasticity on cyclic response. J. Geotech. Eng., ASCE, 117:1, 89-107.
- Warnitchai, P. and Lisantono, A. (1996): Probabilistic seismic risk mapping for Thailand. Proc. 11<sup>th</sup> World Conf. on Earth. Eng. , Acapulco, Paper No. 1271.



*Dr. Pennung Warnitchai*





# **APPLIED ELEMENT METHOD: A NEW EFFICIENT TOOL FOR DESIGN OF STRUCTURE CONSIDERING ITS FAILURE BEHAVIOR**

KIMIRO MEGURO

International Center for Urban Safety Engineering (ICUS/INCEDE),  
Institute of Industrial Science (IIS), The University of Tokyo, Japan

## **ABSTRACT**

*A new efficient numerical model termed Applied Element Method (AEM), which can be a new tool for discussing a new philosophy of design of structure, is introduced. Although formulation and material model adopted in the method are simple, highly nonlinear behavior of structures in both static and dynamic conditions can be simulated accurately in reasonable CPU time. Conventionally, structures were designed based on the assumption that an engineering designed structure would never collapse, however, this was wrong and it miss-guided people in some sense not to think seriously about the chaotic situation. To show the accuracy and applicability of the method, numerical results of nonlinear behavior of reinforced concrete structures obtained by the AEM are compared with experimental results.*

## **1. INTRODUCTION**

During earthquakes, buildings suffer from the different types of damage. Structure damage is classified into seven groups, as shown in Table 1, according to the Architecture Institute of Japan (AIJ)<sup>1)</sup>. In the first five groups, partial damage occurs to the structural and non-structural elements without collapse of the structure. Partial and complete collapse of structures is important topic under research because it causes extensive casualties inside and outside of the structures. In addition, collapse of a structure may lead to failure or collapse of neighbor structures. Recent earthquakes, like Hyogo-Ken Nanbu Earthquake (Kobe Earthquake), show that structural failure was major cause of death toll<sup>2)</sup>.

Many important questions can not be answered unless the numerical technique can follow detailed collapse behavior. For example, "What is the effect of collision between falling structural elements and neighbor structures", "What happens if structures having different dynamic characteristics collide during earthquakes?", "If a structure collapse, where and how do they undergo collapse?" and "What is the duration of collapse?". From the experience of Kobe Earthquake, Science and Technology Agency of Japan decided to build huge capacity (1,200 tf, over 0.9 G,  $\pm 200$  kine,  $\pm 100$  cm) three dimensional shaking table facility up to 2005. Using the

facility, we can construct real-scale building and/or structure on the table and simulate complete collapse behavior of them. However, it is still impossible to carry out many experiments of every different type of structures. To fulfill this, an accurate but simple numerical technique is important. This numerical technique should satisfy the conditions of "*accuracy*", "*simplicity*" and "*applicability*". The term, "*accuracy*", means that realistic results should be obtained. "*Simplicity*" indicates that the method should not be complicated. Finally, "*applicability*" means that the method can be applied for a wide range of applications in reasonable CPU time. Studying the existing numerical techniques, we can find easily that these three conditions can not be fulfilled by one specified numerical technique.

To clarify the problems, a brief overview about the advantages and disadvantages of existing numerical technique are introduced. Numerical methods for structural analysis can be classified into two categories. In the first category, model is based on continuum material equations. The Finite Element Method (FEM) is typical example of this category. Smearred Crack approach<sup>3)</sup> can not be adopted in zones where separation occurs between structural elements. While, Discrete Crack Methods<sup>3)</sup> assume that the location and direction of crack propagation are predefined before the analysis. With this group of the methods, analysis of structures, especially concrete structures, can be performed at most before collapse. The FEM can fulfill only the conditions of "*accuracy*". On the other hand, it is difficult to accept that the FEM fulfills the second requirement, which is "*simplicity*". Many complications arise if the behavior is highly nonlinear from either material or geometrical point of view. For example, it is very difficult or impossible to use the FEM to study behavior of materials or structures that change their status from continuum state to perfectly discrete state, like behavior of structures before and during collapse. In brief, the FEM can answer only the following question which is "Will the structure fail or not?" Unfortunately, it is very difficult to use the FEM for the second important question, which is "How does the structure collapse?" Although displacement of structural elements at failure may become tens of meters, analysis using the FEM could be performed till the start of failure, which means tens of centimeters at most.

The second group of methods uses the discrete element techniques, like the Rigid Body and Spring Model (RBSM)<sup>4)</sup> and the Modified ( or Extended) Distinct Element Method (MDEM<sup>5)</sup>, EDEM<sup>6)</sup>. The main advantage of these methods is that they can simulate the cracking process with relatively "simple" techniques compared to the FEM, while the main disadvantage is that crack propagation depends mainly on the element shape, size and arrangement<sup>7), 8)</sup>. Analysis using the RBSM could not be performed up to complete collapse of the structure. On the other hand, the EDEM can follow the structural behavior from zero loading and up to complete collapse of the structure. However, the accuracy of EDEM in small deformation range is less than that of the FEM. Hence, the failure behavior obtained by repeated many calculations is affected due to cumulative errors and it can

Table 1: Damage level of structures as defined by the AIJ<sup>1)</sup>

Damage level	Damage of members
1- No damage	No damage is found.
2- Slight damage	Columns, shear walls or non-structural walls are slightly damaged.
3- Light damage	Columns or shear walls are slightly damaged. Some shear cracks in non-structural walls are found.
4-Moderate damage	Typical shear and flexural cracks in columns, shear cracks in shear walls, or severe damage in non-structural walls are found.
5- Heavy damage	Spalling of concrete, buckling of reinforcement, and crushing or shear failure in columns are found. Lateral resistance of shear walls is reduced due to heavy shear cracks.
6- Partial collapse	The building is partially collapsed due to severely damaged columns and/or shear walls.
7- Total collapse	The building is totally collapsed due to severely damaged columns and/or shear walls.

Table 2: Organization of research results

Geometry	Material	Static		Dynamic	
		Monotonic	Cyclic	Monotonic	Cyclic
Small deformation (linear)	Elastic	I	III	V	VI
	Nonlinear	II			
Large deformation (nonlinear)	Elastic	IV			
	Nonlinear	Covered in dynamics			
Collapse process		No meaning			

not be predicted accurately using the EDEM. This means that the EDEM can answer qualitatively only the second question, "How does the structure collapse?" The EDEM fulfill totally the conditions of "simplicity" and partially fulfills the "applicability", however, the "accuracy" requirements are still questionable.

From the fact discussed above, we can say that there is no proper method among current available techniques by which total behavior of structures from zero loading to collapse can be followed with reliable accuracy, reasonable CPU time and with relatively simple material models.

The major advantages of the Applied Element Method (AEM) are simple modeling and programming, and high accuracy of the results with relatively short CPU time. Using the AEM, highly nonlinear behavior, i.e. crack initiation, crack propagation, separation of structural elements, rigid body motion of failed elements and collapse process of the structure can be followed with high accuracy<sup>9)</sup>.

To cover a wide range of applications, analyses should be performed for different fields of application and the results should be verified by comparing with theoretical and/or experimental results whenever possible. The main factors affecting structural analysis can be categorized as:

1. Effects of inertia forces: The loading types are divided into two categories, static and dynamic loading conditions. In dynamic loading case, the inertia and damping forces should be taken into account and hence, loading is a function of time.
2. Effects of the direction of loading: The analyses are divided into two categories, monotonic and cyclic loading conditions. In monotonic

- loading condition, the load direction is constant while its value increases, and in case of cyclic loading, the load direction and values are changing.
3. Effects of geometrical changes: In some analyses, the deformations are considered small with respect to the structural dimensions. It can be assumed that the structure geometry is constant and effects of geometrical changes on the stiffness matrix or internal forces are negligible. In other cases, like buckling cases, deformations are large and geometrical nonlinear behavior should be discussed.
  4. Effects of material properties: The material behavior can be assumed as linear or nonlinear behavior. In linear behavior, all stress-strain relations are constant while in nonlinear case, cracking, yield of the material and nonlinear stress-strain relations should be considered.

The organization of the research done is shown in Table 2. This table shows all meaningful application ranges, which should be covered by the proposed numerical model. The dark area indicates that there is no meaning to perform simulation, like simulation of collision effects in static loading condition. In the lightly hatched area, application in static loading conditions is not reasonable sometimes because in case of nonlinear material, structural elements, like concrete elements in large deformation range, tend to separate and become unstable. This indicates that the effects of inertia forces and rigid body motions become dominant. Therefore, this range is covered in dynamics. The main purposes of this paper are to explain the background and outline of newly proposed model, AEM, and to introduce some of the results of AEM in order to show the applicability of the method.

## 2. OVERVIEW OF THE AEM

With the AEM, structure is modeled as an assembly of small elements, which are made by dividing the structure virtually, as shown in Fig. 1 (a). The two elements shown in Fig. 1 are assumed to be connected by pairs of normal and shear springs located at contact points, which are distributed around the element edges. Each pair of springs totally represent stresses and

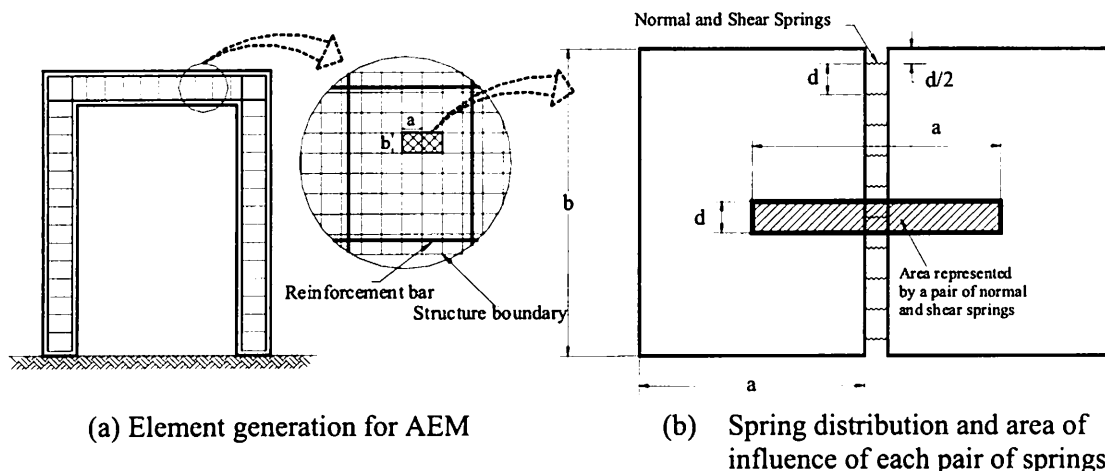


Figure 1: Modelling of structure to AEM

deformations of a certain area (hatched area in Fig. 1 (b)) of the studied elements. In case of reinforcement, two pairs of springs are used, for concrete and for reinforcement bar. This means that the reinforcement spring and concrete spring have the same strain and the effects of separation between reinforcement bars and surrounding concrete can not be easily considered within an element. However, when we look at the behavior of element collection as a unit, due to the stress conditions, separation between elements occurs because of failure of concrete-springs before the failure of reinforcement-springs and hence, relative displacement between reinforcement bars and surrounding concrete can be taken into account automatically. This is a unique point which continuum equation based models, like FEM, do not have. In the proposed method, reinforcement springs can be set at the exact location of the reinforcement bars in the model. It should be emphasized that effects of stirrups, hoops and concrete cover can be easily considered. Each of the elements has three degrees of freedom in two-dimensional model. These degrees of freedom represent the rigid body motion of the element. Although the element motion is as a rigid body, its internal deformations are represented by the spring deformation around each element. This means that although the element shape doesn't change during analysis, the behavior of assembly of elements is deformable.

The global stiffness matrix is determined by summing up the stiffness matrices of individual pair of springs around each element. The developed stiffness matrix has total effects from all of the pairs of springs according to the stress situation around the element. This technique can be used both in load and displacement control cases.

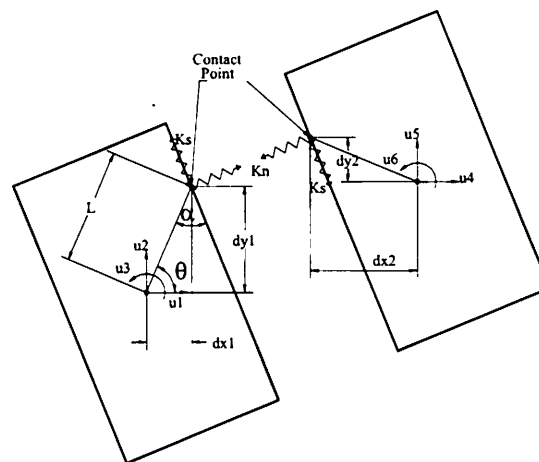


Figure 2: Element shape, contact point and degrees of freedom

### 3. STATIC SMALL DEFORMATION ANALYSIS

In this section, the applicability of the AEM for RC structures in small deformation range is discussed. Simulation results of elastic materials and nonlinear behavior of RC structures under monotonic and cyclic loading conditions are introduced and compared with theoretical or experimental results.

### 3.1 Effect of Element Size (Elastic Material Condition)

Adjustment of element size in the analysis is very important. Simulation of structures using elements of large size leads to increasing the structure stiffness and failure load. This means that the calculated displacements become smaller and the failure load gets to be larger than the actual one. To make this effect clear, we carried out a series of simulations using the laterally loaded cantilever models as shown in Fig. 3. The dimensions of the models are also shown in the figure. The Young's modulus is assumed as  $2.1 \times 10^7$  tf/m<sup>2</sup> and elastic analysis was performed using the proposed method. The results were compared with the theoretical results of elastic structure. The percentage of error in maximum displacement and the CPU time (CPU: DEC ALPHA 300 MHz) are shown in Fig. 4.

To discuss the effect of the number of connecting springs, the analyses were performed using two models with 20 and 10 springs connecting each pair of adjacent element faces for each case of different element size. From Fig. 4, it is evident that increasing the number of base elements leads to decreasing the error but increasing the CPU time. Use of only one element at the base leads to about 30% error of theoretically calculated displacement. This error reduces to less than 1% when the number of elements at the base increases to 5 or more. However, the CPU time increases rapidly. When we compare the results using 20 and 10 springs, although the CPU time in case of 10 springs is almost half of that in case of 20 springs, the accuracy of the results of 10 springs model is same as that in case of 20 springs. From this figure, it can be concluded that usage of large number of elements together with relatively few number of connecting springs leads to high accuracy in reasonable CPU time.

Figures 5 and 6 show the normal and shear stresses distribution at the base of the studied columns for different number of base elements. From these figures, the followings should be noticed:

- Calculated normal stresses are very close to the theoretical values even in case of the smaller number of elements at the base.
- Shear stresses are constant for the same element.
- Shear stresses are far from the theoretical values in case of the smaller number of elements at the base and become close to the theoretical results as the number of elements increases.

This means that behavior in which the effect of shear stresses is minor, like the case of slender frames, can be simulated accurately by elements of relatively large size. To improve the accuracy of analysis using elements of large size, attention should be paid for the unsupported length of the structure. On the other hand, in case of walls and deep beams, elements of small size should be used to follow the fracture behavior in the shear dominant zones.



### 3.2 Effect of Element Arrangement

To verify the accuracy of the proposed method in comparison with other numerical techniques using rigid elements, such as RBSM and DEM, Brazilian test simulation is performed using square shaped concrete specimens subjected to concentrated loads. Three different mesh configurations are used. In Case (1), the elements are set parallel to the specimen edges, while in the second case, the elements are 45 degrees inclined to the specimen edges. In the third case, the load is applied to the diagonal of the square and the elements are parallel to the specimen edges. The distance between loading points is 20 cm in all cases and 10 springs were set between each two adjacent faces. The results are summarized in Table 3. Theoretical failure load is 12.5 tf in Cases (1) and (2). In this simulation, compression failure under the applied load is not permitted. Only tension cracks are permitted.

From the results, it can be noticed easily that the obtained failure load by the proposed model does not change even when different mesh arrangement is adopted, while by RBSM or DEM, failure load can not be calculated in case of 45° discretization mesh in Case (2). Although the normal and shear stress applying to element edges are different in Cases (1) and (2), the principal stresses, which dominate the occurrence of cracking, do not change. This means that results obtained by RBSM or DEM depend

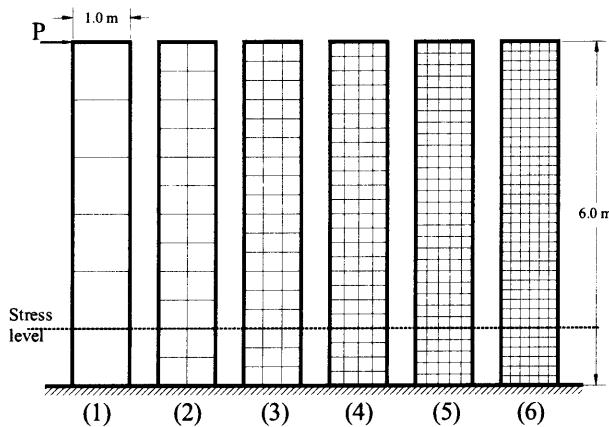


Figure 3: Dimensions and element arrangements of laterally loaded cantilever models

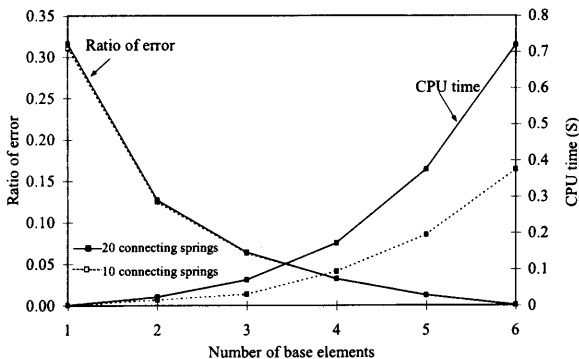


Figure 4: Relations between the number of base elements, ratio of error and CPU time

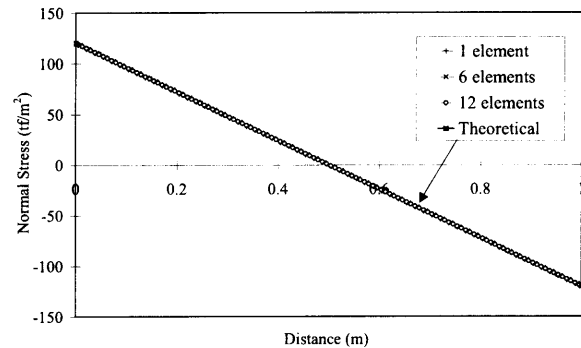


Figure 5: Normal stress distribution at the column base

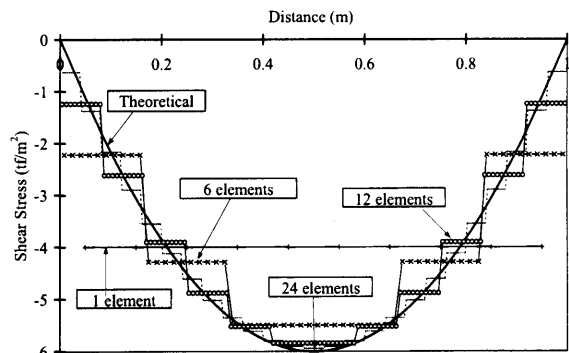


Figure 6: Shear stress distribution at the column base

on the element shape and arrangement because of the use of Mohr-Coloumb's failure criterion based on two components of stresses (not based on principal stresses). This makes the application of Mohr-Coloumb's failure criterion suitable only for brick masonry type of structures but not suitable for continuum materials where the cracking behavior is dominant by the principal stresses.

### 3.3 Verification under Cyclic Loading

This section introduces application of the AEM to cyclic loading conditions. The simulation results are compared with a double cantilever beam subjected to cyclic loading. The dimensions of the beam, reinforcement details and loading points are shown in Fig. 7. For more details about the experiment, refer to Ref. (10). The material properties are:  $\sigma_y=4,600 \text{ kgf/cm}^2$ ,  $\sigma_c=380 \text{ kgf/cm}^2$ ,  $\sigma_t=22.0 \text{ kgf/cm}^2$  and  $E_c=250 \text{ tf/cm}^2$ , following the Ref. (10). In this case, diagonal tension cracks, nonlinear stress-strain relations of concrete<sup>3)</sup>, nonlinear behavior of reinforcement bars<sup>1)</sup> before and after yield are considered.

Half of the structure is modeled using 330 square elements. The number of distributed springs set between each two adjacent faces is 10. Four and half load cycles are applied to the beam in 400 load increments for each. The reinforcement bars are modeled as continuous springs connected elements together at each reinforcement bar location. The total elapsed time of the analysis is about 30 minutes (CPU: DEC ALPHA 300 MHz). It should be noticed also that the loading points and the support locations change during analysis when the load direction is reversed. The applied load cycles are shown in Fig. 8. The numbers inside the figure correspond to the deformed shape and crack patterns shown Fig. 12.

Table 3: Brazilian test results of specimens

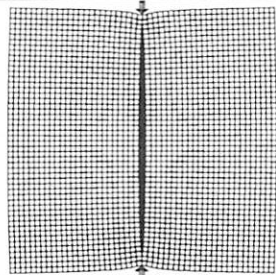
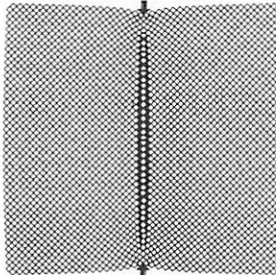
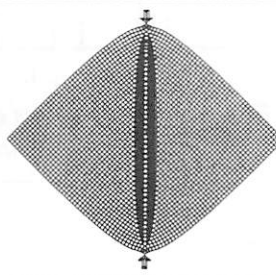
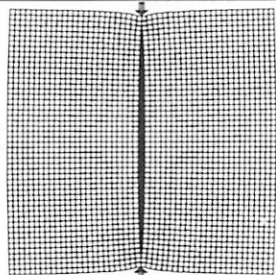
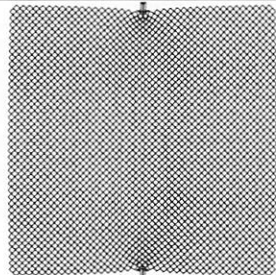
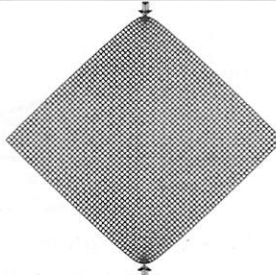
Fracture Criterion	Case (1)	Case (2)	Case (3)
Number of elements	2500	3280	3280
AEM (Principal Stress)			
Failure Load	12.5 tf	12.5 tf	11.7 tf
RBSM or DEM type (Normal and Shear Stresses)			
Failure Load	12.5 tf	Not failed	Not failed

Figure 9 shows the relation between the total applied load and displacement under the loading plates. A good agreement between the calculated and experimental load-deformation relations can be seen. From the figure, it is noticed that the prediction of failure load is very close to the experimental result. However, accuracy of the calculated unloading stiffness, especially before yield of reinforcement, is a little less than that of experiment. This is because of the improper crack closure mechanism.

Using the proposed model, stresses and strains at any point in concrete or steel of the specimen can be calculated easily. Figures 10 and 11 show the stress-strain relations for main reinforcement at point "A" and concrete at point "B", respectively. The location of these points is shown in Fig. 12. It can be noticed from these figures that compression failure of concrete occurs at the connection between the beam and the column together with yield of main reinforcement, which agrees well with the experiment. After yield of reinforcement, stiffness is drastically reduced and relatively large displacement occurs, as shown in Fig. 9.

Figure 12 shows the deformed shapes and crack patterns at different loading stages. Different illustration scale factors are adopted to follow the cracking behavior. Two groups of cracks can be identified easily. During loading

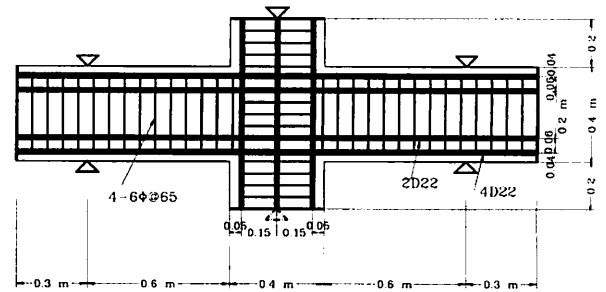


Figure 7: Dimensions and reinforcement of a double cantilever

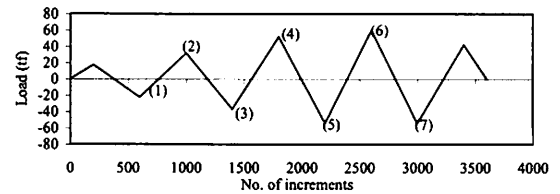


Figure 8: Load cycles applied to a double cantilever

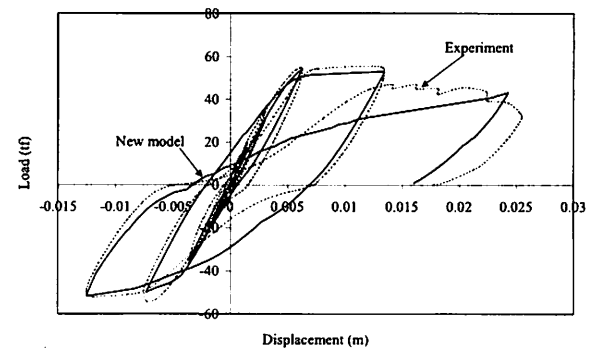


Figure 9: Load-displacement relation of a double cantilever

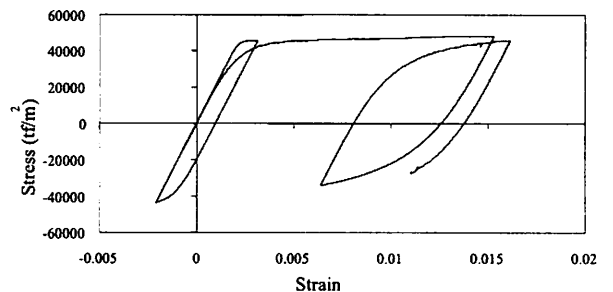


Figure 10: Stress-strain relation for steel at point "A"

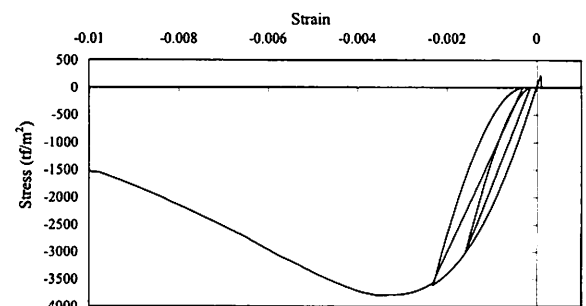


Figure 11: Stress-strain relation for concrete at point "B"

cycles, one group opens while the other group tends to close. The crack width increases when the applied load increases. In addition, tension cracks parallel to centerline of the column appear. Compression failure of elements at the connection between the beam and the column can be seen by following element overlaps. Dislocations of some elements before failure and after repetition of cycles are also obvious.

The above mentioned discussions show that the proposed model can be applied for fracture behavior of RC structures, such as, failure load, deformations, crack generation and propagation, etc. It should be emphasized that although the shape of elements used in the simulations is square, it does not have big effect to the crack generation or propagation in the material. Diagonal cracks, as shown in Fig. 12, coincide well with those obtained from the experiment. In the simulation using rigid elements, like RBSM<sup>4)</sup>, shapes and distributions of elements should be decided before the simulation based on the assumption that crack locations and direction of propagation are known.

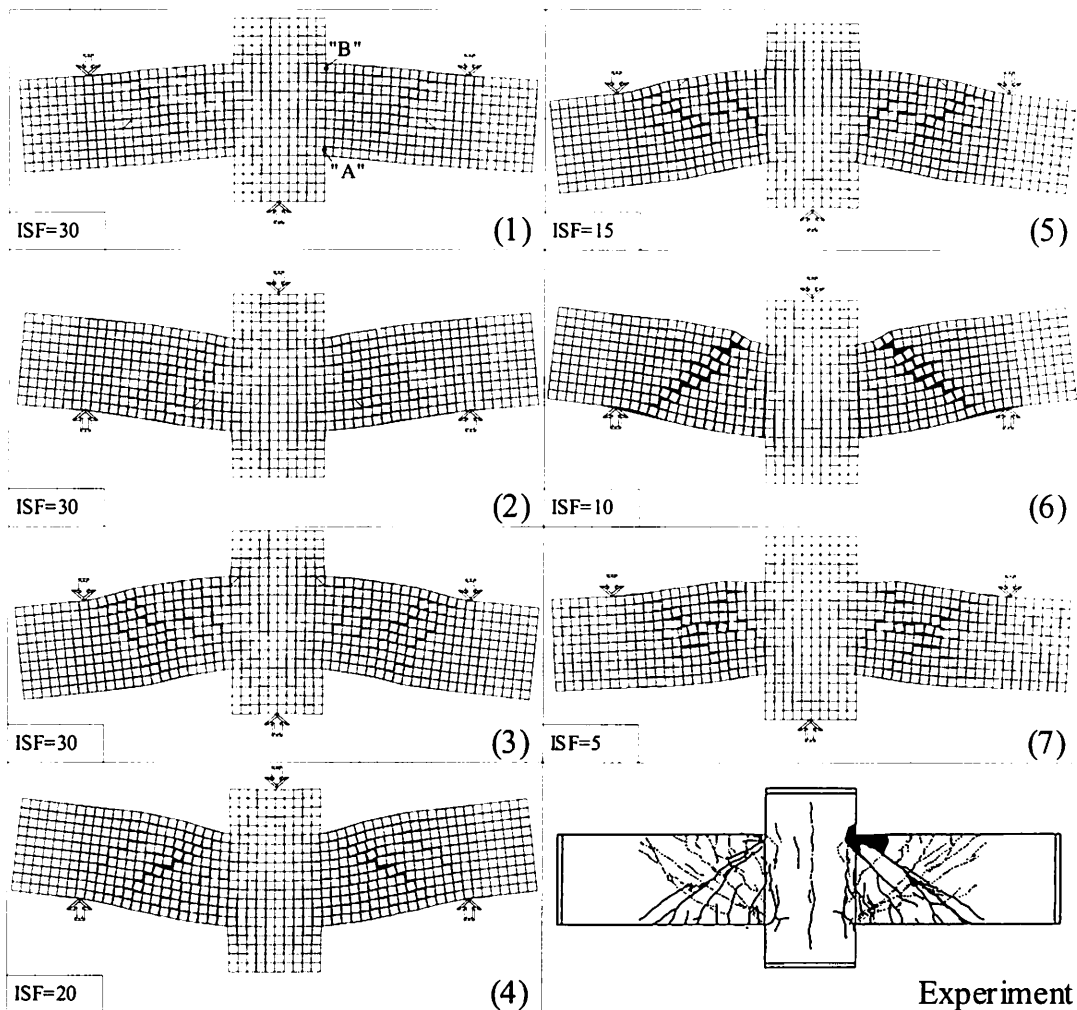


Figure 12: Deformed shape and crack patterns of a double cantilever (ISF: Illustration Scale Factor)

### 4. LARGE DEFORMATION ANALYSIS

In this section, the applicability of the AEM for RC structures in large deformation range is discussed. The applicability of the method for buckling analysis, rigid body motion and collision of structural elements during collapse is addressed. The effects of the geometrical changes of the structure during simulations are considered by adopting the geometrical residuals technique<sup>12), 13)</sup>. The advantage of this technique is that there is no need to determine the geometrical stiffness matrix, resulting in making the simulation easier without affecting the accuracy of the results. This technique can be applied either for static<sup>12)</sup> or dynamic loading cases<sup>13)</sup>.

#### 4.1 Buckling and Post-Buckling Behavior of Structures

In this case study, a fixed base elastic cantilever under axial load is used. The load direction is assumed constant and applied in static way

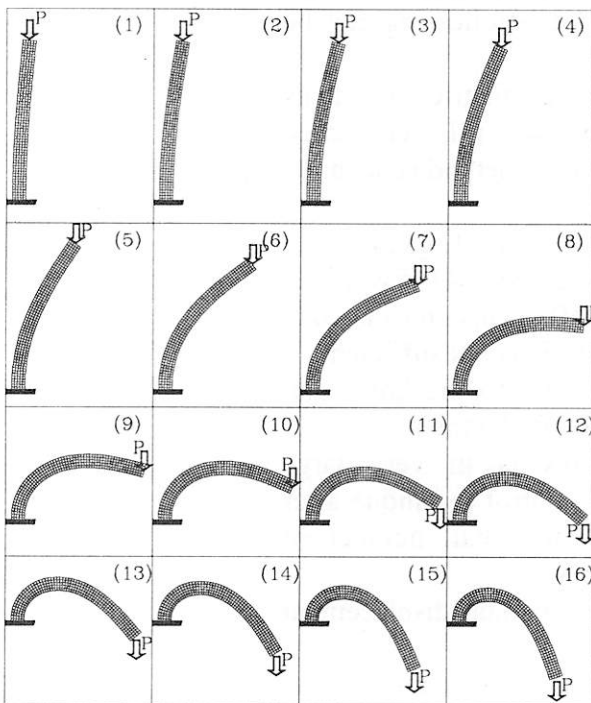


Figure 13: Post buckling behavior of a cantilever

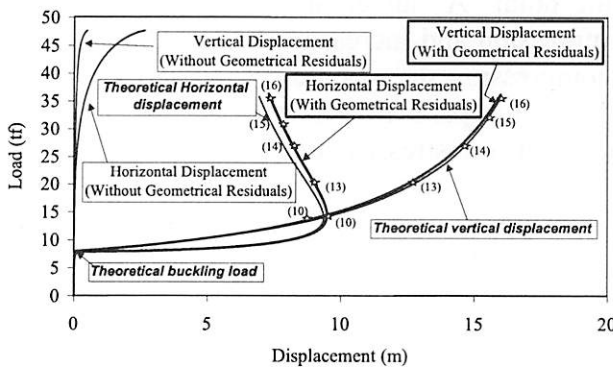


Figure 14: Load-displacement relation of an elastic cantilever under vertical load

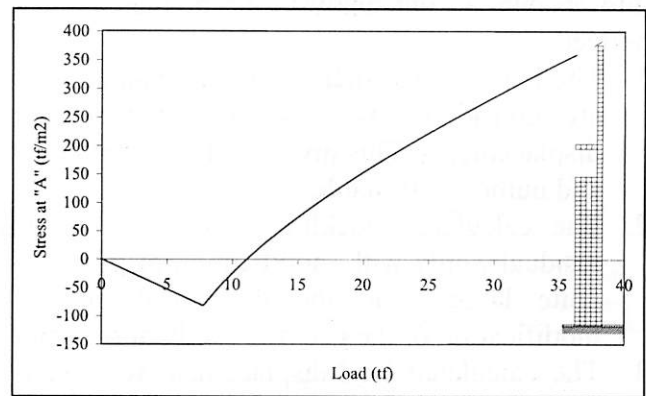


Figure 15: Load-stress relation at point "A"

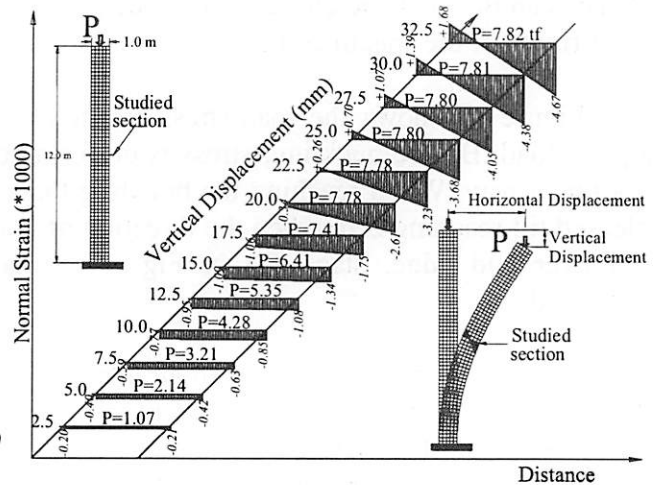


Figure 16: Variation of internal stress distribution during buckling

during analysis. The height of the cantilever is 12.0 m and the cross section is (1.0 m x 1.0 m). The Young's modulus assumed is  $8.4 \times 10^4$  tf/m<sup>2</sup>. The analysis is performed using 300 elements. The load is applied at the top of the column with the constant-rate vertical displacement. To break symmetry of the system, the stiffness of one of edge elements was increased by just 1% relative to the other elements (initial imperfection). The theoretical results of vertical and horizontal displacements can be obtained by following Ref. (14). Figure 13 illustrates the deformed shapes of the cantilever during and after buckling. It is obvious that highly nonlinear geometrical changes can be followed. Figure 14 shows the horizontal and vertical displacements at the loading point in three different cases with and without consideration of the geometrical residuals together with the theoretical load-displacement relations.

In theoretical results, the effects of axial and shear deformations are not considered. Although these effects are relatively small, they are taken into account in our analysis. From Figs. 13 and 14 the following can be noticed:

1. The load-displacement relation obtained when the geometrical residuals are considered is close to the theoretical values till very large displacements. This gives evidence that the proposed method is accurate and numerically stable.
2. The calculated buckling load without consideration of geometrical residuals, only with modification of geometry, was about 47 tf which is quite larger than the theoretical one (7.8 tf). This means that modification of the geometry only during the analysis is not sufficient.
3. The calculated load-displacement relation is tangent to the horizontal line at the buckling load value which agrees well with the theory.
4. Slight increase in the load after buckling results in very large displacements. This indicates that applying load control technique after buckling leads to very large deformations during small number of increments.
5. When the vertical displacement is about 9 m, horizontal displacement begins to decrease.
6. The cantilever shape changes after buckling to an arch, which makes the stiffness of the specimen increase after buckling.

Figure 15 shows the load-stress relation at the point "A" under the applied load. Before buckling, stress is uniform compression and increases in a linear way. When reaching the buckling load, compression stresses are released till reaching zero when the direction of load becomes parallel to the cantilever end edge, stage (8) in Fig. 13. Finally, tension stresses are developed.

Changes in internal stresses of an intermediate section during analysis are shown in Fig. 16. Before buckling, stresses are almost uniform compression and only axial deformations are observed. After reaching the buckling load, although the applied load is constant ( $P \approx 7.8$  tf), bending moments generates and large deformation occurs because of the buckling



bending moments. This shows one of the strong points in our analysis that mechanical behavior of any point in the structure can be followed accurately even if large deformations occur.

## 4.2 Analysis of an RC Building Model Subjected to Series of Base Excitations

Recently, the size of scaled model specimens for structural tests tends to become larger and larger. A large scaled model test enables us to obtain data similar to real structures. However, since it requires large size testing facilities and large amount of research funds, it makes difficult to execute parametric tests. This section introduces the simulation results of a scaled RC building model (1/15) subjected to magnified base excitation. The test structure was an eleven-storied building model. A general view of the model and sections are shown in Fig. 17. For more details about the structure shape or applied load, refer to Refs. (15) and (16). A series of base excitations were applied to the structure in order from small to large amplitudes. The shape of these excitations is same, namely, their frequency characteristics are same while amplitudes are different, from 40 Gal to 800 Gal, as shown in Fig. 18. The excitation G800 was applied twice to the structure, with normal (G800-1) and doubled (G800-2) time scale, respectively. This makes the numerical analysis more complicated because cumulative damage to the structural elements affects the response.

The structure is modeled using 1,232 square-shaped elements. The comparison between the measured and simulated response of different floors is shown in detail in Ref. (9). The following factors are considered in the simulation using the AEM:

1. Stress-strain relation of concrete under cyclic loading<sup>3)</sup>.
2. Stress-strain relation of reinforcement under cyclic loading<sup>11)</sup>.
3. Additional bending moments because of load eccentricities at columns during tests.
4. Large deformation, separation and rigid body motion of structural members during failure<sup>13)</sup>.
5. Collision of structural members with each other and with the ground<sup>17)</sup>.

The natural periods and modes, shown in Fig. 19, could be calculated using eigen value analysis. Different mode shapes and natural periods could be obtained easily. This indicates that the analysis can be performed in frequency domain as well as in time domain.

Because of limitations of space, selected samples of the results are introduced in this paper. The calculated and measured responses of the roof in case of G600 and G800 are shown in Figs. 20 and 21, respectively. Although the structural behavior is highly nonlinear, with cracking, yield of reinforcement and crushing of concrete, excellent agreement between calculated and measured displacement responses could be obtained. Moreover, it is clear that the effects of cumulative damage during the applications of G40, G200 and G400 are considered automatically.

Most of experiments of RC structures have been performed till failure but before complete collapse, where geometrical changes are generally small. It is very difficult to extend the experiments to follow the collapse process of structures. Difficulty arises from the fact that capacities of shaking tables have been limited and even when the capacity is enough, it is not safe to perform such kind of experiments, especially for full-scaled structures. It may also result in damage of shaking table or surrounding area due to large collision forces.

The experiment was performed up to the G800-2 with doubled time scale, where the structure failed from the structural viewpoint, but it did not collapse. Therefore, numerical results of the same building subjected to a destructive excitation are also introduced. The amplitude of the base excitation of G800 is multiplied by 1.5 and its time scale is doubled. This destructive acceleration is applied to the same structure and the structural response during the process of failure including complete collapse is studied. As the collapse process is very complicated and it may not be represented accurately using two-dimensional model, relatively simple models for

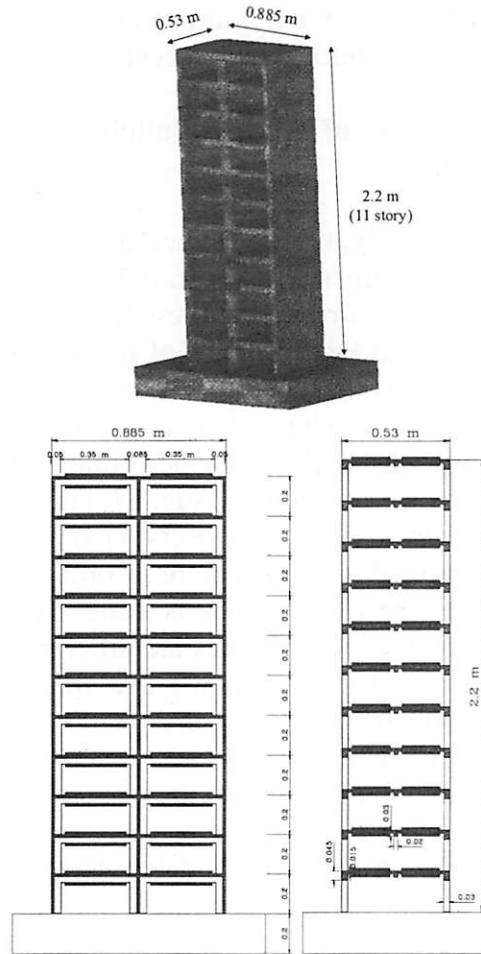


Figure 17: Shape, dimensions and loading of a small-scaled RC building model under lateral excitation

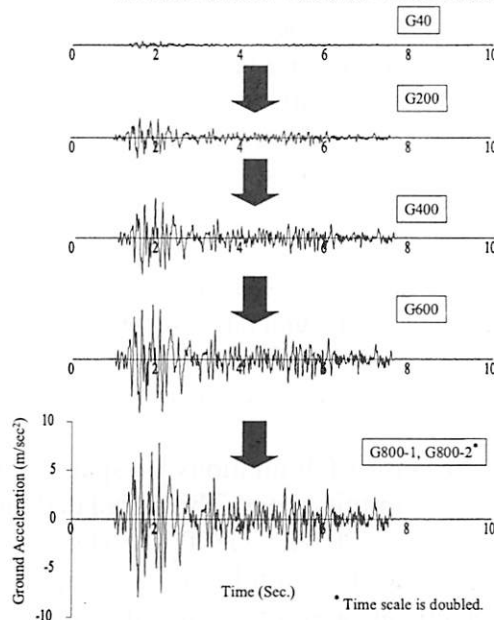


Figure 18: Input base accelerations, G40, G200, G400, G600, G800-1 and G800-2 used for shaking table experiments.

concrete crushing and reinforcement cut are adopted<sup>17)</sup>. The analysis is performed using time increment of 0.0025 and 0.0005 seconds before and after re-contact between elements occurs, respectively. The collapse history, shown in Fig. 22, can be summarized as follows:

1. Failure starts by excessive cracking, yield and cut of reinforcement at base floors.
2. Columns and beams of lower floors suffered complete damage while the upper floors suffered slight damage but it moves together in rigid body motion and rotates around the failed structural elements till they collide with the ground.

### 5. CONCLUSIONS

In the paper, the Applied Element Method for structural analysis is introduced. The main advantage of this method is that it is simple, accurate and applicable to wide range of problems. For the accuracy, it can be said that it has the same accuracy as the FEM where it can be used and better accuracy compared with the RBSM or EDEM. The formulations used are simpler than that of the FEM. The main advantages of the AEM are:

1. The formulations used are simple compared to the FEM.
2. All reinforcement details, like reinforcement bar location and concrete cover, can be considered easily and without any additional complications in the element shape or arrangement.
3. In case of RC structures, material models used are for plain concrete and reinforcement bars separately. This means that the adopted material

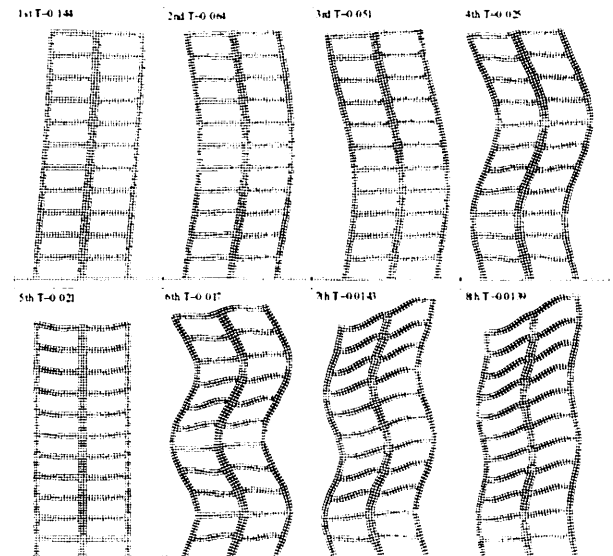


Figure 19: Eigen values and modes of the building model.

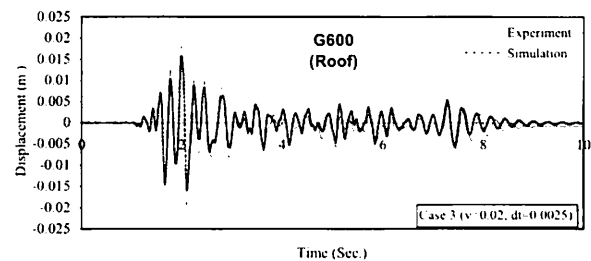


Figure 20: Displacement response at the roof for G60 (damping ratio=0.02, simulation time increment=0.0025)

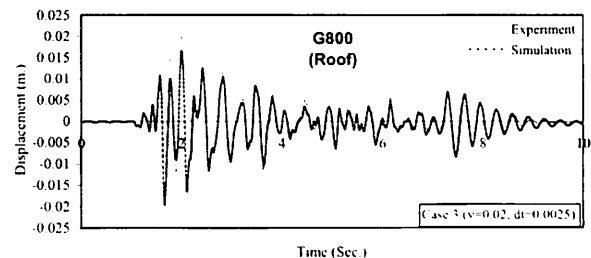


Figure 21: Displacement response at the roof for G800-1 (damping ratio=0.02, simulation time increment=0.0025)

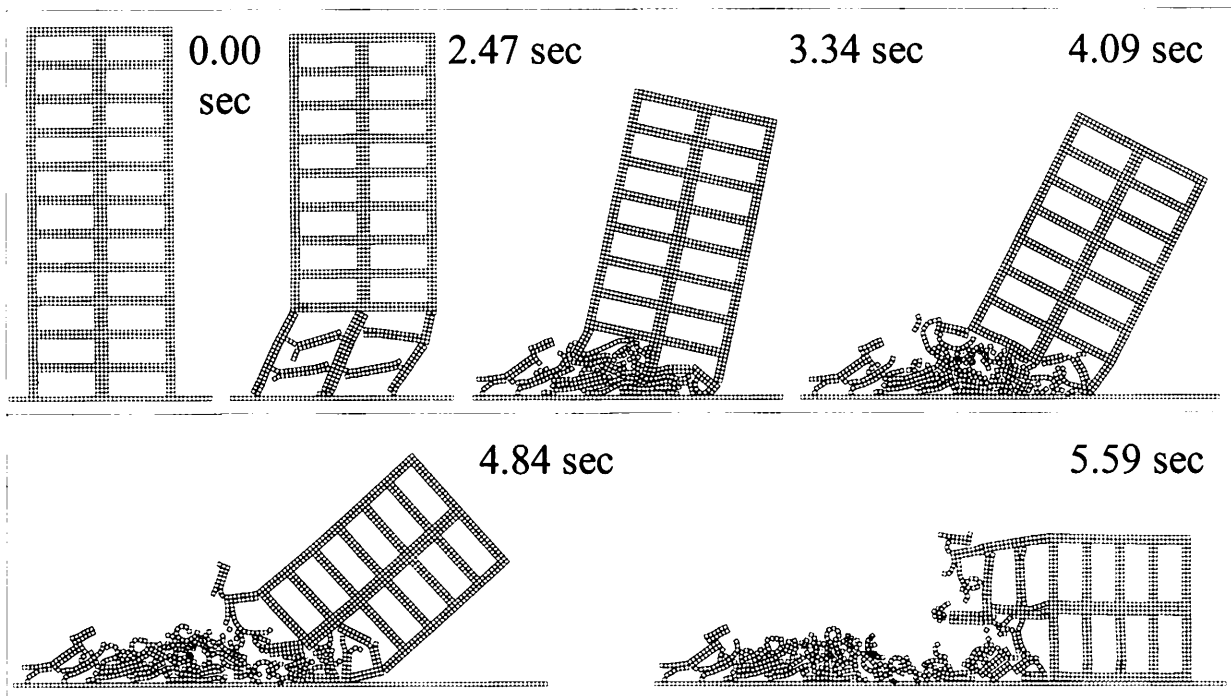


Figure 22: Simulation of collapse process (Amplitude: 1200 Gal, Time scale: double)  
 (In the experiment, this case could not be performed because of limitation of shaking table capacity.)

models are not affected by the reinforcement ratio. While in the Smeard Crack approach, material models are different and based on to the reinforcement ratio<sup>3)</sup>.

4. Internal stresses and strains of any point in the material, either reinforcement bars or concrete, can be followed easily.
5. The AEM has wide range of application. It can be applied to static and dynamic cases, monotonic and cyclic loading conditions. It can be applied for small and large deformation ranges.
6. Although the shape of adopted elements is square, it has almost no effect on the crack propagation direction, especially in monotonic loading condition. While in the RBSM and EDEM methods, the crack propagation is strongly affected by the element shapes and arrangement.
7. The AEM can be applied for studying the nonlinear dynamic behavior of structures. Effects of cracking, concrete crushing, yield of reinforcement can be considered.
8. The rigid body motion and collision of structural elements during collapse can be followed with reliable accuracy.
9. No previous knowledge about the collapse process is needed before the analysis.
10. For future study of detailed collapse mechanism of structures, additional effects like buckling of reinforcement bars and spalling of concrete cover, etc. are needed to be modeled which are not taken into account yet.
11. It is very difficult, or impossible, to follow complete collapse behavior using methods that assumes continuum material, like FEM and BEM,

where failure analysis is still restricted to cases where crack locations are known before the analysis.

12. The EDEM is one of the few models that can simulate such collapse behavior. The main advantages of the AEM compared to the EDEM are high accuracy and short CPU time. With the AEM, the time increment can be enlarged before collision starts while with the EDEM, the time increment is restricted to a certain small value, which is function of the material type and element size. It can not be enlarged even before collision starts. In the AEM, longer time increment can be used before collision and it makes the CPU time required shorter.

## REFERENCES

1. Architectural Institute of Japan: A report on damage during Miyagiken-Oki Earthquake of 1978, 1979 (in Japanese).
2. Nishimura A. et. al.: Statistical report on casualty of the Great Hanshin Earthquake, Advances in Legal Medicine 3, July 1997.
3. Okamura H. and Maekawa K.: Nonlinear analysis and constitutive models of reinforced concrete, Gihodo Co. Ltd., Tokyo, 1991.
4. Kawai T.: Recent developments of the Rigid Body and Spring Model (RBSM) in structural analysis, Seiken Seminar Text Book, Institute of Industrial Science, The University of Tokyo, pp. 226-237, 1986.
5. Meguro K. and Hakuno M.: Fracture analyses of structures by the modified distinct element method, Structural Eng./Earthquake Eng., Vol. 6. No. 2, 283s-294s., Japan Society of Civil Engineers, 1989.
6. Meguro K. and Hakuno M.: Application of the extended distinct element method for collapse simulation of a double-deck bridge, Structural Eng./Earthquake Eng., Vol. 10. No. 4, 175s-185s., Japan Society of Civil Engineers, 1994.
7. Kikuchi A., Kawai T. and Suzuki N.: The rigid bodies-spring models and their applications to three dimensional crack problems, Computers & Structures, Vol. 44, No. 1/2, pp. 469-480, 1992.
8. Ueda M. and Kambayashi A.: Size effect analysis using RBSM with Vornori elements, JCI (Japan Concrete Institute) International Workshop on Size Effect in Concrete Structures, pp. 199-210, 1993.
9. Tagel-Din H.: A new efficient method for nonlinear, large deformation and collapse analysis of structures, Ph.D. thesis, Civil Eng. Dept., The University of Tokyo, Sept. 1998.
10. Oscar A. and Lopes Batiz: Earthquake Resistance of Precast Reinforced Concrete Structures, Doctor thesis, The University of Tokyo, 1992.
11. Ristic D., Yamada Y., and Iemura H.: Stress-strain based modeling of hystertic structures under earthquake induced bending and varying axial loads, Research report, No. 86-ST-01, School of Civil Engineering, Kyoto University, March, 1986.
12. Meguro K. and Tagel-Din H.: Simulation of buckling and post-buckling behavior of structures using applied element method, Bulletin of Earthquake Resistant Structure Research Center, IIS, University of Tokyo, No. 32, pp. 125-135, 1999.

13. Meguro K. and Tagel-Din H.: A new simple and accurate technique for failure analysis of structures, , Bulletin of Earthquake Resistant Structure Research Center, IIS, University of Tokyo, No. 31, pp. 51-61, 1998.
14. Timoshenko S. and Gere J.: Theory of Elastic Stability, McGraw-Hill Inc., 1961.
15. Okada T., Kumazawa F., Horiuchi S., Yamamoto M., Fujioka A., Shinozaki K. and Nakano Y.: Shaking table tests of reinforced concrete small scale model structure, Bulletin of Earthquake Resistant Structure Research Center, IIS, University of Tokyo, No. 22, pp. 13-40, 1989.
16. Kumazawa F. and Okada T.: Shaking table tests of reinforced concrete small scale model structure (Part 2), Bulletin of Earthquake Resistant Structure, IIS, University of Tokyo, No. 25, pp. 25-37, 1992.
17. Tagel-Din H. and Meguro K.: Applied element simulation for collapse analysis of structures, Bulletin of Earthquake Resistant Structure Research Center, IIS, University of Tokyo, No. 32, pp. 113-123, 1999.



*Dr. Kimiro Meguro*



# **URBAN WARMING AND ITS CONTROL TECHNIQUES**

RYOZO OOKA

International Center for Urban Safety Engineering (ICUS/INCEDE),  
IIS, The University of Tokyo, Japan

## **1. URBAN DEVELOPMENT AND URBAN WARMING**

In recent years the population has been concentrated in urban areas due to economic development, generating megalopolises such as Tokyo throughout the world. A change in land coverage conditions and an increase in energy consumption due to the development of urbanization have caused a climatic phenomenon termed “urban climate,” which is peculiar to urban area. It is now widely recognized that this has caused various environmental problems such as urban warming, ozone concentration increases, contaminant detention, etc. The scale of this urban climate is said to be 10 ~ 100 km horizontally and 100 ~ 1,000 m vertically in a large city such as Tokyo. This is therefore a local phenomenon that cannot actually be captured through normal meteorological observation stations. However, though small in scale, the phenomenon itself is evident and has a great influence on actual urban living. This paper explains the generation mechanism of urban warming represented by a heat island, a methodology to control it, and an comprehensive evaluation method. Ground surface temperatures in summer in the Kanto area based on the artificial satellite data (NOAA-AVHRR) are shown in Fig. 1. It can be confirmed from these pictures that the urban area shows higher temperature than does its suburbs. Changes in the urbanization of Tokyo during the last 100 years are shown in Fig. 2; changes in temperature in Tokyo during the past 100 years are shown in Fig. 3. The radius of metropolitan Tokyo has increased from 5 km to 50 km in approximately 100 years, and the average urban temperature has risen by approximately 2°C. The warming of large urban area such as Tokyo due to urbanization is progressing several times faster than global warming.

## **2. FACTORS CAUSING URBAN WARMING**

The primary factors causing urban warming are considered to be as follows:

### **a. Increase in the amount of artificial heat release in urban areas**

Urban areas consume more energy than suburbs due to the requirements of creating a comfortable living environment as well as the mass transport of information/materials, and consumption levels have continued to increase. Particularly, the amount of public energy consumption for the control of the living environment has increased significantly in recent years, which has led to a vicious cycle of further urban warming. The amount of artificial waste

heat in three wards in the Metropolitan Tokyo reached approximately 700,000 Gcal/year· km<sup>2</sup> in 1986, which exceeds the income of solar heat radiation: approximately 650,000 Gcal/year· km<sup>2</sup>. The distribution of amount of artificial waste heat in the Tokyo area is shown in Fig. 4.

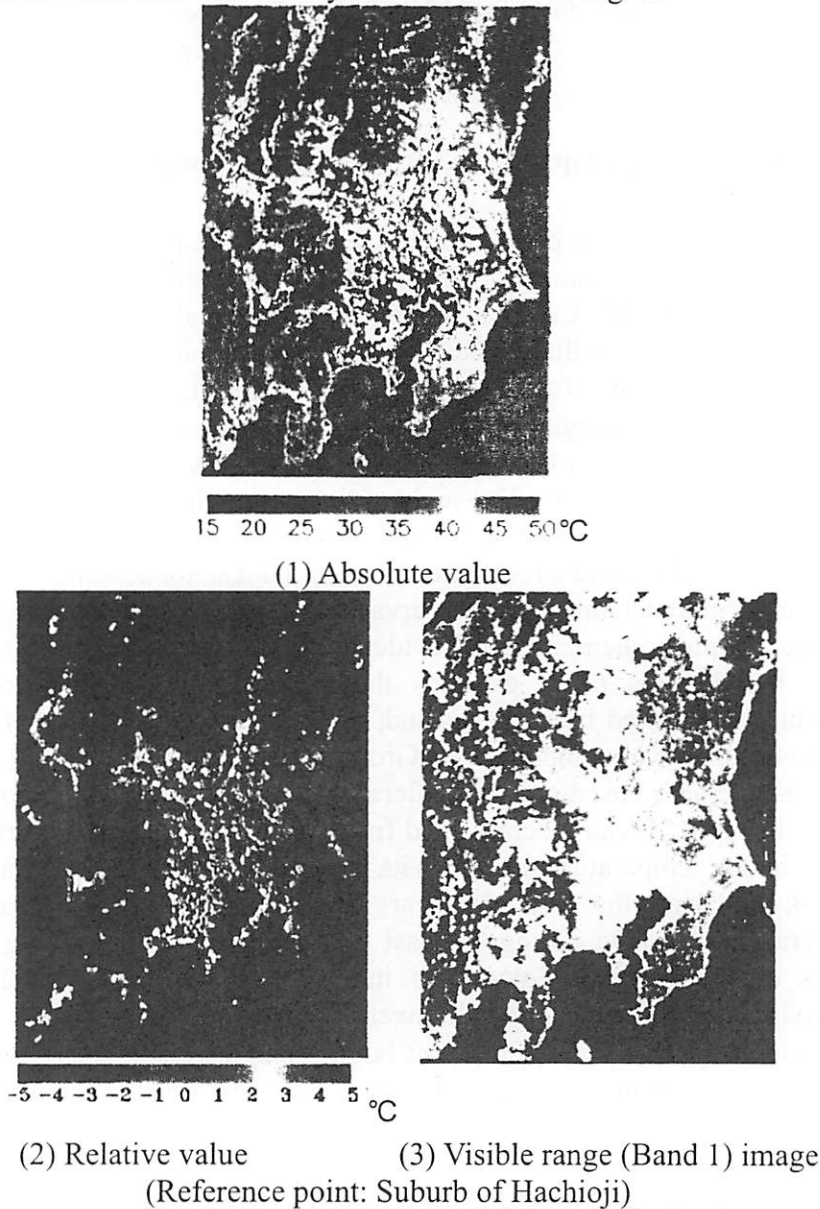


Figure 1: Ground surface temperatures in the Kanto area by NOAA-AVHRR [1] (13:20, July 24, 1995)

**b. Decrease in evaporation from the land surface due to decrease in permeable surfaces**

Permeable areas such as green space, marshland, rivers, ponds, etc., are covered by asphalt, concrete, etc., due to urbanization. This affects the latent heat by evaporation from the land surface, causing the surface temperature in urban area to rise higher than in the suburbs. Especially, the park area per city is very small in Japan, and this cannot be expected to fill the role of green space in relieving urban warming at present. Also, as shown by the example

of the Nogawa river, Tokyo, in Fig. 5, the rate of river flow through the urban area has decreased due to the spread of the drainage system in recent years. This reduction in the permeable area has caused the humidity in urban areas to drop. Changes in relative humidity in Tokyo and its surrounding area are shown in Fig. 6. This shows an outstanding decrease in humidity in Tokyo compared to other areas such as Tateno, Choshi, and Katsuura.

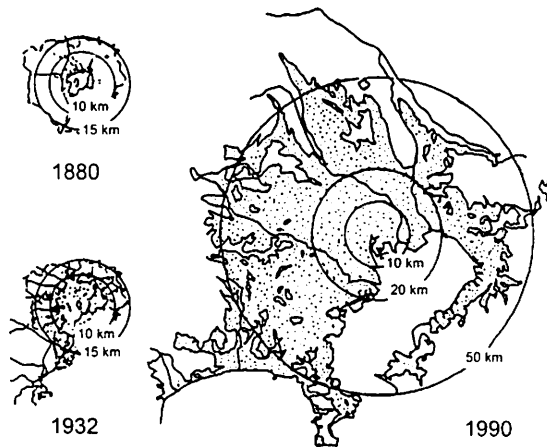


Figure 2: Changes in the urbanization of Tokyo [2]

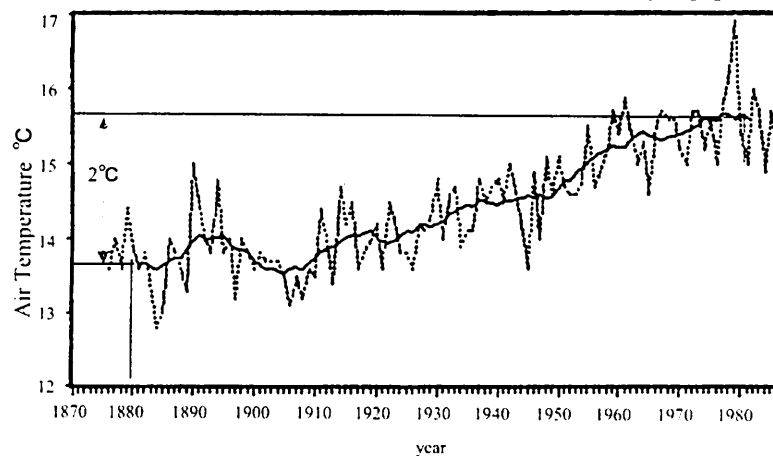


Figure 3: Changes in year-averaged temperature in Tokyo (at 1.5m height)

**c. Effects of heat storage through the heat capacity of urban structural materials**

In the metropolis, there are many structural materials with a large heat capacity, such as concrete and asphalt, slowly radiating at night, the heat that has been stored during the day. This large amount of stored heat in the urban structures raises the nighttime temperature, and becomes a factor in causing the summer “tropical nights”, the days of which lowest temperature is higher than 25°C. The number of tropical nights in Tokyo significantly rose from 2.6 in the 1920s to 13.6 in the 1980s.

**d. Decrease in heat exchange with the atmosphere due to urban structure**

The wind velocity in the urban area crowded with buildings becomes extremely low compared to that in the free atmosphere. Therefore, heat

exchange between the urban interior and the free atmosphere decreases, preventing the urban heat from escaping. Also, rows of high-rise buildings increase the urban surface area and inter-reflection among the surface of the buildings, practically contributing to an approximate 10% increase in the rate of solar radiation absorption in the urban area.

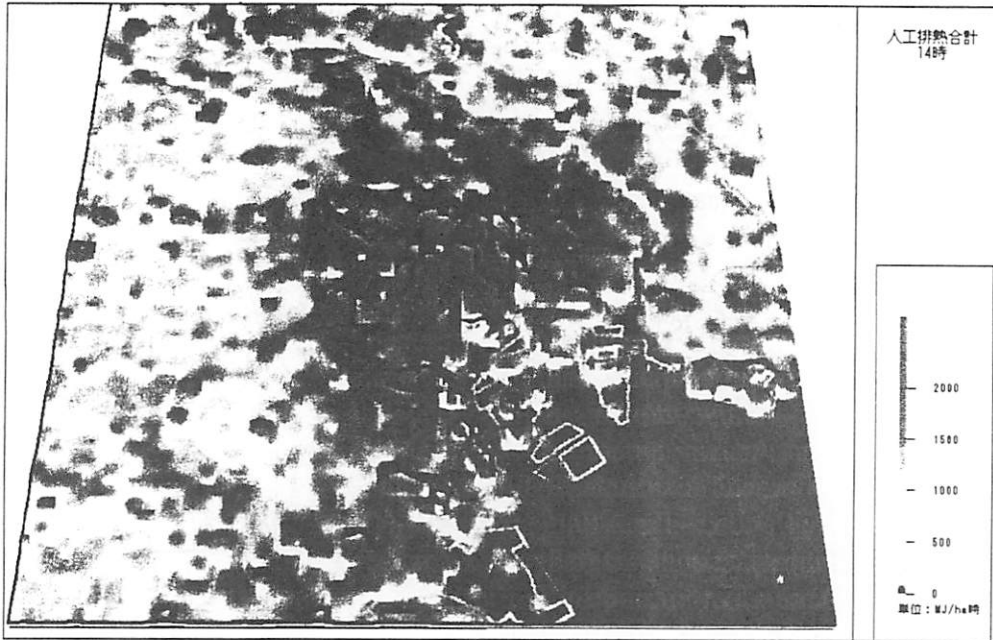


Figure 4: Distribution of amount of artificial heat release in Tokyo (at 14:00 in summer)

**e. The greenhouse effect due to fine dust and atmospheric contaminants**

Contaminants generated in the urban area are detained there or in the surrounding areas due to the structure of circulating current and boundary layers of the area. Table 1 shows the concentration differences of atmospheric contaminants between a large city and its suburbs as represented by a large industrial city in the United States and its suburbs (according to Landsberg) as well as Tokyo and its suburbs (according to Kawamura). These detained contaminants will increase the greenhouse effect in the city.

Table 1: Concentration differences of atmospheric contaminants between the large city and its suburbs [4]

Atmospheric contaminants	Large industrial city (Landsberg)	Tokyo (Kawamura)
Solidified cores	Increase of 15 times or more	
Extremely large dust particles	Increase of 10 times or more	Increase of 10 times or more
SO <sub>2</sub>	Increase of 5 times or more	Increase of 10 times or more
CO <sub>2</sub>	Increase of 10 times or more	
CO	Increase of 25 times or more	Increase of 50 times or more

**3. Influence of Urban Warming on Climatic Change**

A conceptual diagram of the urban climate associated with urban warming is shown in Fig. 7. Warmed air in the urban area rises through

buoyancy, is cooled in the upper air, and descends into the surrounding suburbs. Also, the air currents that have descended further converge in the metropolis, generating so-called urban circulating currents. An example of observation on convergent currents toward the metropolis from the suburbs is shown in Fig. 8.

These urban circulating currents detain contaminants generated in the city (the dust dome), often generating highly concentrated contamination in the suburbs surrounding the city. Fig. 9 shows an example of observations on highly concentrated contamination generated in the south of Saitama prefecture.

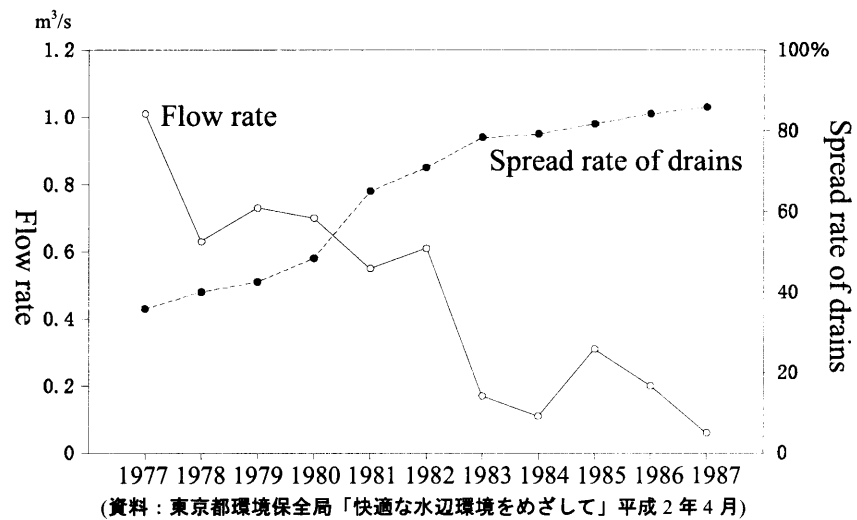


Figure 5: River flow rate and spread rate of drains (at the case of Nogawa-river) [3]

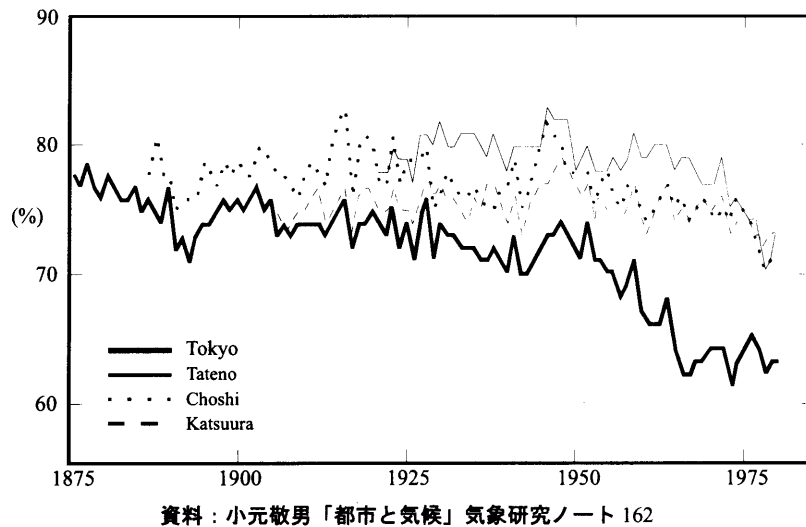


Figure 6: Changes in relative humidity in Tokyo and its surrounding area

#### 4. Various Measures to Control Urban Warming

If the concentration of the population and functions into large cities continues as it does at present, the deterioration of the urban environment will

likely become a serious problem. Various ideas of so-called environmentally symbiotic urban planning have been proposed to control urban warming, seeking to reduce the amount of artificial waste heat, appropriately arrange green spaces, rivers, etc., through the promotion of various energy-conservation measures or by decreasing the environmental load through the use of water permeable building materials, etc. Various representative control techniques will be introduced below in response to the aforementioned factors concerning urban warming.

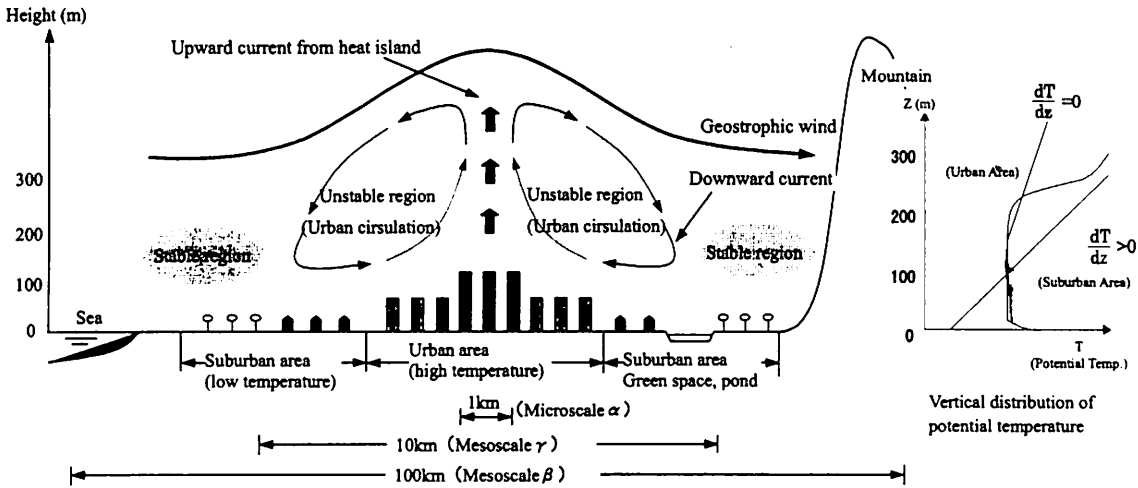


Figure 7: Conceptual diagram of urban climate

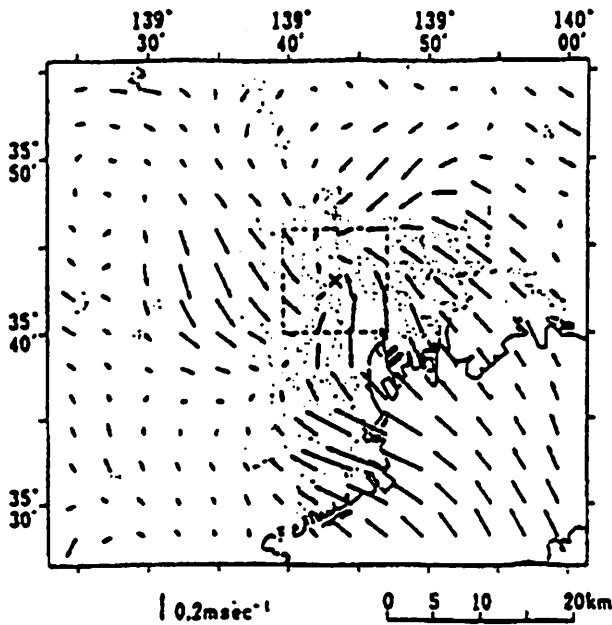


Figure 8: Convergent currents in the Tokyo metropolis [5]

**a. Control of the amount of artificial heat release in the urban area**

Measures to reduce the amount of energy consumption, such as by insulating buildings and developing highly energy-efficient products may be

listed as techniques concerning such factors. Also, from the viewpoint of improving the energy consumption system for the entire city, various energy consumption control measures may be listed, such as use of natural energy through naturally symbiotic buildings, hybrid environmental control techniques, etc., or the effective use of unused energy through efficient heat storage systems, or efficient use of energy through introduction of cogeneration systems. In addition, the reduction of industrial waste through improvements in the production process and the reuse of resources through recycling are expected to contribute to reducing the total amount of energy input.

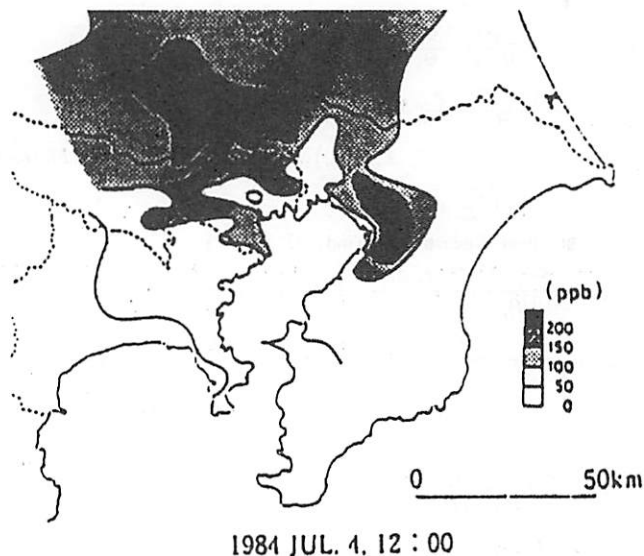


Figure 9: Highly concentrated contaminants detained in south Saitama [6]

#### b. Promotion of evaporation from land surfaces

This refers to seeking an increase in the water permeable surface area and helping to diffuse evaporative latent heat from urban areas through actively introducing green space, waterfront space, etc., and using water-retentive building materials, etc. It is important to increase green space in cities from the standpoint of adsorption of atmospheric contaminants as well as for improving landscapes.

#### c. Promotion of heat absorption by heat sinks

This refers to absorbing heat in the urban area by using heat sinks that have an enormous heat capacity such as the underground train system, sea and rivers. Also, technologies to reuse absorbed heat are being developed.

#### d. Promotion of heat exchange between the urban structures and the atmosphere

It is generally known that a heat island is not likely to be generated if the wind velocity is high in the synoptic field. It is said that a heat island will cease to exist even in a super megalopolis such as Tokyo if the wind velocity exceeds 12m/s. More active ways to exchange heat are being studied, such as

using the wind ventilation effect and appropriately arranging buildings. For example, the “Ventilation Paths” plan implemented in Stuttgart, Germany, may be listed as a representative case.

Table 2: Basic Equations of Mellor-Yamada model(level 2.5)

<p>① Momentum equation at horizontal direction</p> $\frac{DU}{Dt} = f(V - V_g) + g \frac{\bar{H} - z^*}{\bar{H}} \left( 1 - \frac{\langle \Theta_v \rangle}{\Theta_v} \right) \frac{\partial z_g}{\partial x} + \frac{\partial}{\partial x} \left( K_{xx} \frac{\partial U}{\partial x} \right) + \frac{\partial}{\partial y} \left( K_{xy} \frac{\partial U}{\partial y} \right) + \frac{\bar{H}}{H - z_g} \frac{\partial}{\partial z^*} (-\overline{uw}) \quad (1)$ $\frac{DV}{Dt} = -f(U - U_g) + g \frac{\bar{H} - z^*}{\bar{H}} \left( 1 - \frac{\langle \Theta_v \rangle}{\Theta_v} \right) \frac{\partial z_g}{\partial y} + \frac{\partial}{\partial x} \left( K_{xy} \frac{\partial V}{\partial x} \right) + \frac{\partial}{\partial y} \left( K_{yy} \frac{\partial V}{\partial y} \right) + \frac{\bar{H}}{H - z_g} \frac{\partial}{\partial z^*} (-\overline{vw}) \quad (2)$ <p>where <math>g</math> is gravity accelerate, <math>K_{xx}</math>, <math>K_{yy}</math> (<math>= K_{xy}</math>), <math>K_{xy}</math> are eddy viscosity for horizontal diffusion.</p> $\frac{D}{Dt} = \frac{\partial}{\partial t} + U \frac{\partial}{\partial x} + V \frac{\partial}{\partial y} + W^* \frac{\partial}{\partial z^*} \quad (3)$ <p>② Horizontal component of geostrophic wind <math>U_g(z^*)</math>, <math>V_g(z^*)</math></p> $fU_g(z^*) = fU_g(\bar{H}) \frac{\langle \Theta_v \rangle}{\langle \Theta_v(\bar{H}) \rangle} + g \frac{H - z_g}{\bar{H}} \int_{z^*}^H \frac{1}{\langle \Theta_v \rangle} \frac{\partial}{\partial y} \Delta \Theta_v dz' - \frac{g}{\bar{H}} \frac{\partial z_g}{\partial y} \int_{z^*}^H \frac{\Delta \Theta_v}{\langle \Theta_v \rangle} dz' \quad (4)$ $fV_g(z^*) = fV_g(\bar{H}) \frac{\langle \Theta_v \rangle}{\langle \Theta_v(\bar{H}) \rangle} - g \frac{H - z_g}{\bar{H}} \int_{z^*}^H \frac{1}{\langle \Theta_v \rangle} \frac{\partial}{\partial x} \Delta \Theta_v dz' + \frac{g}{\bar{H}} \frac{\partial z_g}{\partial x} \int_{z^*}^H \frac{\Delta \Theta_v}{\langle \Theta_v \rangle} dz' \quad (5)$ <p>where <math>\Delta \Theta_v = \Theta_v - \langle \Theta_v \rangle</math> and <math>\langle \rangle</math> means horizontal averaging operation</p> <p>③ Continuity equation</p> $\frac{\partial U}{\partial x} + \frac{\partial V}{\partial y} + \frac{\partial W^*}{\partial z^*} - \frac{1}{H - z_g} \left( U \frac{\partial z_g}{\partial x} + V \frac{\partial z_g}{\partial y} \right) = 0 \quad (6)$ <p>where <math>W^* = \frac{\bar{H}}{H - z_g} W + \frac{z^* - \bar{H}}{H - z_g} \left( U \frac{\partial z_g}{\partial x} + V \frac{\partial z_g}{\partial y} \right)</math> (7)</p> <p>④ Turbulence energy <math>q^2 / 2</math> equation</p> $\frac{D}{Dt} \left( \frac{q^2}{2} \right) = \frac{\partial}{\partial x} \left[ \frac{K_{xx}}{\sigma_q} \frac{\partial}{\partial x} \left( \frac{q^2}{2} \right) \right] + \frac{\partial}{\partial y} \left[ \frac{K_{yy}}{\sigma_q} \frac{\partial}{\partial y} \left( \frac{q^2}{2} \right) \right] + \left( \frac{\bar{H}}{H - z_g} \right)^2 \times \frac{\partial}{\partial z^*} \left[ q S_q \frac{\partial}{\partial z^*} \left( \frac{q^2}{2} \right) \right] - \frac{\bar{H}}{H - z_g} \left( \overline{uw} \frac{\partial U}{\partial z^*} + \overline{vw} \frac{\partial V}{\partial z^*} \right) + \beta_r g \overline{w \Theta_v} - \frac{q^3}{B_1 l} \quad (8)$ <p>where <math>q^2 = \overline{u^2} + \overline{v^2} + \overline{w^2}</math>, <math>S_q = 0.2</math>, <math>B_1 = 16.6</math>, <math>\sigma_q = 1.0</math>.</p> <p>⑤ Turbulence length scale equation</p> $\frac{D(q^2 l)}{Dt} = \frac{\partial}{\partial x} \left[ \frac{K_{xx}}{\sigma_l} \frac{\partial (q^2 l)}{\partial x} \right] + \frac{\partial}{\partial y} \left[ \frac{K_{yy}}{\sigma_l} \frac{\partial (q^2 l)}{\partial y} \right] + \left( \frac{\bar{H}}{H - z_g} \right)^2 \frac{\partial}{\partial z^*} \left[ q S_l \frac{\partial (q^2 l)}{\partial z^*} \right] - l F_1 \left[ \frac{\bar{H}}{H - z_g} \left( \overline{uw} \frac{\partial U}{\partial z^*} + \overline{vw} \frac{\partial V}{\partial z^*} \right) - \beta_r g \overline{w \Theta_v} \right] - \frac{q^3}{B_1} \left[ 1 + F_2 \left( \frac{l}{kz} \right)^2 \right] \quad (9)$ <p>where <math>S_l = 0.2</math>, <math>F_1 = 1.8</math>, <math>F_2 = 1.33</math>, <math>\sigma_l = 1.0</math>.</p> <p>⑥ Internal energy (virtual potential temperature <math>\Theta_v</math>) equation</p> $\frac{D \Delta \Theta_v}{Dt} = \frac{\partial}{\partial x} \left[ \frac{K_{xx}}{\sigma_{\Theta_v}} \frac{\partial \Delta \Theta_v}{\partial x} \right] + \frac{\partial}{\partial y} \left[ \frac{K_{yy}}{\sigma_{\Theta_v}} \frac{\partial \Delta \Theta_v}{\partial y} \right] + \frac{\bar{H}}{H - z_g} \left[ \frac{\partial}{\partial z^*} (-\overline{w \Theta_v}) + \frac{1}{\rho C_p} \frac{\partial R_N}{\partial z^*} - W^* \frac{\partial \langle \Theta_v \rangle}{\partial z^*} \right] \quad (10)$ <p>where <math>\sigma_{\Theta_v} = 1.0</math> and <math>R_N</math> are net radiation flux.</p> <p>⑦ Total water mixing ratio <math>Q_w</math> equation</p> $\frac{DQ_w}{Dt} = \frac{\partial}{\partial x} \left[ \frac{K_{xx}}{\sigma_{Q_w}} \frac{\partial Q_w}{\partial x} \right] + \frac{\partial}{\partial y} \left[ \frac{K_{yy}}{\sigma_{Q_w}} \frac{\partial Q_w}{\partial y} \right] + \frac{\bar{H}}{H - z_g} \frac{\partial}{\partial z^*} (-\overline{w q_w}) \quad (11)$ <p>where <math>\sigma_{Q_w} = 1.0</math>.</p> <p>⑧ Turbulence flux at vertical direction</p> $\overline{uw} = -l q \tilde{S}_M (\partial U / \partial z) \quad (12)$ $\overline{vw} = -l q \tilde{S}_M (\partial V / \partial z) \quad (13)$ $\overline{w \Theta_v} = -l q \tilde{S}_H (\partial \Theta_v / \partial z) \quad (14)$ $\overline{w q_w} = -l q \tilde{S}_H (\partial Q_w / \partial z) \quad (15)$ <p>where <math>\tilde{S}_M</math>, <math>\tilde{S}_H</math> are modification terms for buoyancy</p>
---



### **e. Control of atmospheric contaminants**

This refers to lowering the concentration of atmospheric contaminants in the urban area through effective ventilation by regulating contaminant discharge, developing adsorptive systems, arranging buildings, etc. Notably, it is necessary to take measures concerning urban structural aspects to rationalize the transportation system as well as develop technologies for automobiles from which most nitrogen oxides are discharged. These control techniques against urban warming are currently being researched in their respective areas; however, it is often difficult to correctly evaluate their effects when an individual measure is taken to reduce the influence on the environment because there are so many factors that are intricately involved in the actual urban environment. It is hoped to establish a total environmental assessment technique coupled with each factor based on the numerical analysis method, which has recently seen remarkable developments.

## **5. ESTIMATION OF URBAN WARMING USING A NUMERICAL CLIMATE MODEL**

### **a. Numerical climate model for total environmental assessment**

Viewed from the perspective of a comprehensive environmental assessment technique, it is expected that an environmental estimation technique based on a numerical climate model will be a powerful tool. A model based on static equilibrium, developed in the field of meteorology, is often used as a local weather model for this type of simulation. This local weather model was developed to estimate local winds such as land and sea breeze and local temperature distribution, which is used to analyze heat transfer by sensible heat, latent heat, and radiation through solving the moisture transport equation and radiative transfer equation rather than the motion equation and potential temperature transport equation. The local weather model developed by Mellor and Yamada [7] is representative. Basic equations for this model are shown in Table 2 (Mellor-Yamada model level 2.5). The authors developed a new numerical weather model based on the Mellor-Yamada model, verified its accuracy through comparison with observational data (Fig. 10), and used it to clarify the mechanism of urban warming.

### **b. Influence of land use and artificial waste heat on urban warming - Analysis of climatic changes in Tokyo from the Edo era to the present**

Fig. 11 shows an example of the analysis results on climatic changes in Tokyo from the Edo era (Tempo period, 1830–44) to the present. This analysis covered an area of 480km x 400km horizontally and 5km vertically, centered around Tokyo. Here, conditions of land surface use, distribution of waste heat amount, etc., were integrated into the computation through land surface boundary conditions. Fig. 11 shows a comparison of land surface temperature distribution at 3 pm in early August. The analysis covering present Tokyo reflects the land coverage, artificial waste heat, etc., associated

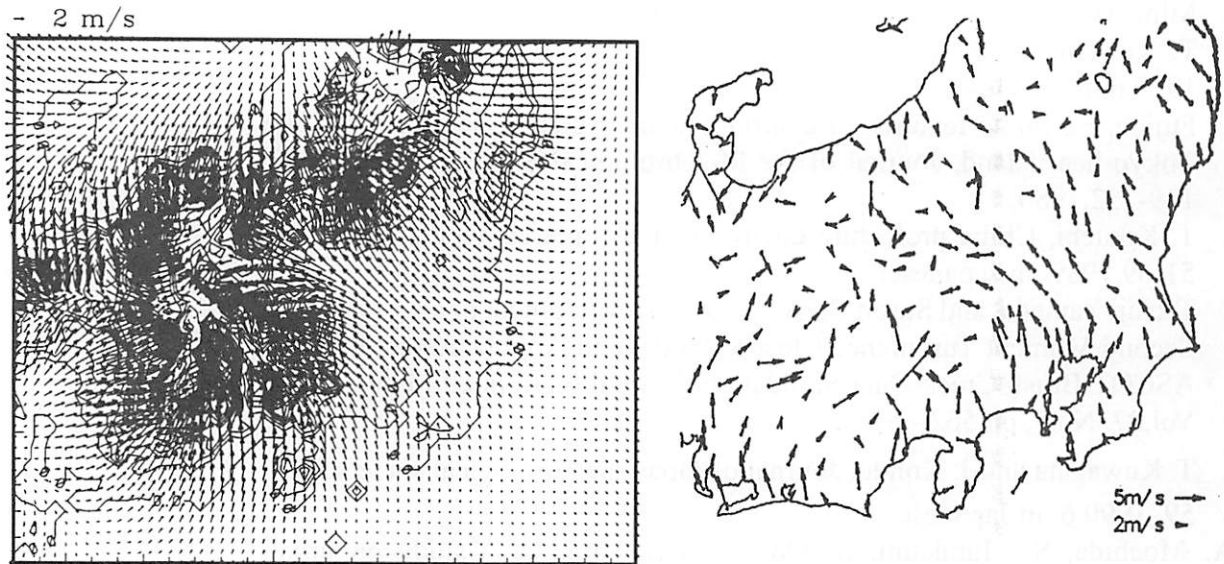
with present land usage, allowing the largest value (approximately 34°C) to appear in the metropolis (Fig. 11 (2)). This estimation result roughly coincides with existing actual measurement results. On the other hand, the largest value was approximately 30°C in the case of the Edo era in Fig. 11 (1); therefore, the land surface temperature in the present metropolis has risen approximately 4°C compared to that in the Edo era. The temperature rise at the elevation of 10m was approximately 1°C, and these estimation results corresponded well with the temperature rise (2°C) during the 100 years of observation (El. approximately 1.5m above ground) (Figure 3), reproducing the urban warming associated with urbanization. This temperature rise is due to the decrease in the amount of generated moisture, which is associated with the decrease in the green space area and an increase in the amount of artificial waste heat during recent years. Also, as a result of comparing the wind velocities in the upper air, though not shown here, the wind velocity in the metropolis when sea breezes were generated was higher in the present condition than that in the Edo era. This is interpreted as a result of the increase in the temperature difference between the land and sea surfaces, the driving force of sea breeze, due to the general rise in the land surface temperature in present conditions.

### **c. Future problems concerning the total environmental assessment technique**

As described above, these numerical climate models were capable of accurately expressing the influence of characteristics such as land form, etc., on a scale from several 10 km to several 100 km on meteorological phenomena, and achieved results in their application to analyzing phenomena, heat, and contaminant transfer models, etc. However, in order to use them for more sophisticated analyses concerning phenomena on an urban weather scale, it will be necessary to resolve such problems as follows:

1. Errors due to the hydro-static equilibrium assumption will be problematic if a weather structure on a small scale corresponding to cities is to be expressed accurately. Therefore, if the structure remains as it is, its horizontal grid size will be limited to 2 km.
2. Very simplified canopy models have been used until now, such as treating the urban structure as “roughness” while complicated wind, sensible heat, latent heat transfer and radiation processes are not specifically covered.
3. There is no data or sub models to accurately understand land surface boundary conditions, such as the amount of evaporation.

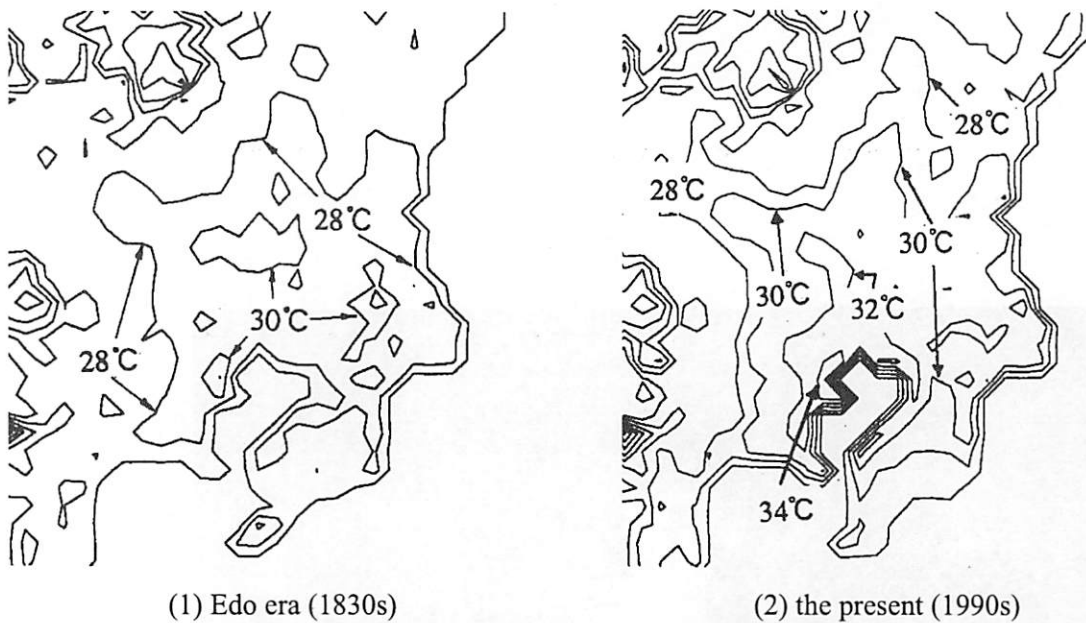
These limitations are expected to be resolved through preparing comprehensive platform integrating various models that cover the range on smaller scale.



(1) Numerical analysis (early August)

(2) Observation result[9]  
(average of the 50 days in the summer, 1985)

Figure 10: Comparison of numerical analysis and observation results  
(average wind velocity vectors at 100m height at 3:00 pm)



(1) Edo era (1830s)

(2) the present (1990s)

Figure 11: Analysis of climatic changes in Tokyo from the Edo era to the present [10]  
(surface temperatures at 3 pm, early August)

## REFERENCES

1. Environmental Assessment Dept. National Institute for Resources and Environment. Development of assessment for countermeasure for urban warming, Research report 19-1, 1997.3. in Japanese.
2. T. Ojima, Changing Tokyo Metropolitan Area and its Heat Island Model, Energy and Buildings, 15, 191-203, 1991.

3. Ministry of Environment 1990.12, in Japanese
4. T. Kawamura ed. Atmospheric science 3, University of Tokyo press., 1979.6 in Japanese
5. Fujibe, F., Some features of a surface wind system associated with the Tokyo heat island, Journal of the Meteorological Society of Japan, 58, 149-152,1980.
6. T. Kikuchi, Chiba prefecture environmental research center report, 21, 51-69,1989. in Japanese.
7. Tetsuji Yamada. and Susan Bunker., 1988, Development of a Nested Grid, Second Moment Turbulence Closure Model and Application to the 1982 ASCOT Brush Creek Data Simulation, Journal of Applied Meteorology, Vol.27, No.5, pp 562 - 578.
8. T. Kuwagata and J. Kondo, Journal of Japan meteorological society 55 ~ 59, 1990.6. in Japanese
- A. Mochida, S. Murakami, R. Ooka and S. Kim, CFD study on urban climate in Tokyo, 10th international conference on wind engineering, Copenhagen, Denmark, 1999.



*Dr. Ryoza Ooka*

# **THE CHANGING ROLE OF CIVIL ENGINEERS IN URBAN SAFETY**

WORSAK KANOK-NUKULCHAI

School of Civil Engineering, Asian Institute of Technology,  
Thailand

## **1. INTRODUCTION**

*When a doctor makes a mistake, he kills one; when an engineer makes a mistake, he kills many.* This has become a well-known quote in Thailand after the tragic collapse of Royal Plaza Hotel in 1993, which killed 137 unsuspecting occupants.

The civil engineering profession has recently been a subject of critical debate. Most deliberations call for a review of current engineers' roles in society at the level of individual as well as at the professional level. Discussions also point to a re-evaluation of the profession from the perspective of the country (national scope) as well as globally. One of the major concerns of the entire engineering community is the ensuing negative image of engineers, brought about mainly by the undesired impacts of engineering products that affect not only the lives of people but also the environment and natural resources.

## **2. THREE BUILDING DISASTERS IN THAILAND**

In Thailand, three building catastrophes that caused scores of deaths remain vivid in the memories of people.

On 10 May 1993, the four-storey Kader doll factory, Fig. 1, an unprotected steel building, collapsed just after 20 minutes of fire, killing 188 and injuring 469 workers. The author served as member of an official investigation panel set up by the Government. Among the many recommendations approved by the Government, the panel was able to facilitate the imposition of a regulation that required all steel buildings to be protected by a 3-hour fire rating insulation. In addition, the new policy imposed the hiring of safety officers in factories. It took such a long time to implement the first policy that another fire disaster occurred 4 years later, not benefiting from the new regulation.

On 13 August 1993, the Royal Plaza, Fig. 2, a 6-storey hotel complex in the northeastern province of Thailand collapsed with little warning, killing 137 and injuring 227. The investigation committee chaired by the author found that three additional stories were constructed without permit and without strengthening the structure. Most columns on the ground floor carried a load near their strength limit for almost 6 years before one of them

failed due to a long-term creep. The failure of one column caused the progressive collapse of all the other columns within a very short time, leaving little time for occupants to escape. While a new regulation was put in place requiring an independent third-party check for all public buildings, the engineer ended up in jail.

Then, in the morning of 11 July 1997, the coffee shop of Royal Jomtien Resort Hotel, Fig. 3, in the seaside resort city of Pattaya caught fire.



Figure 1: Fire in naked steel toy factory killing 188 in 1993.

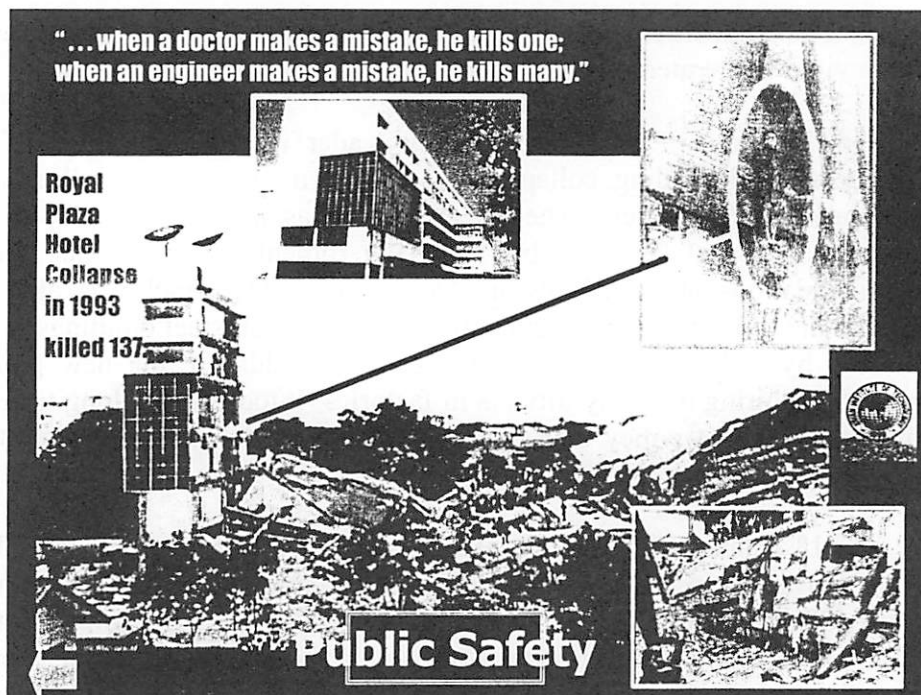
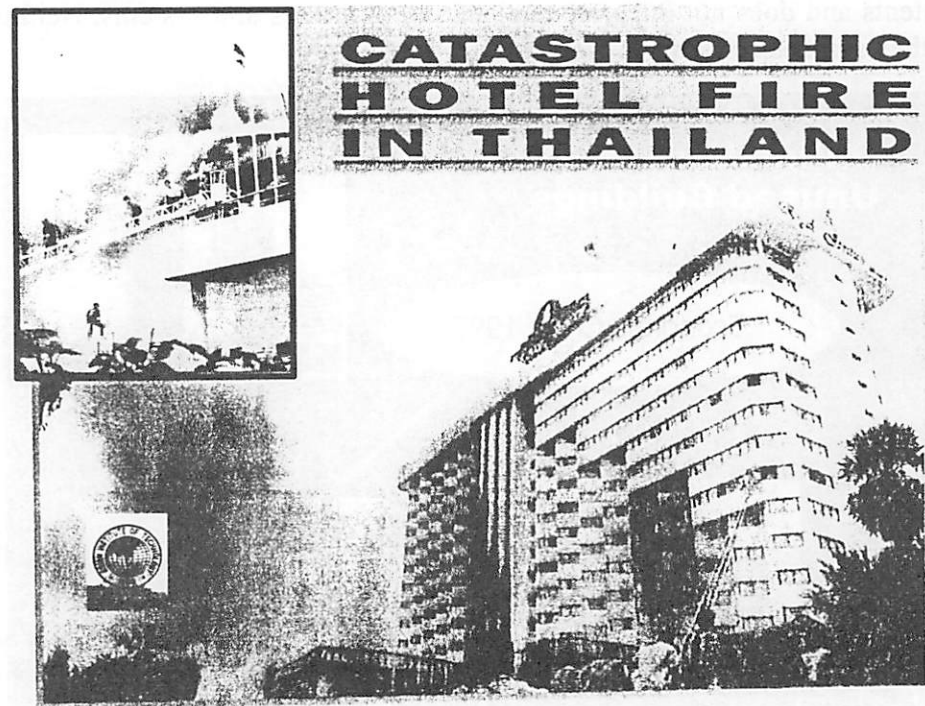


Figure 2: Sudden collapse of overloaded hotel killing 137 in 1993



Despite the presence of staff and fire mitigating utilities, the fire engulfed the entire building. What aggravated casualties was that to prevent burglary, the fire stair was kept locked causing 93 deaths. The disaster was reported as world's 'deadliest' hotel fires since 1971 when a hotel fire in Korea killed 166. The panel, chaired by the author, found that the hotel was well-equipped with sprinkles and fire equipment but they were not in proper condition. Its recommendations led to a number of new regulations including the requirement for all public buildings to be operated under a fixed-term permit renewable only upon certification of all fire equipment by registered engineers.



*Figure 3: Hotel fire in Pattaya killing 93 in 1997*

### 3. LESSONS

Regardless of what triggered these incidents, the root cause of these catastrophes points to the inherent deficiency of engineers in realizing their role in preventing public hazards emanating from their 'engineering outputs'. If this devastating trend is allowed to continue, engineers will be transformed from being leaders to merely followers, from being enablers to merely being tools, and eventually to becoming like cheap commodities in the world market.

### 4. PROPER ROLE OF CIVIL ENGINEERS

Aside from public safety, civil engineers must understand the social and environmental impacts of their products. During the period of economic

bubble, many tall buildings were constructed in Bangkok by investors in hope of making quick profits. Their demands were immediately responded to by engineers who were happy serving as merely tools to investors. Some engineers were even glad that their role was confined to the technical side of projects. After the crisis, a lot of these engineering products, Fig. 4, were left either unfinished or unused. No doubt, the public had to carry the tap, as corporate debt was transformed into public debt.

This undesirable role is rooted from an engineering education that shapes engineers through outdated engineering curricula and teaching methods. The traditional engineering curriculum is limited to technical contents and does not integrate engineering processes and systems. Neither do they synthesize technical and worldly domains.

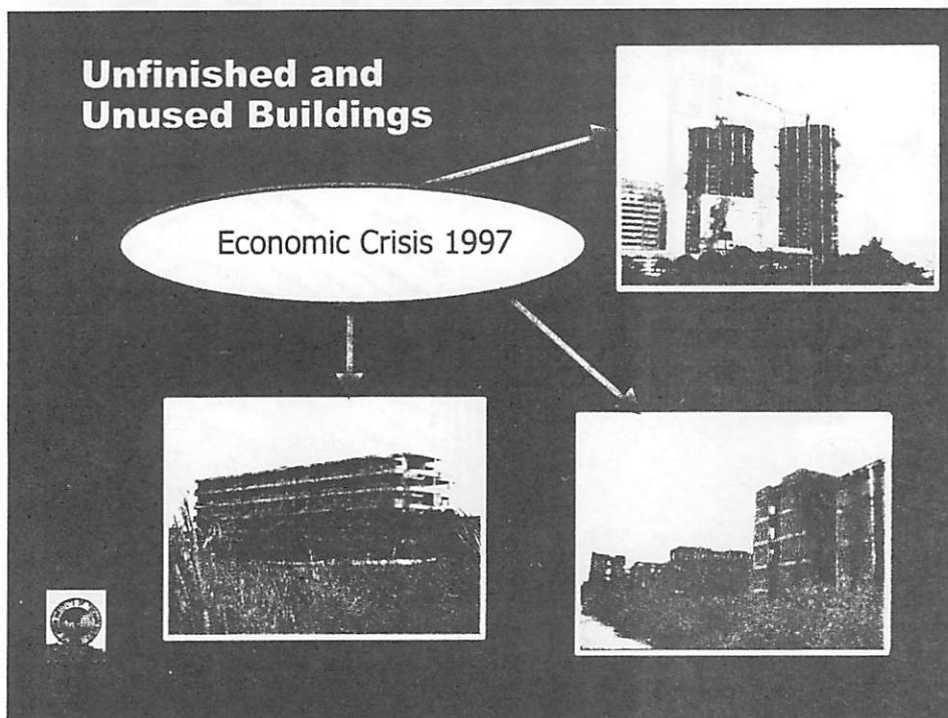


Figure 4: Large number of unfinished and unused tall building after 1997 economic crisis

## 5. RETHINKING OF CIVIL ENGINEERING EDUCATION

There's so much literature calling for changes in engineering education that range from adaptation to radical phases. This paper calls for a systems-related approach that results from a broader, more reconciling view by first identifying major interactions and hierarchies within engineering itself and between the engineering system and various non-engineering systems related to natural resources, environment, ecology and society. These non-engineering systems represent the different views of various actors that are affected directly or indirectly by engineering activities. Presented in this way, the fundamental nature of the problem can be easily perceived and explained. As shown in Fig. 5, the green solution of



engineering projects must consider environmental and social factors in the inception of the projects.

The traditional engineering curriculum is rigid in identifiable division hence, engineers have become rigid in their outlook. Their capability to adapt to rapidly changing working conditions have stagnated. The context of change is critically reviewed together with many different views of engineering educators. Curriculum differentiation should be made from the undergraduate to graduate and life-long education, and also from a narrow and specific to broader and more balanced structure that accommodates current and future market differentiation.

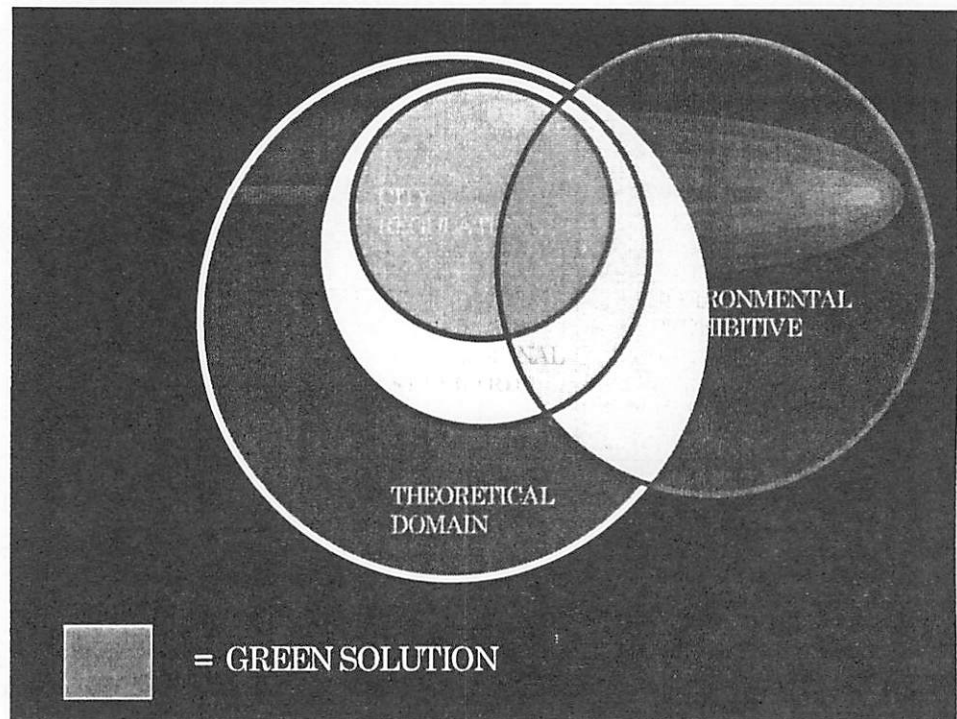


Figure 5: Green solution for engineering projects

## 6. CONCLUSIONS

To accomplish the above redefinition, an educational institute must affirm the constituents it serves, assess its activities, identify its comparative advantages, and develop an institution-specific vision. The new breed of civil engineers must recognize that they operate in a world where their accomplishments may be limited by societal considerations more than by technical capabilities; hence, they must understand the social, economic, and political contexts of engineering practice. Modern civil engineering curriculum must combine the elements of traditional technology-based engineering education with a strong emphasis on broader skills such as written and oral communication, management, economics and international relations. This aims to prepare a new generation of civil engineers conscious of their roles in public safety through technological decision-making and policy-setting.

Finally, the issue of professional ethics must be strongly addressed at all times. Whether engineers are conducting engineering research, managing a company, or building bridges and office buildings, their decisions affect the lives and property of the greater community. Civil engineers must therefore be sensitive to and understand the importance of securing public trust.



***Prof. Worsak Kanok-Nukulchai***

# **APPLICATION OF NON-DESTRUCTIVE INSPECTION TO CONCRETE STRUCTURES**

TAKETO UOMOTO  
International Center for Urban Safety Engineering (ICUS/INCEDE), IIS,  
The University of Tokyo, Japan

## **1. INTRODUCTION**

A large amount of concrete structures have been made in Japan since 1950's. Especially, just before 1964, when Olympic game was held in Tokyo, not only the facilities for the Olympic games but also traffic facilities such as "Shinkansen" (rapid train railways), "Shutokousoku-doro" (metropolitan express way), and "Toumei kousoku-doro"(high way connecting Tokyo and Nagoya) had been made. Many projects have been proposed and numerous facilities have been constructed since then, using concrete. Recently, three huge bridges connecting Honshu island and Shikoku island (Honshu-Shikoku Renraku-kyo) have been made and people can travel to 4 main islands (Hokkaidou, Honshu, Shikoku and Kyusyu) by land.

Although there are still many structures to be made, one of the most important works to be done by the civil engineers in Japan today is to maintain these structures. Such as Shinkansen and Shutokousoku-doro have been in use for more than 35 years and without these important facilities, the economy of Japan cannot be maintained.

Recently, spalling of concrete from concrete structures, such as bridges, tunnels, etc., has become a big problem in the field of mass media. Although the spalling of concrete may not be a big problem considering the load carrying capacity of the structure, they may cause traffic accident when cars or trains run underneath at a high speed, such as in the case of Shinkansen, which runs at the speed above 210km/hr. In 1999, a block of concrete hit Shinkansen in Fukuoka tunnel, and the top of several cars were damaged partly. The ministry of transportation and port and harbor organized a special committee to investigate the causes, and concluded that a part of the concrete lining spalled off due to insufficient consolidation at the time of construction and formation of inner cracks from the early age. Since then, many engineers and researchers brought a keen interest on non-destructive inspection (NDI) of existing structures.

## **2. METHODS FOR INSPECTION AND EVALUATION OF CONCRETE STRUCTURES IN GENERAL**

The maintenance of concrete structures are done by the owners of the structures. In case of public structures, the ministries, etc. maintain the structure as soon as they are completed. For the time being, the methods for

the maintenance differ according to the owners of the structures. Although there are some differences, the main concept of the maintenance can be summarized as in Figure 1.

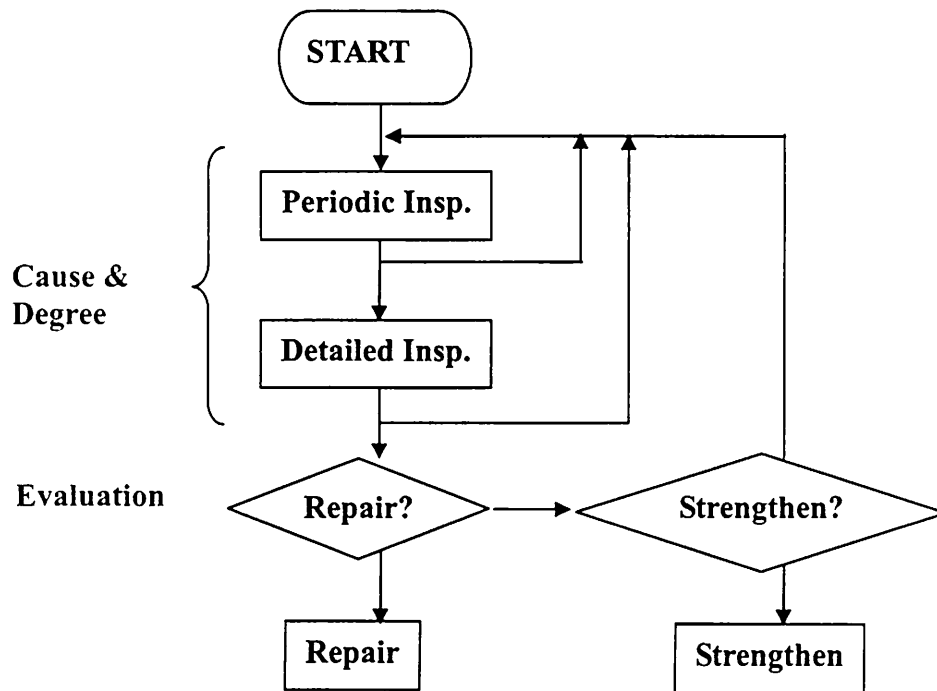


Figure 1: Flow chart for maintenance of concrete structures

## 2.1 Periodic inspection

Periodic inspection is essential in most cases. The inspectors inspect the structures visually, sometimes with the help of binoculars, once a year or once in several years according to the importance and the time after the structure is completed. In some cases, sonic inspection is carried out along with hammers. The inspectors are mostly trained engineers with experiences.

The periodic inspection covers not only the degree of deterioration but also the estimated main cause of the deterioration. For example, when a crack was found at the corner of openings and increased, the inspector may estimate the main cause as drying shrinkage with restraint. As shown in Table 1, in most cases, the appearance and crack formation may offer good data for the inspector. In our laboratory, we developed a system using handy type computers estimating the possible causes and degree of deterioration [1]. The system is composed of sample photographs and questionnaire to be answered by the inspectors by looking at the inspecting concrete structures, and the answers are stocked as individual data to be transported to the main computer from any place within Japan. This system runs with expert system eliminating the personal errors of the inspectors.

In some cases, visual inspection is also used to decide whether further inspection is needed or not. In Tables 1 and 2, an example of the actual visual

evaluation making criteria is briefly shown. From these evaluations, when the structure is ranked equal or above 2, careful inspection or detailed inspection of the structure is performed. According to the table, for the sake of simplicity, the items to be inspected are limited to cracks, stains and spallings.

*Table 1: Evaluation of deterioration degree by periodic inspection (example) [2]*

Degree of deterioration	Steel bar corrosion	Cracks	Spalling
0	none	none	none
1	Some stains on concrete surface	partial cracks	none
2	Stains are observed Partially	Some cracks	Partial rise at surface
3	Fair amount of Stains observed	Fair amount of cracks (width: Several mm)	Partial spalling observed
4	Fair amount of Rusts observed	Large amount of cracks (width: several mm)	Fair amount of rise and spalling
5	Large amount of Rusts observed		Large amount of rise and spalling

*Table 2: Evaluation for detailed inspection and need for repair (example) [2]*

Deterioration degree	Detailed inspection	Need of repair
0	no	no
1	no	no
2	yes	no (may need)
3	yes	yes
4	yes	yes
5	yes	yes(may strengthen)

## 2.2 Detailed inspection

The detailed inspection is done when the estimated degree of deterioration exceeds certain limit, or when some new phenomenon is found during the periodic inspection. The inspection is done normally by using non-destructive tests or taking core samples out from the inspected structure. The purpose of the inspection is to decide the cause of the deterioration and also to evaluate whether repair and/or strengthening is needed or not. In Table 3, the available non-destructive inspection methods being used are listed with some comments of the individual methods [4].

In case of large concrete structures, such as bridges, tunnels, dams, buildings, etc., the structures are too large to be inspected in details. To overcome the problem, the following methods are being used. 1) Overall inspection techniques, such as using digital still camera, thermography, radar, sonic and laser technique are often used to sweep the whole area to be inspected and find out the distribution of defects within the structure. Then, 2) other techniques, such as X-ray, ultra-sonic, natural potential, acoustic emission, etc. can be applied to get more detailed information.

Some movable inspection cars and trains have been developed for the overall inspection 1). In case of tunnel linings, an inspection train mounting both heating facility and thermograph has been developed to obtain the crack distribution and spalling portions for the subways. To inspect the voids at the back of tunnel linings or pavements, radar mounted cars have been developed for railways, waterways and highways. To digitize the surface cracks of reinforced concrete slabs, laser mounted car has been developed by the Technology Center of Metropolitan Expressway. These techniques are important for obtaining inspected data without any personal errors and can be used to check whether the deterioration advanced since the previous inspection.

For detailed inspection, many new non-destructive inspection techniques have been developed. The details of the techniques are explained in the next chapter.

### **3. NON-DESTRUCTIVE INSPECTION METHODS**

As shown in Table 3, many NDI methods have been applied to inspect concrete structures. Brief explanations are given in the followings [3,4].

#### **3.1 Compressive strength of concrete**

For most of the civil engineers, compressive strength of concrete is the most important item to be inspected. The most popular methods being used are to use rebound hammer or to measure the ultrasonic velocity of concrete. In case of rebound hammer, the strength is estimated from the surface hardness of concrete as shown in Figure 1. One of the problems of this method is that the hardness of concrete may vary according to the location of the aggregates at the surface. To deal with the problem, many points are tested at the surface. As shown in Figure 2, Ultra-sonic velocity measurement is used to estimate the strength from the elastic modulus of concrete; velocity is a function of elastic modulus and Poisson's ratio and there is a good correlation between strength and elastic modulus. When cracks or deterioration exist within concrete and different material is used, the estimated strength may not be accurate.

Recently, due to the accuracy of above-mentioned methods, pull out test method, break off test methods, etc. have been developed and used. As shown in Figure 3, these method measures the tensile strength or shear strength of concrete at the surface. Compared to the methods using rebound hammer and ultra-sonic, these methods measures the strength directly and have better correlation with compressive strength of concrete. The only problem is that they are not non-destructive but partially destructive.

Table 3: Application of NDI for existing concrete structures [4]

Time	Items	Measurement	Methods	Comments
Just after construction	Dimension	Cross sectional dimension	Measure, Transit, Laser	When the structure is in the open air
			Ultra-sonic, Impact echo, Radar	When a part of the structure is embedded
	Arrangement of steel reinforcement	Concrete cover	Radar, Electro-magnetic, X-ray	Surface bars only
		Bar spacing	Radar, Electro-magnetic, X-ray	Surface bars only
		Bar diameter	Electro-magnetic method	Surface bars only
Structure	Overall stiffness	Oscillation test	Amplitude, frequency	
After several years of usage	Appearance	Deterioration	Visual inspection, Photograph	Stain, cracks,
		Defects (Surface)	Digital still camera, Thermograph	Including honeycomb, cold joints
		Defects (Inside)	Sonic, Thermograph, Radar U-sonic, X-ray, Impact echo	VOIDS inside and at the back of the structure
	Stress & Strain	Deformation(Macro)	Measure, Transit, Laser	
		Deformation(Micro)	Dial gauge, Strain gauge	
		Vibration	Acceleration Sensor, LVDT Laser deformation measurement	
		Stress	Mold gauge, Optical sensor	
	Strength & Stiffness	Concrete strength	Core sample test Rebound hammer, Pull-out test	General method Problem of accuracy
		Modulus of Elasticity	Core sample test Ultra-sonic velocity	
	Cracks & Spalling	Distribution	Digital still camera, Thermograph	
		Crack width	Digital still camera, Thermograph	Direct measurement possible
		Crack depth	Ultra Sonic	Effect of bars
		Cracking	Acoustic Emission	Continuous measurement required
	Diffusion Depth	Carbonation	Core sample test	Analysis by core samples
		Chlorides	Core sample test	
		Acids	Core sample test	
		Other substances	Multi-spectrum method	Limited to concrete surface
	Permeability	Permeability	On-site permeability test	
	Steel Corrosion	Location	Natural potential	Location at that time
		Corrosion degree	Natural potential, Electric current analysis	periodic measurement required

Note: indicates application of NDI.

### 3.2 Appearance and surface deterioration of concrete structures

When inspection of existing concrete is performed, the most essential method is to inspect the structure visually. If the inspector is well trained, visual inspection is the most simple and economical method especially in case of periodic inspection. The problem is that visual inspection offers no objective document, which can be compared in the next inspection by different inspector. To deal with the problem, sketches and photographs have been used to record the inspected results.

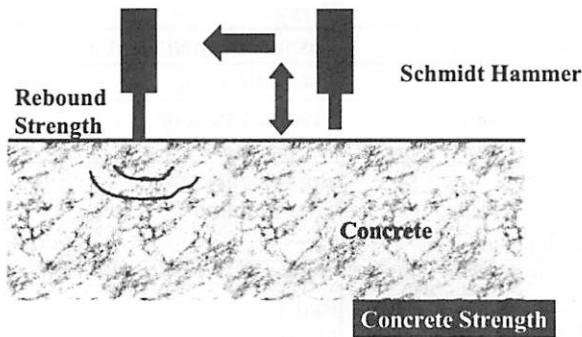


Figure 1: Rebound hammer

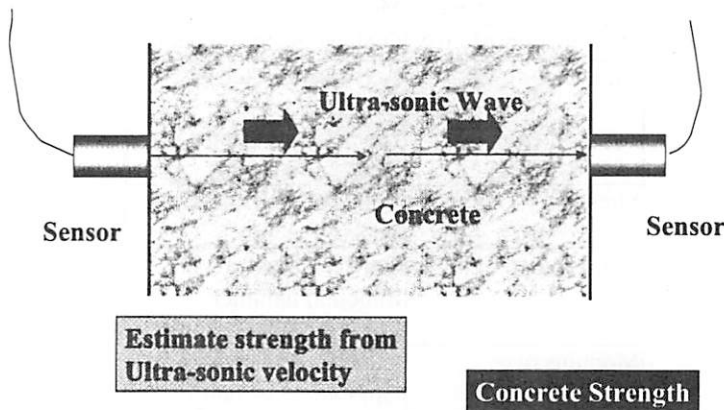


Figure 2: Ultra-Sonic Measurement

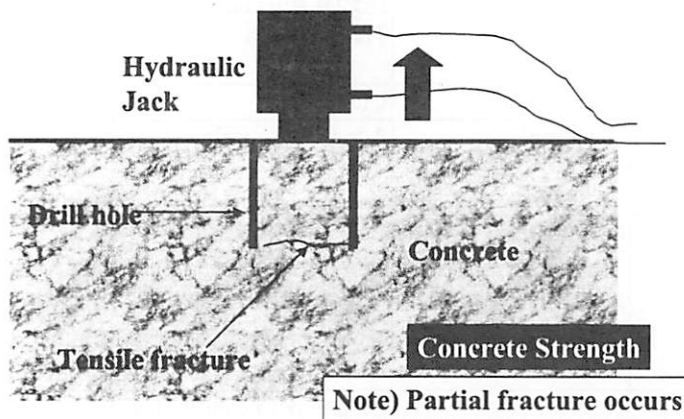


Figure 3: Pull Out Strength

Recently, digital still camera has been used for recording the inspected results, such as distribution of cracks and honeycombs that can be seen by



visual inspection. The photographs taken by the digital still camera can be easily mounted on a computer and the distorted portion can be modified, especially the corners of the photograph. Also, the results of other inspected data can easily mounted on the photograph [4]

Thermograph is another valuable tool. When any void exist close to the surface of concrete structure, they can easily detected by using thermograph as shown in Figure 5. The tool looks the same with digital still camera but the information we can obtain is different. When a void with certain size exists close to the surface, due to sun light, etc., surface temperature of concrete becomes slightly higher (less than 1 degree in most cases) than the surroundings. As a result, the voids underneath can be easily detected.

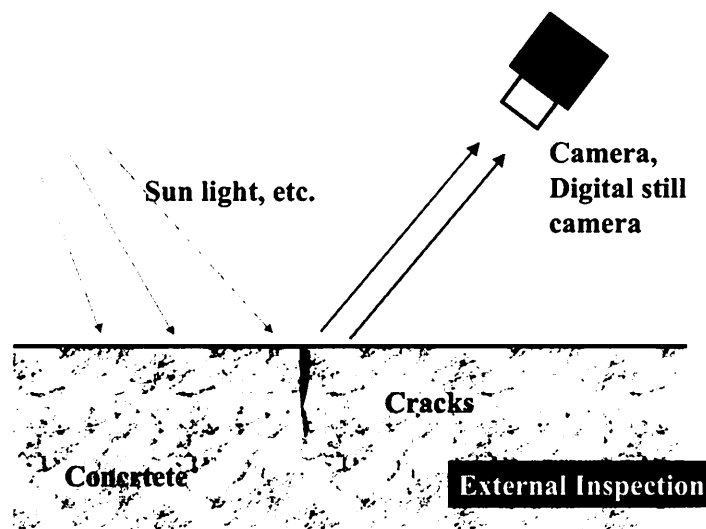


Figure 4: Digital still camera

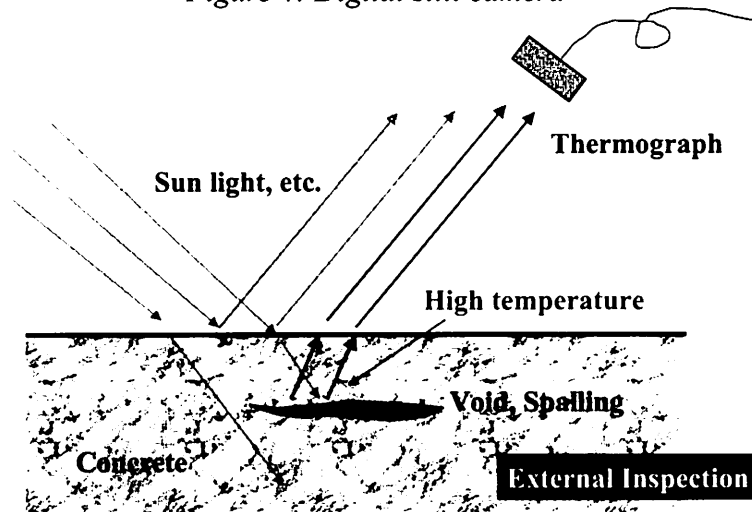


Figure 5: Thermograph

### 3.3 Crack depth and cracking

When cracks are observed by visual inspection, the inspectors wish to know the depth of the cracks. The popular method being used is to measure

the depth using ultra-sonic, such as BS method, T0-Tc method, etc. The principle of the method is to measure the arrival time of the induced elastic wave that diffracted at the tip of crack. Care must be taken to consider that the diffracted wave may be affected by the existence of reinforcing bars in concrete. In our laboratory, a new method is developed to eliminate the effect of reinforcing bars at the time of measurement.

In case of monitoring crack formation of a concrete structure under fatigue load, etc. acoustic emission (AE) monitoring is useful. As shown in Figure 7, when fracture occurs in concrete, not only cracks but also elastic waves are transmitted from that point. AE monitoring method is to monitor these elastic waves and find out both the location and degree of fracture. It can be said that monitoring of earthquake waves is just the same as monitoring of concrete fracture by AE.

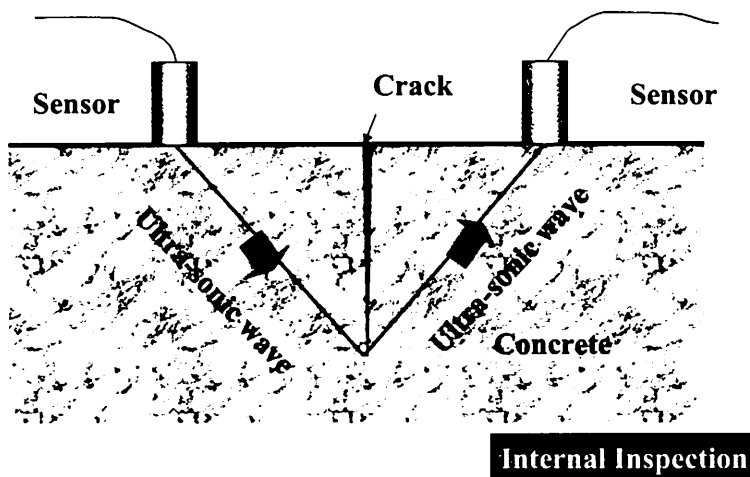


Figure 6: Crack depth measurement

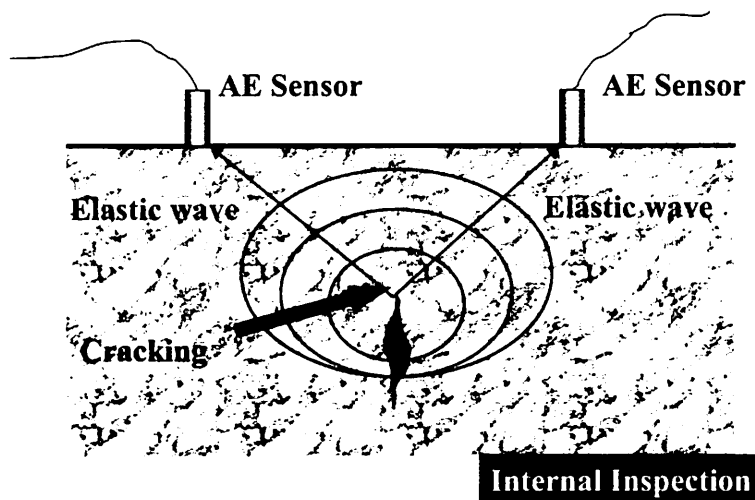


Figure 7 Acoustic emission monitoring by ultrasonic

### 3.4 Location and cover depth of reinforcing steel bars

In case of old concrete structures, it is quite difficult to obtain detailed drawing of reinforcements. Both electro-magnetic method and radar systems

are often used to clarify the arrangement and location of reinforcing steel bars within concrete structure or to measure the cover to the bars.

The principle of electro-magnetic method is explained in Figure 8. A magnetic field is formed around the sensor and if there is any steel bar in the field, electric current is formed in the steel bar. Due to the current in the bar, a new magnetic field is formed, which induces the current in the sensor. The relation between the induced current in the sensor and cover thickness is used to estimate the thickness of cover and size of the steel bar. In order to obtain accurate values, it is better to check either cover thickness or the size of the bar beforehand.

Radar system is often used to measure the cover thickness of the reinforcing bars and location of voids. As shown in Figure 8, the microwave transmitted from radar reflects at the surface of concrete, steel bars or voids. The time difference is used to measure the depth of the target [5].

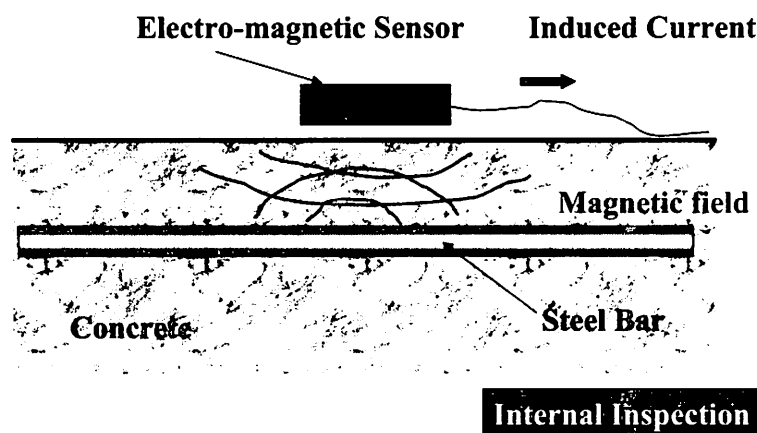


Figure 8: Electro-magnetic apparatus

### 3.5 Detection of voids in concrete

To investigate internal voids and defects in concrete, acoustic (sound) measurement is often used. The principle of the method is simple. The inspector listens the sound he hears when he hits the structure. If the inspector

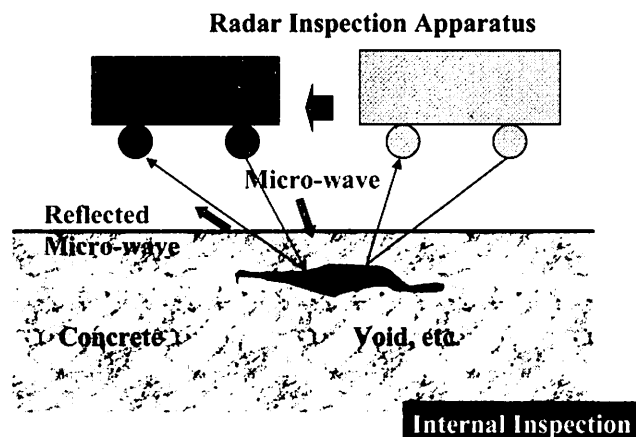


Figure 9: Radar system for bars and voids

is well trained and has enough experience, he can easily find out the location of these defects without any apparatus. To reduce the personal errors, sensor and recorder are combined in a system. Due to the surrounding noise, analysis of the data is performed using both the amplitude and frequency of the obtained sound.

X-ray is used to detect voids, defects and bar arrangements in concrete. The results can be easily understood by civil engineers. When more than 2 photographs are taken at different locations, three-dimensional information can be obtained. The only problem is that x-rays are harmful and it is difficult to use high-energy rays at field [6]. Normally, with compact apparatus, the thickness of concrete is limited to less than 40cm.

### 3.6 Corrosion of reinforcing steel

Corrosion of reinforcing steel deteriorates reinforced concrete structures easily. Cover concrete may easily spall off due to cracks formed by corrosion of steel bars. To inspect the corrosion of embedded steel, natural potential measurement is often used as shown in Figure 12. When corrosion takes place, the potential of the bar changes to negative, and ASTM standard is often used to identify the corroded portion and the degree of corrosion. To

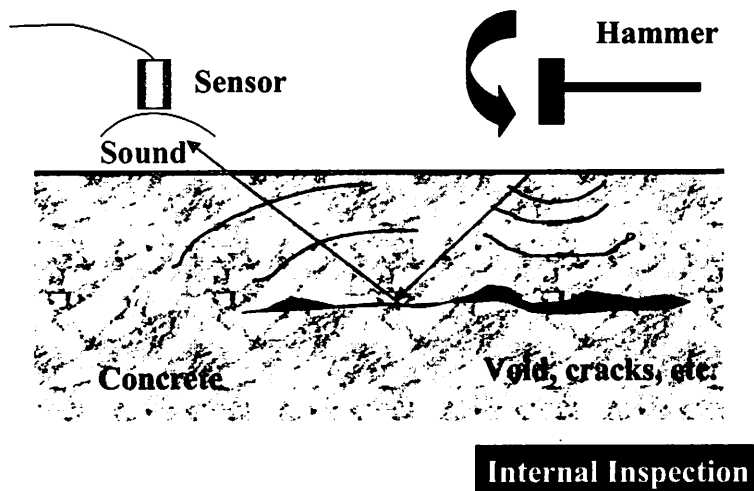


Figure 10: Acoustic measurement

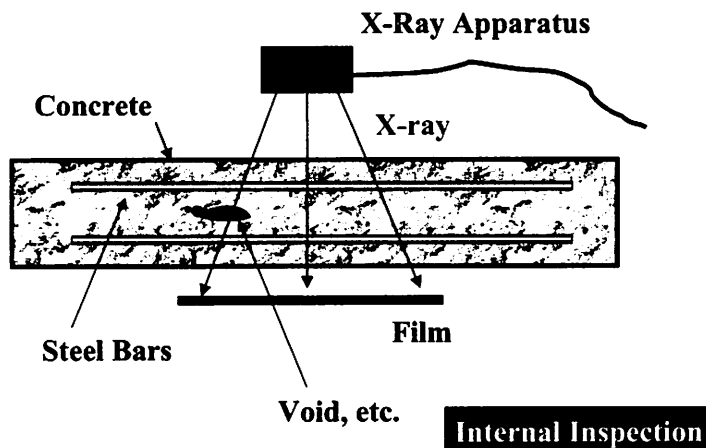


Figure 11: X-ray for concrete

obtain the amount of corrosion, integration of the induced electric current obtained from periodic natural potential measurement [7] is useful.

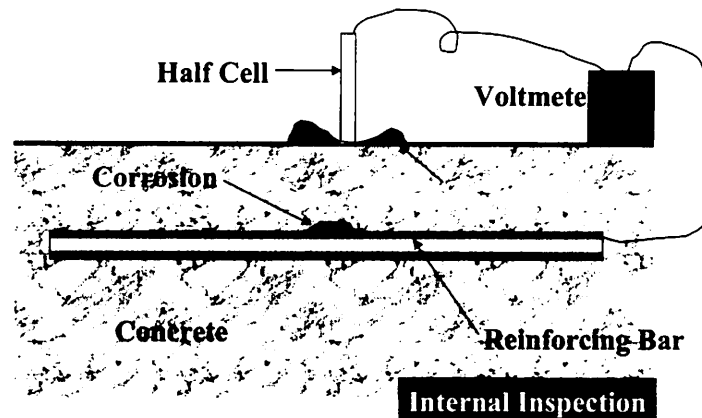


Figure 12: Natural potential measurements for corrosion

#### 4. PREDICTIONS AND EVALUATION OF DETERIORATION

Evaluation of existing structures is one of the most difficult thing to be done. The engineer must predict the remaining lifetime of the structure if the structure is kept un-repaired. To predict the lifetime, not only the mechanism of the deterioration must be clarified but also accurate calculation and enough data is needed. Although the data is limited, JSCE and JCI committees have been trying to propose an accurate and practical prediction method to avoid big mistakes in the prediction [2].

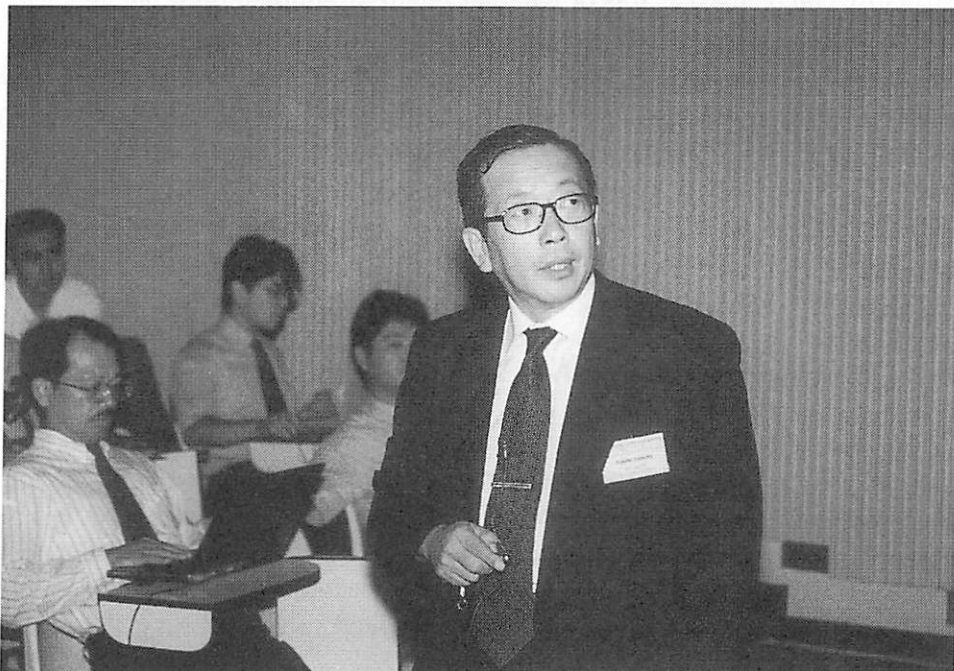
The engineers with above mentioned prediction method, whether the structure can be used as it is or whether repair/strengthening is needed, can do the decision. But whether to demolish and construct a new structure must be done considering engineering, social and economical views. Up till now, none of the important structures, such as Shinkansen, highways, Honshu-Shikoku Bridges, etc., deteriorated to a dangerous level but sooner or later we may encounter such a problem in the 21<sup>st</sup> century. It will become especially important in Japan how to decide such a problem, obtaining consensus of the public.

#### 5. CONCLUDING REMARKS

Engineering is not always complete, and further research works are needed. To set up a good system for maintenance of existing concrete structures, there are still many things to be done: not only researches but also education to the students and engineers about durability and maintenance of concrete structures. I hope this paper may become a help to the concrete engineers and NDI engineers who are involved in maintaining the existing concrete structures.

## REFERENCES

1. T. Uomoto: Development of Deterioration Diagnosis for Reinforced Concrete Structures, Report of Grant-in-Aid from Ministry of Education, IIS, University of Tokyo, March, 1992
2. Research Committee on Repair of Concrete Structures: Committee Report on Analysis for Evaluation of Repair Methods, Japan Concrete Institute, October, 1996
3. T.Uomoto, K.Kato, S.Hirono: Non-Destructive Inspection Method of Concrete Structures, Morikita-Shyuppan, 1990.5
4. T.Uomoto: Non-destructive Inspection of Concrete Structures, pp.3-11, Dam Engineering, November 1999
5. S.K.Park et al: Estimation of the Volume of Three-Dimensional Subsurface Voids by Microwave Polarization Method, pp.13-24, JSCE No.592/V-39, 1998.5
6. S.Izumi et al: Application of High Energy X-ray CT/DR to Non-Destructive Testing of Thick Concrete Structure, 3<sup>rd</sup> Non-destructive Symposium using X-rays, 1999 .11
7. E.Tsukahara et al: Basic Study on Corrosion of Reinforcement in Cracked Concrete, General Meeting of JSCE, 1999.9



*Prof. Taketo Uomoto*

# **DURABILITY PROBLEMS OF CONCRETE STRUCTURES IN THAILAND AND THEIR SOLUTIONS**

SOMNUK TANGTERMSIRIKUL  
Sirindhorn International Institute of Technology,  
Thammasat University, Thailand

## **ABSTRACT**

*This paper introduces some problems on deterioration of concrete structures in Thailand and some concepts on their future solutions. A survey of damages due to durability problems of some structures in the central and eastern parts of Thailand was carried out to explore the level of severity of the problem. It could be summarized that problems occurred in various states of the works i.e. from design, material selection, construction and maintenance. Some examples of problems in each state are illustrated. Solutions were offered in two categories i.e. that for new construction and that for the existing structures. For new construction, the performance based analysis and design taking into account the service life of the structures is proposed. For the existing structures, good protection, repair, strengthening shall be carried out.*

## **1. INTRODUCTION**

The current design and construction of concrete structures in Thailand are based on working stress and ultimate stress design concepts. Civil engineers concern much only on a few properties of the concrete such as workability and mechanical properties like strength and Young's modulus, etc. at the design age which is usually 28 days rather than considering the long term properties which involve various durability problems. As shown in Fig.1, for the whole life cycle of the concrete, the mentioned considered properties in the design are just a few of the overall properties of the concrete that is supposed to be under service for long time. In addition, since Thailand can be considered in a state of developing the nation with many infrastructures being constructed within the past decade, there may still be no serious accident based on the failure due to deterioration of the built concrete structures. Many may think in a way that the mentioned concrete structures are still new when compared to those in the previously developed nations in Europe, America or even in Japan. However, based on the survey of the situation of some concrete structures in the central and eastern part of Thailand, many signs of various degree of deterioration from light to serious were observed. The deterioration was caused by insufficient knowledge and attention in various steps of the practice starting from analysis and design, material selection, construction and maintenance

planning. It is necessary to plan for a solution to this problem for the sake of economic and safety.

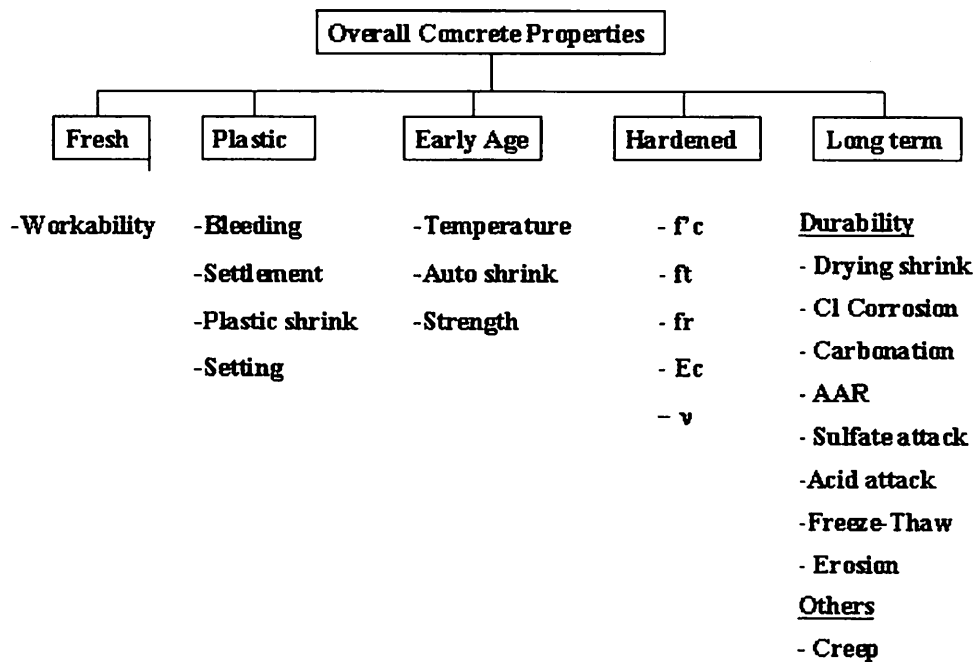


Figure 1: Properties throughout service life of concrete

## 2. A SURVEY ON DETERIORATION OF CONCRETE STRUCTURES SHOWING DURABILITY PROBLEMS

A survey on situation of deterioration of some concrete structures in Thailand was conducted for 4 years starting from 1997 to 2001 with the aim of gathering data on the types and degree of deterioration of the surveyed structures. Two regions were selected for the survey namely central region (including Bangkok) and eastern region with different categories of environment. The main difference of the two regions is on the existing of chloride problem. Eastern part of Thailand is the region closed to sea and is subjecting to attack by salts. Fig.2 shows the map of Thailand and the survey area denoted by the name of the provinces in the map. According to this survey, the following summary can be drawn.

- 1) There were various causes of deterioration including those due to load and due to environmental attack such as drying shrinkage, thermal crack, sulfate attack, acid attack, alkali aggregate reaction, carbonation, chloride attack, etc., and those occurs during construction like plastic shrinkage, bleeding and settlement, etc..
- 2) Most of the damages were visible in form of steel corrosion. Damage due to steel corrosion is much more serious in the eastern part than in the center of Thailand.



- 3) Most of the steel corrosion problems were due to poor construction such as insufficient concrete cover or honeycombing and no maintenance program.



Figure 2: Map of Thailand showing the surveyed regions

- 4) The selection of raw materials and mix proportion of concrete was only based on a few performances such as strength and workability. The concept of selecting proper materials and proper mix proportion for different environment is still dilute.

The problems in all stages of practice can be observed, starting from stage of analysis and design, raw materials selection and mix proportioning, construction and maintenance. Fig.3 to Fig.9 show some examples of the problem in each stage. The current practice is considered not reasonable in terms of economic and public safety.

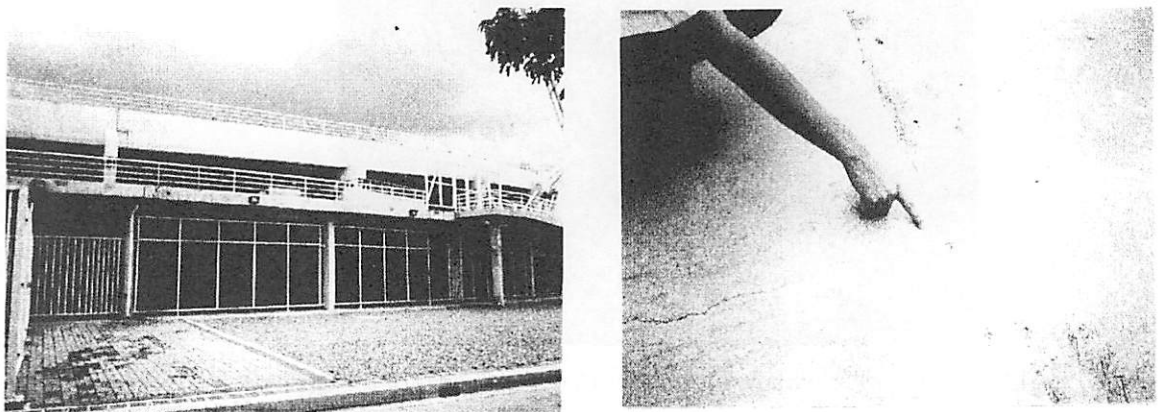
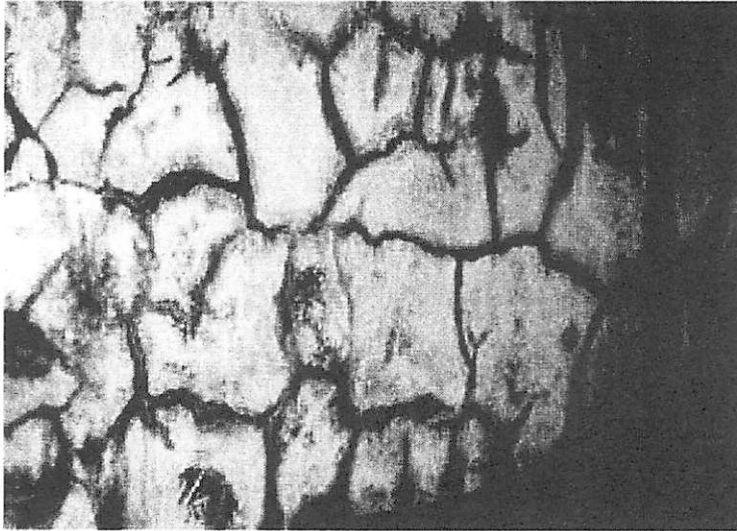
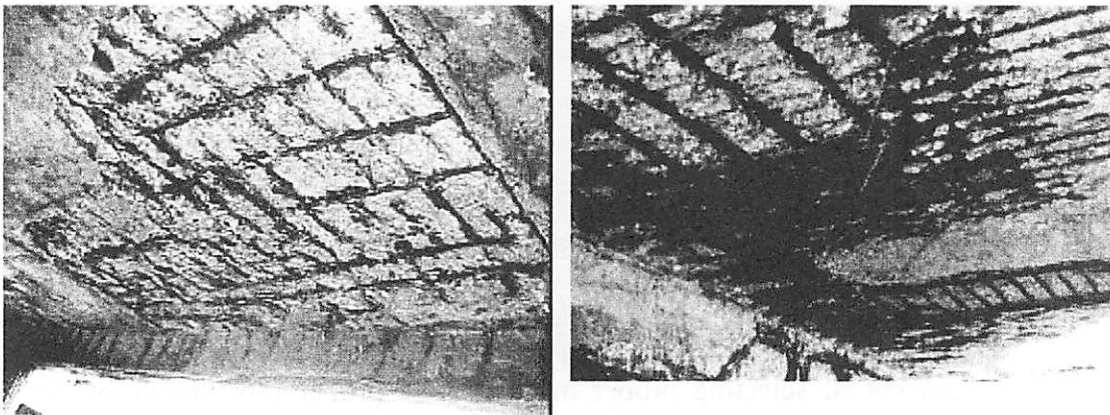


Figure 3: Crack on a roof slab of a stadium (Analysis and design problem)



*Figure 4: Cracking due to alkali aggregate reaction  
(Raw materials selection problem)*



*Figure 5: Severe honeycombing due to segregation (Problem of concrete  
mix proportion)*



*Figure 6: Drying shrinkage cracks (Mix proportioning problem)*

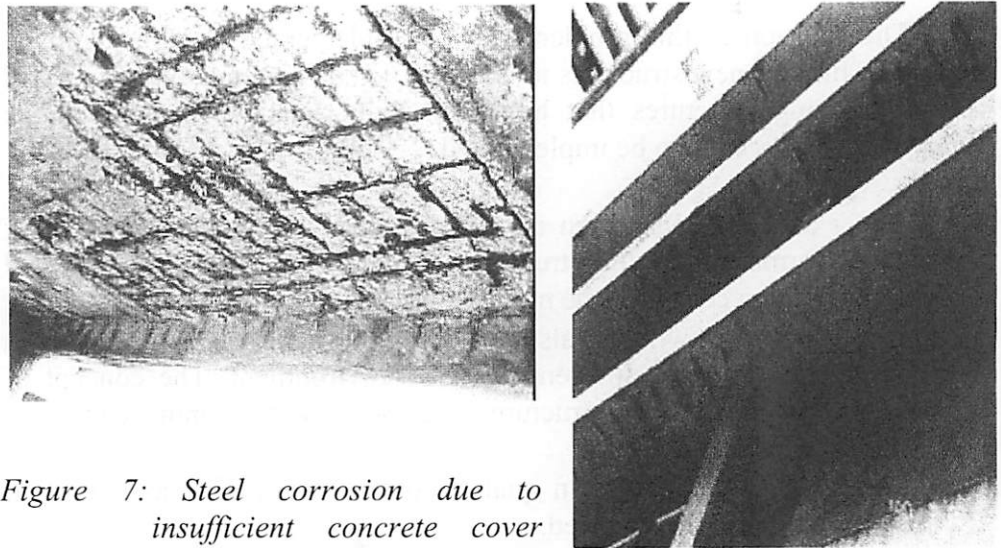


Figure 7: Steel corrosion due to insufficient concrete cover under bridge (left) and under building balconies (right) (Construction problem)

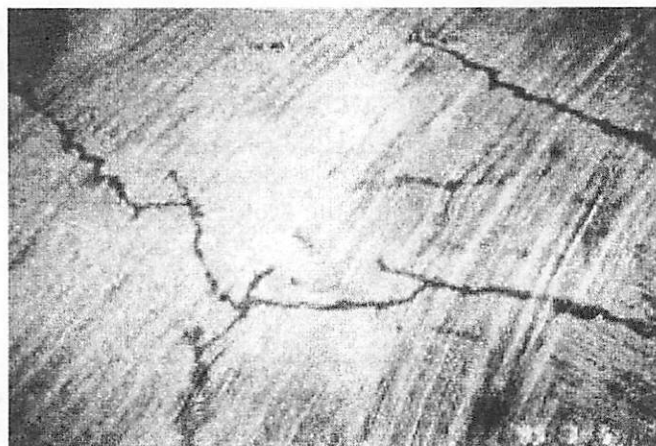


Figure 8: Plastic shrinkage cracking due to insufficient early curing and moisture loss prevention (Construction problem)

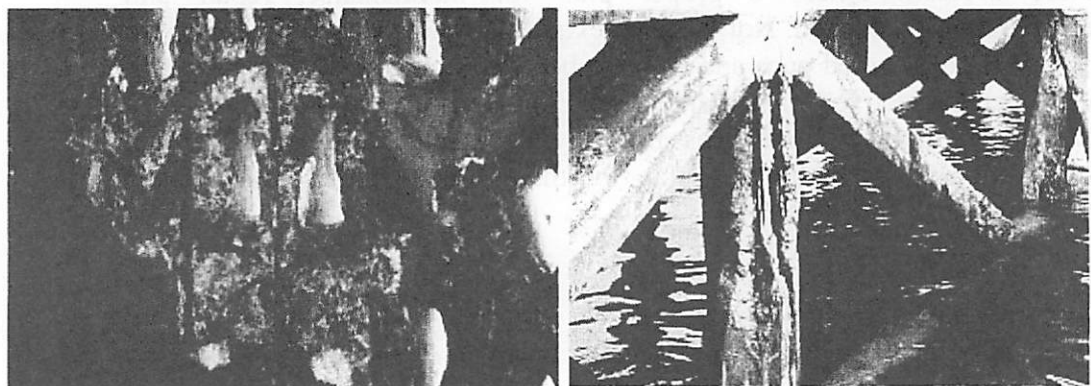


Figure 9: Severe steel corrosion due to carbonation (left) and chloride attack (right) (Maintenance problem)

### 3. SOLUTIONS

The solution to this problem can be implemented by considering 2 measures, first for new structures to be constructed from now on and second for the existing structures that had been built. For new structures, the following measures are to be implemented.

- A better analysis and design considering not only short term but long term performances of the structures (Performance based analysis and design). Design code shall be modified in the mentioned way.
- Selecting proper raw materials and mix proportion of concrete for each type of structure and different types of environment. The concept of proper concrete for each structure type and each environment must be seriously considered.
- A much more seriousness in quality control and quality assurance of construction must be practiced.
- The existing of good plan of protection and maintenance which will prevent intensive repair or strengthening in the future has to be considered from the beginning of the project.

For the already built structures, there is a need to create a database indicating the cause and degree of deterioration of the existing structures in order to conduct a proper protection, maintenance, repair, strengthening or reconstruction program for each case. There is a strong need to publish higher level of appropriately advanced codes and standards of practice and to provide more education in order to get the problems solved.

### 4. CONCLUDING REMARKS

Based on a survey on the deterioration situation of some concrete structures in the central and eastern parts of Thailand, it was found that even though most of those structures were constructed just in the past decade, there were many problems regarding deterioration which would lead to future accident unless a proper plan for maintenance, repair and rehabilitation is realized. Not only the existing damaged structures, but also the newly constructed ones and those to be constructed must be considered. A proper protective maintenance plan for newly and still undamaged structures and proper practices in analysis, design, materials selection, construction and maintenance plan for those to be constructed must be available.

### ACKNOWLEDGEMENTS

The author would like to express appreciation to Dr. Toshiharu Kishi, former seconded faculty member to Asian Institute of Technology and many graduate and undergraduate students from Sirindhorn International Institute

of Technology and Asian Institute of Technology for their contribution to the survey.

## **REFERENCES**

- Tangtermsirikul, S., et.al., 2000. Durability of Concrete. Engineering Institute of Thailand, ISBN 978-974-87684-5-7, Thailand.
- Wongtanakitcharoen, T., 1999. A Study of Deterioration of RC Structures in Central and Seaside Areas of Thailand. A Master thesis No. ST-99-32, Asian Institute of Technology, Thailand.



*Dr. Somnuk Tangtermsirikul*



# **APPLICATIONS OF REMOTE SENSING AND GIS FOR DAMAGE ASSESSMENT**

FUMIO YAMAZAKI

School of Advanced Technologies, Asian Institute of Technology, Thailand  
Earthquake Disaster Mitigation Research Center, NIED, Hyogo, Japan  
Institute of Industrial Science, University of Tokyo, Japan

## **ABSTRACT**

*Remotely sensed imagery data from satellites and airborne platforms have become important tools to assess vulnerability of urban areas and to grasp damage distribution due to natural disasters. The platform and sensors of remote sensing should be selected considering the area to cover, urgency, weather and time conditions, and resolution of images. Satellites with optical and/or SAR sensors can cover much larger areas than other platforms, and hence, they can be used for macro-scale urban modeling and damage detection in large-scale natural disasters. Aerial television imagery and photography are very useful to observe buildings and infrastructures with high resolution. Thus automated detection of damage is possible using only post-event images or both pre- and post-event images. Use of airborne SAR is also highlighted for 3D urban modeling. In this paper, recent developments and applications of advanced technologies, notably, remote sensing and GIS, are reviewed from the viewpoint of risk assessment and post-event disaster management.*

*Keywords: remote sensing, GIS, damage assessment, aerial imagery, SAR, natural disasters*

## **1. INTRODUCTION**

In the last decade of the 20th century, although it was designated as the International Decade for Natural Disaster Reduction (IDNDR), a large number of devastating natural disasters attacked highly populated urban areas in the world, and a huge amount of human, structural, and socio-economic losses were brought due to them. Thus, vulnerability assessment before and after natural disasters has attracted significant attentions among researchers and practitioners of disaster management. In this regard, advanced technologies, notably remote sensing and GIS, have become important new tools in disaster management.

Recent advancements in remote sensing and its application technologies made it possible to use remotely sensed imagery data for assessing vulnerability of urban areas and for capturing damage distribution due to natural disasters (Shinozuka & Rejaie 2000). To obtain pre- and post-event information on built environment, several methods exist, such as field sur-



vey, aerial videography and photography, and satellite imagery. Figure 1 shows various platforms and sensors used for remote sensing. The platform and sensors should be selected considering the area to cover, urgency, resolution of images, and weather and time conditions. The first three items are closely related. If we want to get images over a large area, satellite imagery may be the most suitable tool although its resolution is in the order of several ten meters and return period is several weeks for commonly available earth observation satellites. On the contrary, aerial videography and photography from helicopters and light planes can be obtained much faster with higher resolution despite the fact that the area to cover is much small.

Regarding sensors on board platforms, synthetic aperture radar (SAR) can be used irrespective of sunlight and weather conditions, hence this feature is highly effective in damage surveys when optical remote sensing, such as multispectral scanning and aerial photography, is difficult. Massonet et al. (1993) introduced interferometric SAR (IFSAR) analysis using phase information to estimate the distribution of ground displacement due to the 1992 Landars earthquake. Laser altimeter (LIDAR) is another new technique to profile 3D elevations of the earth surface (Gamba & Houshmand 2000).

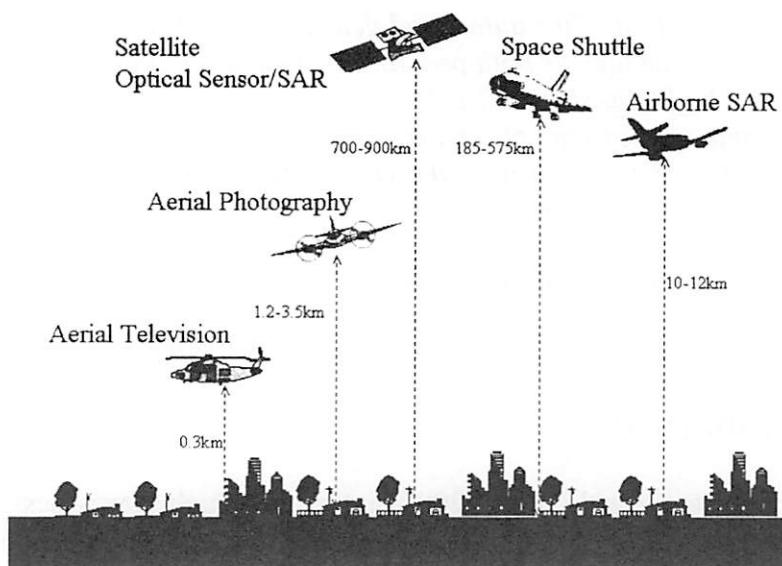


Figure 1: Platforms and sensors of satellite and airborne remote sensing

Capability of optical/SAR satellite imagery has been demonstrated for damage detection in large-scale natural disasters. Using the pre- and post-event images of the 1995 Hyogoken-Nanbu (Kobe) earthquake observed by Landsat/TM, JERS/SAR, and ERS/SAR satellites, the areas with heavy building damage, fire and liquefaction were identified (Matsuoka & Yamazaki 1999, 2000a). In the study, the results of field surveys stored in GIS were employed as supervised learning data. Similar approaches comparing the pre- and post-disaster satellite images were carried out for the 1999 Kocaeli, Turkey earthquake (Estrada et al. 2000, Matsuoka & Yamazaki 2000b) and the 1990 Luzon, Philippine earthquake (Yamazaki & Matsuoka



1999). The satellite images together with GPS were also employed in a damage survey (Eguchi et al. 2000b) after the Kocaeli earthquake.

Airborne remote sensing is more suitable to obtain detailed inventory and to collect damage data of built environment. SAR imagery is one of the most promising techniques in this objective and a pioneer study on mathematical theory and image simulator has been conducted by Shinozuka et al. (2000). Interpretation of airborne SAR data was also attempted for the purpose of inventory development (Eguchi et al. 2000a) and urban modeling (Aoki et al. 1999). Although these investigations are still preliminary, airborne SAR imagery will be used for risk assessment and post-disaster damage detection of urban areas in the near future.

Aerial photography and videography from helicopters and light planes are practical and powerful tools to survey urban and suburban areas in pre- and post-event periods. Using aerial photographs, liquefaction induced permanent ground displacements were investigated for several damaging earthquakes in Japan (Hamada 1992, Hamada et al. 1995) and in the United States (O'Rourke et al. 1992, Sano et al. 1999). More recently, building damage due to the 1995 Kobe earthquake was interpreted visually using aerial photographs (Ogawa & Yamazaki 2000) and high-definition television (HDTV) images (Hasegawa et al. 2000a). Damage detection of buildings is further being developed to automated damage detection methods (Hasegawa et al. 2000b, Mitomi et al. 2000, 2001a, b) using the edge and color information of the post-earthquake images. Helicopters or light planes installing video and still cameras can provide damage information soon after the occurrence of a disaster. Hence such images are particularly useful in the early post-disaster damage detection as well as in the collection of inventory data in the ordinary period.

Use of GIS in disaster management has been accelerated in the last decade. Databases on built and natural environment have been developed on GIS platforms and damage assessments to natural disasters, especially urban earthquakes, have been conducted in many countries. One of the most enhanced damage databases has been developed for Kobe area after the 1995 Kobe earthquake and it has been used for the estimation of strong motion distribution (Yamaguchi & Yamazaki 2001) and for the construction of building fragility curves (Yamazaki & Muraio 2000). GIS models are extensively utilized in real-time damage assessment systems (Yamazaki et al. 1994, 1998, Whitman et al. 1997, Shimizu et al. 2000).

In this paper, recent developments and applications of advanced technologies, notably, remote sensing and GIS, are reviewed from the viewpoint of risk assessment and disaster management. These technologies were born and developed in the different areas from "structural safety and reliability", but their application to our area is quite attractive and promising. Recent examples in the field of earthquake disaster mitigation are presented in the following.

## 2. SATELLITE REMOTE SENSING FOR DAMAGE DETECTION FROM THE 1995 KOBE EARTHQUAKE

### 2.1 Damage Survey Data and Satellite Data

Several satellites with optical sensors and/or SAR observed Kobe area before and after the Kobe earthquake on January 17, 1995. Since a part of the damage survey results is maintained as GIS data, a quantitative analysis on the surface changes in the damaged areas is possible. Liquefied areas were plotted on a GIS map based on the 1/50,000-scale ground-failure survey map (Hamada et al. 1995). The building damage data based on detailed survey results compiled by AIJ (the Architectural Institute of Japan) and CPIJ (the City Planning Institute of Japan), and digitized by BRI (Building Research Institute, Ministry of Construction) were utilized as the ground truth data (Fig. 2). In the GIS data, the building damage level was classified into five categories: damage by fire, severe damage, moderate damage, slight damage and no damage (BRI 1996).

We prepared several satellite images taken after the Kobe earthquake. Landsat/TM with optical sensors observed the area of interest on January 24, 1995, one week after the earthquake. We used the images taken on August 17, 1994 by Landsat for the data before the earthquake, and aimed to extract the change in the spectral characteristics of the damaged area. JERS/SAR image (Fig. 3) observed on February 5, 1995, 20 days after the Kobe earthquake, and five pre-event images were employed to examine the change in the backscattering characteristics of the area. SAR systems have the capability of recording complex signals including the amplitude (intensity) and phase of backscattered echoes from the objects on the earth's surface.

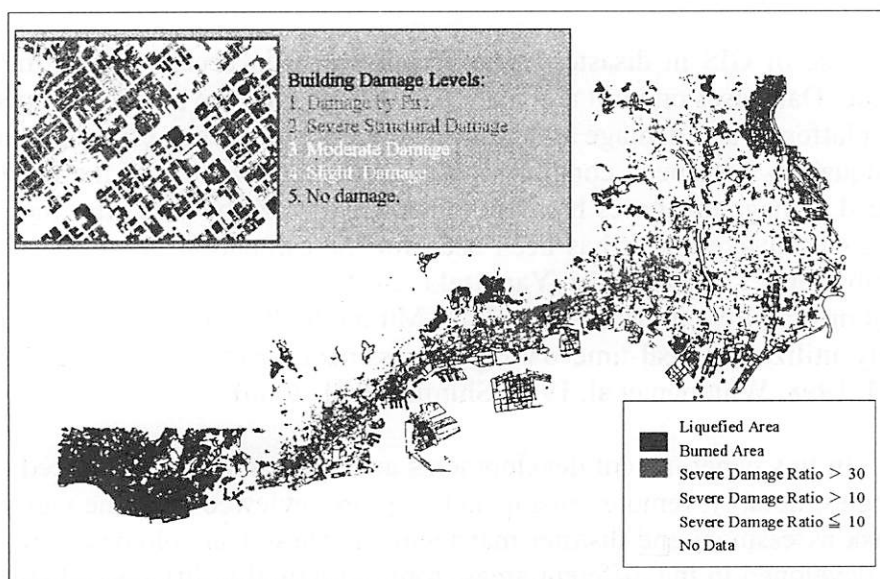


Figure 2: Building damage distribution due to the 1995 Kobe earthquake based on detailed survey results compiled by AIJ and CPIJ and digitized by BRI (BRI 1996)

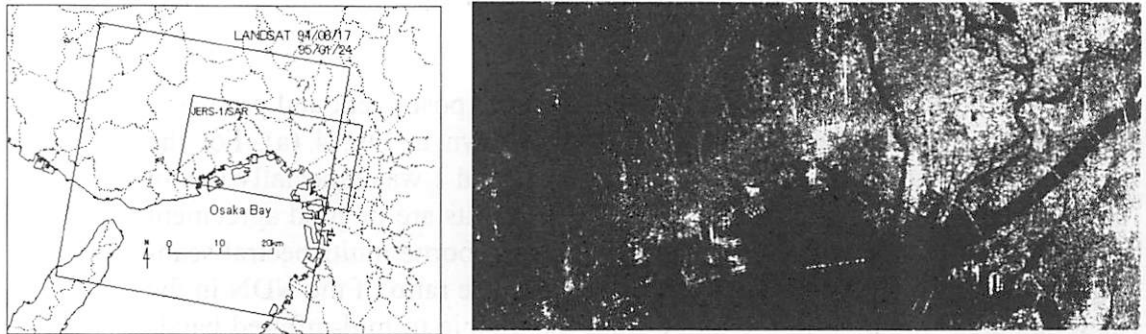


Figure 3: The area of the satellite images used in this study (left) and the backscattered intensity image of JERS/SAR taken after the Kobe earthquake (right)

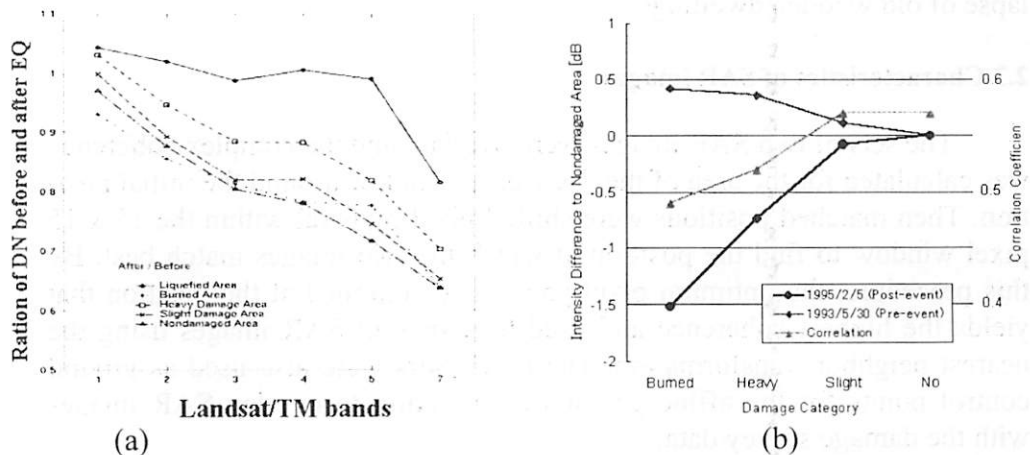


Figure 4: (a) Ratio of digital numbers of Landsat/TM bands for the damaged areas before and after the earthquake and (b) comparison of backscattered intensity between the damaged and nondamaged areas and the correlation coefficient of JERS-1/SAR images taken before and after the earthquake

### 2.2 Characteristics of optical images

Because the digitized values in the satellite images were different depending on the observation and surface conditions, digital number (DN) normalization is required before starting a study. The characteristics of the reflection of electromagnetic waves from the surface differ depending on the season because the sunlight and vegetation are different. One common technique to eliminate the seasonal difference is the band ratioing, which is defined as the ratio of the DN of each band to the DN of a reference band (Campbell 1996). We calculated the normalized DN (NDN) based on the band ratioing using band 6 as a reference band. The pre- and post-event images were registered after the affine geometric correction using ground control points. The correlation coefficients between the two sets of images were calculated using a 5 x 5 pixel window filter. Clouds and cloud shadows covering the area were removed using proper threshold values of several spectral bands. Areas with vegetation were also excluded from these images, based on the normalized difference vegetation index (NDVI). The pixels that represent the areas of liquefaction, fire, and heavy damage, slight dam-

age and no damage of buildings were selected from the images to characterize the DN in the damaged areas.

The ratios of mean values of the NDN in the post-event and pre-event images for the classified damaged areas are shown in Fig. 4 (a). For the burned area, the ratio in the blue-light range of band 1 was especially low in comparison with the nondamaged area. These results are in good agreement with those of the damage survey performed by airborne multispectral scanner remote sensing (Mitomi & Takeuchi 1995). The ratio of the NDN in the liquefied area was high in the range from the visible to mid-infrared bands because of the higher reflectance of sand than the surface of asphalt. It is also conceivable that the ratio was raised in infrared bands in the heavy damage area due to the exposure of soil under walls and roofs upon the collapse of old wooden dwellings.

### 2.3 Characteristics of SAR images

The sets of two SAR images were overlain and the complex coherence was calculated for the area of the 7 x 7 pixel window around the initial position. Then matched positions were shifted pixel by pixel within the 15 x 15 pixel window to find the position at which the two images match best. By this procedure, the optimum pixel pair was determined at the position that yields the highest coherence and used to match all SAR images using the nearest neighbor transformation. The pixel pairs were also used as ground control points for the affine geometric correction to overlay SAR images with the damage survey data.

The coherence, which is the correlation calculated from the phases of the backscattering echoes of two co-registered complex SAR images, is a suitable and sensitive parameter for change detection and land-use classification. The complex coherence is usually adopted between two co-registered complex images acquired under slightly different geometrical configurations. However, decorrelated areas exist in the coherence image due to spatial and temporal decorrelation. The spatial decorrelation is resulted from the difference in the geometry of observation between two acquisitions, which is called baseline length  $B$ , shown in Fig. 5 (a). The temporal decorrelation is related to atmospheric effects such as moisture and surface changes in two acquisitions.

The pixels that represent the areas of fire, heavy damage, slight damage and no damage of buildings were selected from the SAR images. Although a slight influence of vegetation exists even in the SAR images, we disregarded it in this analysis. The trends of the mean values of intensity difference to the non-damaged area before and after the earthquake are shown in Fig. 4 (b). It is observed that the intensity values of the severely damaged area in the post-event image are smaller than those of the non-damaged area while such trend is not observed in the pre-event image. Generally, buildings show high reflectance because of the specular characteristics of the structure and ground surface (Fig. 5 (b)). Open spaces or damaged buildings have low reflectance because the microwaves are scattered in different directions. Following the earthquake, buildings were

rections. Following the earthquake, buildings were destroyed and in some cases, the debris was cleared leaving the ground exposed. Thus the intensity determined in the damaged areas is considered to be lower than that in the non-damaged areas. The mean values of the correlation coefficients between the pre- and post-event images for each damage class are also shown in the figure. A decreasing trend of the correlation coefficient with increasing the damage level is observed and it is coincidental with the difference of the backscattered intensities.

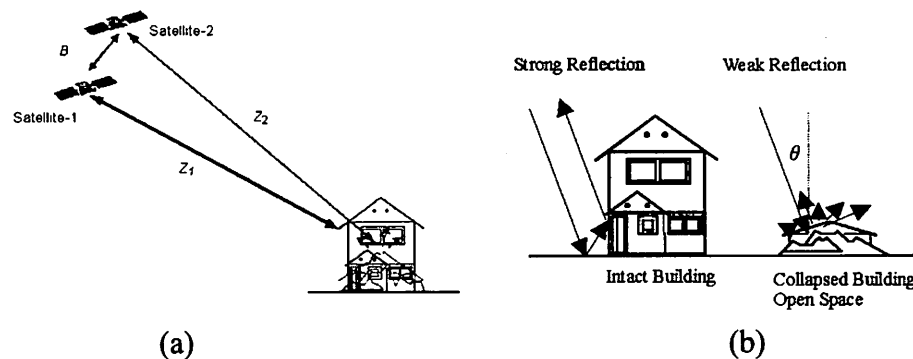


Figure 5: (a) Basic principle of the repeat pass radar interferometry and (b) schematic diagram for surface objects and backscattered echoes

### 3. CHARACTERISTICS OF AIRBORNE SAR IMAGES IN AN URBAN AREA

#### 3.1 CRL/NASDA airborne SAR and its images of Shinjuku, Tokyo

Seismic risk in an urban area is closely related to the structure, material and dimension of buildings and their mutual distances. Hence it is important to study the plan, elevation and structure of buildings for evaluating seismic vulnerability of urban areas. Building inventory can be obtained by field surveys. However, a large amount of time and effort is required. Thus an easier method to develop building inventory is being sought. Airborne remote sensing can be an effective solution for the development of inventory since it can provide high-resolution images of the earth's surface and individual buildings can be identified in the images.

The Communications Research Laboratory (CRL), Japan and the National Space Development Agency of Japan (NASDA) have developed in collaboration an airborne high-resolution multiparameter SAR (Polarimetric and Interferometric SAR: PI-SAR). The airborne SAR is able to provide full-polarization information. The polarization characteristics are highly suitable for the identification of detailed surface conditions of objects because they differ according to the factors such as the building material and the density of city blocks. If we can identify the structures on the basis of their areas and heights from the polarization characteristics, the results can be used in seismic damage assessments. The relationship between the structures and the backscattering characteristics was investigated (Aoki et al. 1999) using airborne SAR data (CRL & NASDA 1999).

The PI-SAR observed a part of Tokyo Metropolitan area on September 30, 1997, and X-band full polarization data were acquired. The backscattering intensity images shown in Fig. 6 for a 3km x 3km area in Shinjuku, a new city center of Tokyo, were used. Comparing the backscattering intensity images in the HH, HV, VH, and VV polarizations, the intensities of the co-polarization (HH, VV) were larger than those of the cross-polarization (HV, VH), and the HH polarization intensity was largest. High-rise buildings were indicated as a cause of strong backscattering reflection whereas low-rise buildings, forests and ponds in parks were found to have weak backscattering reflection.

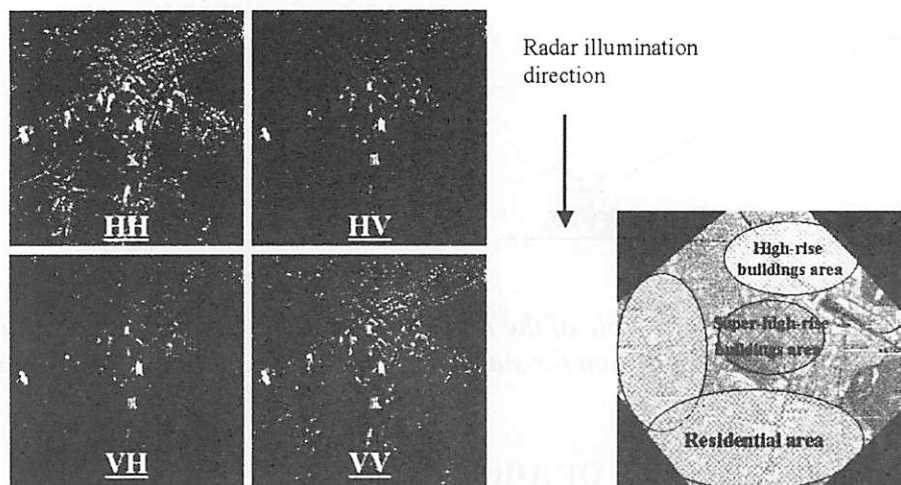


Figure 6: Backscattering intensity images of Shinjuku, Tokyo by CRL/NASDA PI-SAR

### 3.2 Polarization signature and polarized intensity

The detailed polarization characteristics were investigated using the polarization signature of representative city blocks. These blocks labeled as  $\max(R_{hh})$ ,  $\max(R_{vh})$  and  $\max(R_{vv})$  were selected from the pixels having the maximum values of normalized polarization intensities. The details of wave polarization generation can be referred to Van Zyl et al. (1987) and Zebker (1987). The co- and cross-polarized signatures of each extracted pixel are shown in Fig. 7. In the figure, the cross-polarized intensity for  $\max(R_{hh})$  is very low compared with the co-polarization intensity. As expected, the  $\max(R_{hh})$  area exhibited co- and cross-polarized signature shapes similar to those of the simple backscattering model from an object with a horizontal component. Thus it is estimated that the area of  $\max(R_{hh})$  have a scattering object normal to the radar illumination direction, which is a building along the street normal to the radar illumination direction. The entire polarized intensity for  $\max(R_{vh})$  is very low compared with those of  $\max(R_{hh})$  and  $\max(R_{vv})$ . The area of  $\max(R_{vh})$  exhibited co- and cross-polarized signature shapes similar to those of the simple backscattering model from an object with a 45 degree inclined corner reflector component. The area of  $\max(R_{vv})$  showed co- and cross-polarized signature shapes similar to those of the simple backscattering model from an object with a vertical component. Since the  $R_{vv}$  value is high for tall buildings in the commercial area, the VV polarization intensity seems to have a relation with the building height.



The characteristics of the buildings in the studied area were examined by a field survey and aerial photographs. The actual structure at the max ( $R_{hh}$ ) area was found to be a wooden house with a large wall almost normal to the radar illumination direction. The surrounding was a densely built-up residential district as seen by an aerial photograph shown in Fig. 8. The actual structure at the area of max ( $R_{vh}$ ) was confirmed to be a low-rise building 45 degree inclined to the radar illumination direction. It is confirmed from the aerial photograph that this area is a residential district with the similar environment to that of the area of max ( $R_{hh}$ ). The actual structure in the area of max ( $R_{vv}$ ) is a super high-rise building. The surrounding area is a business district with many super high-rise buildings. Based on this study, it was found that the predominant polarization intensity differed with the height, shape, and alignment direction of buildings. A future study will be carried out to investigate the potential of polarimetric characteristics of airborne SAR for the development of building inventory.

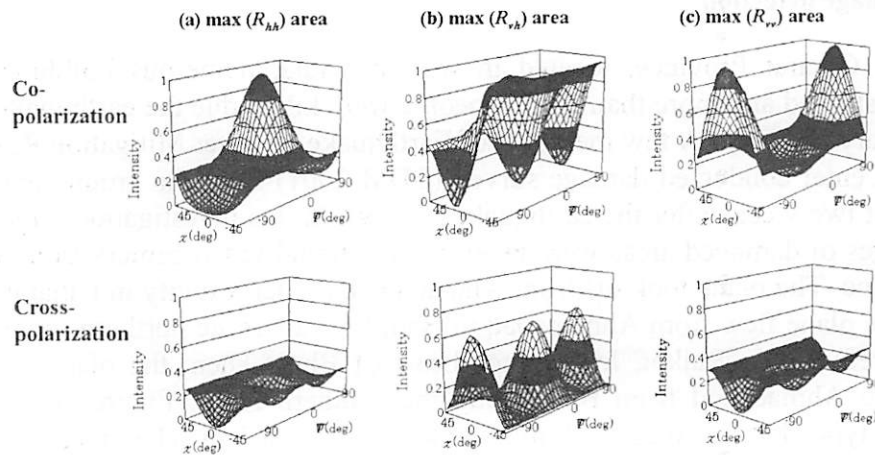


Figure 7. Polarization signatures for the three pixels with maximum polarized intensity.

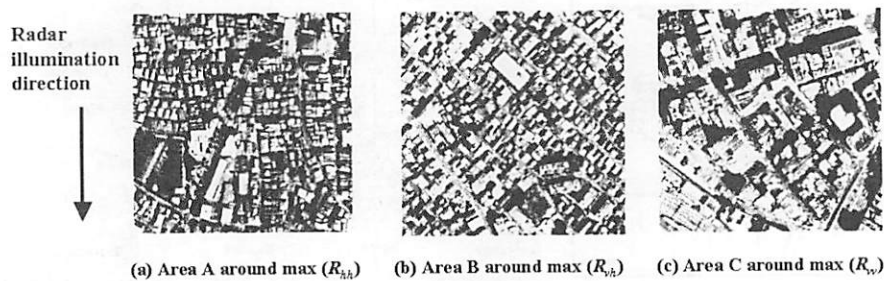


Figure 8: Aerial photographs of the surroundings of the selected areas in Figure 7

#### 4. AUTOMATED DAMAGE DETECTION OF BUILDINGS FROM AERIAL TELEVISION IMAGES AFTER NATURAL DISASTERS

##### 4.1 Use of aerial television images

Airborne remote sensing is one of the promising techniques to capture damage information at an early stage of natural disasters. The present au-

thors performed preliminary studies on the automated detection of building damage, and developed a method of automated damage detection based on only post-event images from the Kobe earthquake (Hasegawa et al. 2000b). The damage distribution estimated using the threshold values of color indices and edge elements (the multi-level slice method) agreed relatively well with the ground truth data. The method was also applied to the post-event images of the 1999 Kocaeli, Turkey and 1999 Chi-Chi, Taiwan earthquakes (Mitomi et al. 2000). Furthermore, an automated method of detecting areas with building damage based on the maximum likelihood classifier was devised (Mitomi et al. 2001a, b) in order to further improve the accuracy of automated damage detection. The results of automated detection of building damage from aerial images taken after the Gujarat, India earthquake are reported in the following.

#### 4.2 Aerial images of the 2001 Gujarat, India earthquake and automated damage detection

In Gujarat Province, located in western India, numerous buildings were destroyed and more than 20,000 people were killed due the earthquake on January 26, 2001. A few members of Earthquake Disaster Mitigation Research Center conducted damage survey (EDM 2001) from the ground and air about two weeks after the earthquake (Fig. 9). In this investigation, digital images of damaged areas were taken with a digital video camera from a light plane. The plane took off from Ahmadabad, the largest city in Gujarat. After the plane flew from Ahmadabad to Bhuj by way of the northern route, it was refueled in Rajkot, located southeast of Bhuj. Then, the plane returned to Ahmadabad from Bhuj along the southern route. Figure 10 (a) shows a typical aerial image of building damage in Bhachau. The image has 640 pixels x 480 lines saved in the bitmap format.

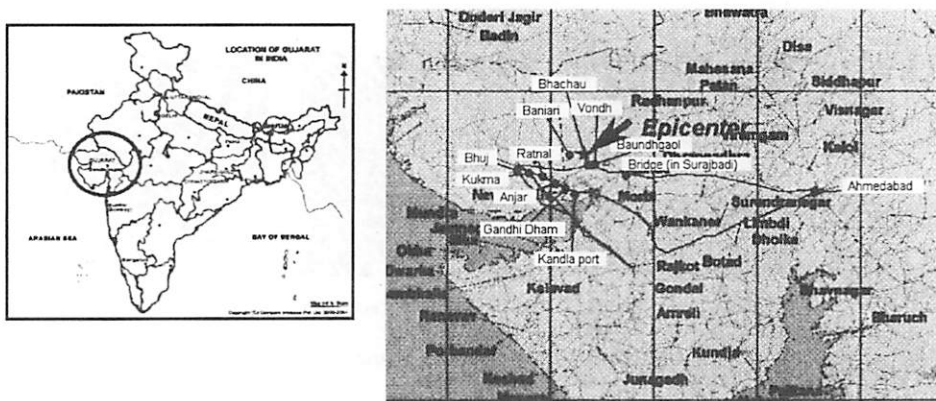


Figure 9: Aerial survey route by EDM for the damage due to the 2001 Gujarat, India earthquake

Color indices and edge elements of image characteristics were used to identify severely damaged buildings. In the color indices, using image signals of the NTSC, which is one of the image transmitting systems for television, a tabular color system of RGB planes was transformed to the bare color system, HSI, which is close to the color perception of humans. Hue and saturation were derived by processing RGB components and brightness



in order to remove the influence of sunshine on buildings. The median of a 7 x 7 pixel window in each HSI image was adopted as a representative value of each HSI component. The edge intensity, its variance and the uniformity of edge direction were derived using a Prewitt filter to detect the change in density among neighboring pixels. The six image characteristics (hue, saturation, brightness, edge intensity, its variance and the uniformity of the edge direction) were represented as raw eight-bit data.



Figure 10: (a) Aerial image of Bhachau for automated damage detection and (b) the extracted collapsed buildings by the multi-level slice method after spatial filtering

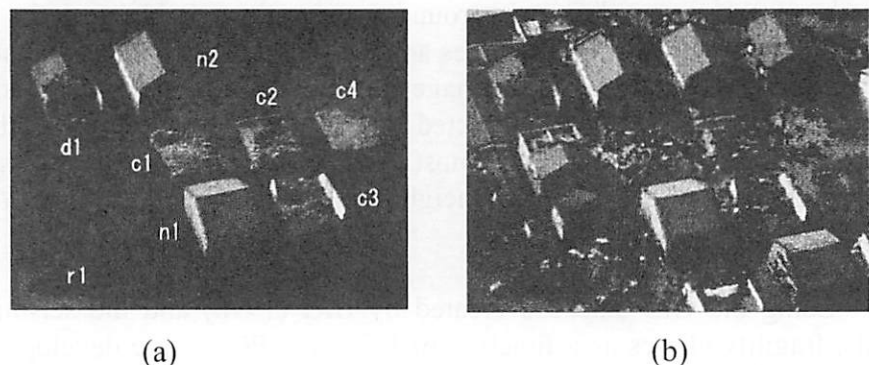


Figure 11: (a) Training data for automated damage detection (c: collapsed buildings, d: damaged building, n: non-damaged buildings, r: asphalt road) and (b) the extracted pixels as damaged buildings from the image of Anjar

Training data shown in Fig. 11 (a) were selected from the aerial image of a few houses in Anjar taken by the telephoto lens of the video camera. The cumulative relative frequency for each training datum was examined for each image characteristic, and the cumulative relative frequency of the training data was modeled by a line and the threshold value is determined for each image characteristic. Pixels within the ranges of all threshold values were regarded as corresponding to damage. Using only color indices, it was difficult to distinguish between severely damaged buildings and roads, however they could be distinguished using edge elements. The extraction result for Anjar is shown in Fig. 11 (b). Pixels of building debris were mostly extracted as damage. The extraction of pixels corresponding to building damage was also applied to aerial images of Bhachau and Bhuj using the threshold values for Anjar.

Then a spatial filtering operation was carried out to decrease surplus pixels and make it easy to identify the areas with building damage. The local density of the selected pixels was calculated by texture analysis. The window size corresponding to one building generally depended on factors such as the resolution of the image and built environment. A 31 x 31 pixel window was selected to be proportional to the scale of about one building in the aerial images and the result for Bhachau is shown in Fig. 10 (b). The result for the Bhachau image, which was obtained using the threshold values based on the Anjar image, seem to be close to the actual damage distribution. Although a good result was obtained in this example, it is suggested that threshold values for the image characteristics should be changed for each image or built environment because of the difference in some factors in each image, such as the influence of sunshine and built environment.

## **5. USE OF GIS FOR THE ESTIMATION OF SEISMIC GROUND MOTION IN THE KOBE EARTHQUAKE**

In order to evaluate the structural damage in the area affected by earthquakes, it is important to estimate the distribution of earthquake ground motion. For the 1995 Kobe earthquake, several approaches have been conducted by a number of researches. As a method to estimate the intensity of seismic motion, e.g., the peak ground acceleration (PGA) and the peak ground velocity (PGV), the damages and effects to structures/objects are often used. Because the building damage was so extensive and several coordinated damage surveys were conducted after the Kobe earthquake, the building damage distribution might be most useful to estimate the detailed strong motion distribution in Kobe and neighboring cities (Yamaguchi & Yamazaki 2001).

Using the GIS database created by BRI (1996) and the seismic records, fragility curves as a function of PGA and PGV were developed and they were used to estimate the spatial distributions of PGA and PGV. From the strong motion records obtained in the earthquake, 17 free field records were selected. Some records were not used since the number of buildings around an observation point was not enough or severe liquefaction was reported around a recording site. To construct fragility curves for buildings, the building damage ratio around each observation point was calculated. The district block (corresponding to the postal address) where a reference seismometer is placed and its surrounding blocks were selected for the corresponding area of the seismometer. In selecting the surrounding blocks, the extent of damage and the soil condition were considered. Using the relationship between the damage ratio of low-storied residential buildings and the strong motion indices, the fragility curves were constructed by the least square method on the lognormal probability paper. Based on the obtained fragility curves and the building damage ratios in all the district blocks, the spatial distributions of the strong motion indices were back-calculated for the stricken area of the Kobe earthquake as shown in Fig. 12. The estimated strong motion distribution is consistent with the string motion data used and

the reported seismic intensity distribution by the Japan Meteorological Agency (JMA 1997).

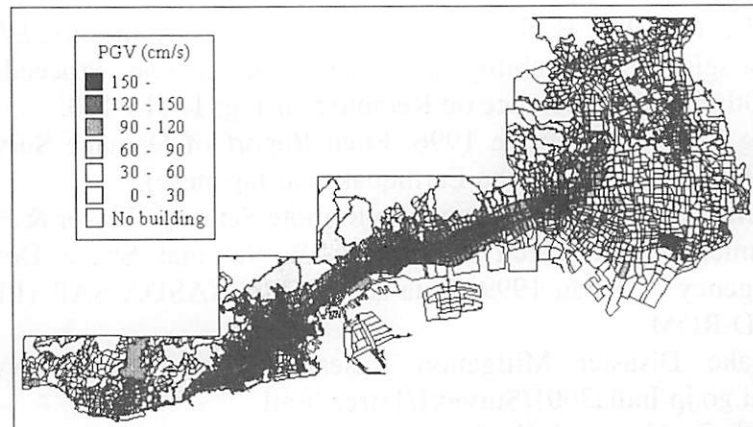


Figure 12: Distribution of the peak ground velocity (PGV) in the 1995 Kobe earthquake estimated from the damage ratio of low-storied residential buildings

## 6. CONCLUSIONS

Recent developments and applications of advanced technologies, notably, remote sensing and GIS, have been reviewed from the viewpoint of risk assessment and disaster management. Applications of these technologies in the field of “structural safety and reliability” are quite attractive and promising. Recent examples in the field of earthquake disaster mitigation were presented in this paper. Satellites with optical and/or SAR sensors can cover much larger areas than other platforms, and hence, they can be used for macro-scale urban modeling and damage detection from large-scale natural disasters. Example of change detection using the pre- and post-event satellite images were shown for the 1995 Kobe earthquake. Aerial television imagery and photography are very useful to observe buildings and infrastructures with high resolution. Thus automated detection of damage is possible using only post-event images or both pre- and post-event images, and an example of building damage detection after the 2001 Gujarat, India earthquake was provided. Use of airborne SAR for the purpose of 3D urban modeling and application of GIS to evaluate seismic ground motion from building damage data were also demonstrated.

## ACKNOWLEDGEMENT

The research outputs introduced in this paper have been produced by Dr. Masashi Matsuoka, Mr. Hirotsada Hasegawa, Mr. Naoki Ogawa, Mr. Hisashi Aoki, Mr. Hijime Mitomi and Mr. Jun Saita of Earthquake Disaster Mitigation Research Center (EDM), and Dr. Naoya Yamaguchi of University of Tokyo. Their contributions are deeply appreciated.

## REFERENCES

- Aoki, H., Matsuoka, M. & Yamazaki, F., Uratsuka, S., Kobayashi, T. & Satake, M. 1999. Backscattering characteristics of airborne SAR images for seismic vulnerability assessment in urban areas: Proceedings of the 20th Asian Conference on Remote Sensing: 1: 115-120.
- Building Research Institute 1996. Final Report of Damage Survey of the 1995 Hyogoken-Nanbu Earthquake (in Japanese).
- Campbell, J. B. 1996. Introduction to Remote Sensing. Taylor & Francis.
- Communications Research Laboratory & National Space Development Agency of Japan 1999. Data set of CRL/NASDA SAR (PI-SAR): 1. CD-ROM.
- Earthquake Disaster Mitigation Research Center: <http://www.edm.bosai.go.jp/India2001/Survey1/1strec.html>
- Eguchi, R.T., Huyck, C.K., Houshmand, B., Tralli, D.M. & Shinozuka, M. 2000a. A new application for remotely sensed data: Construction of building inventories using synthetic aperture radar technology: Proceedings of the Second Multi-lateral Workshop on Development of Earthquake and Tsunami Disaster Mitigation Technologies and Their Integration for the Asia-Pacific Region: 217-228.
- Eguchi, R.T., Huyck, C.K., Houshmand, B., Mansouri, B., Shinozuka, M., Yamazaki, F. & Matsuoka, M. 2000b. The Marmara Earthquake: A View from space: The Marmara, Turkey Earthquake of August 17, 1999: Reconnaissance Report. Technical Report MCEER-00-0001: 151-169.
- Estrada, M., Matsuoka, M. & Yamazaki, F. 2000. Use of Landsat images for the identification of damage due to the 1999 Kocaeli, Turkey earthquake: Proceedings of the 21st Asian Conference on Remote Sensing. 2: 1185-1190.
- Gamba, P. & Houshmand, B. Digital surface models and building extraction: A comparison of IFSAR and LIDAR data. IEEE Transactions on International Geoscience and Remote Sensing: 66 (7): 1959-1967.
- Hamada, M. 1992. Large ground deformations and their effects on lifelines: 1964 Niigata Earthquake. Case Studies of Liquefaction and Lifeline Performance During Past Earthquakes 1: Technical Report NCEER-92-0001: 3:1-123.
- Hamada, M., Isoyama, R. & Wakamatsu, K. 1995. The 1995 Hyogoken-Nanbu (Kobe) Earthquake, Liquefaction, Ground Displacement, and Soil Condition in Hanshin Area. Association for Development of Earthquake Prediction.
- Hasegawa, H., Yamazaki, F., Matsuoka, M. & Sekimoto, I. 2000a. Extraction of building damage due to earthquakes using aerial television images. Proceedings of 12th World Conference on Earthquake Engineering: 8p. CD-ROM.
- Hasegawa, H., Aoki, H., Yamazaki, F., Matsuoka, M. & Sekimoto, I. 2000b. Automated detection of damaged buildings using aerial HDTV images. Proceedings of the IEEE 2000 International Geoscience and Remote Sensing Symposium: 3p. CD-ROM: IEEE.

- Japan Meteorological Agency 1997. Technical Report of the Japan Meteorological Agency: 119: Report on the Hyogo-Ken-Nanbu Earthquake, 1995 (in Japanese).
- Massonnet, D., Rossi, M., Carmona, C., Adragna, F., Peltzer, G., Fiegl, K. & Rabaute, T. 1993. The displacement field of the Landers earthquake mapped by radar Interferometry. *Nature* 364: 138-142.
- Matsuoka, M. & Yamazaki, F. 1999. Characteristics of satellite images of damaged areas due to the 1995 Kobe earthquake. the Second Conference on the Applications of Remote Sensing and GIS for Disaster Management: CD-ROM, The George Washington University.
- Matsuoka, M. & Yamazaki, F. 2000a. Interferometric characterization of areas damaged by the 1995 Kobe earthquake using satellite SAR images. Proceedings of the 12th World Conference on Earthquake Engineering: 8p. CD-ROM.
- Matsuoka, M. & Yamazaki, F. 2000b. Use of Interferometric satellite SAR for earthquake damage detection. Proceedings of the 6th International Conference on Seismic Zonation: 103-108. EERI.
- Mitomi, Y. & Takeuchi, S. 1995. Analysis of spectral feature of the damaged areas by liquefaction and fire using airborne MSS data: 18th Japanese Conference on Remote Sensing: 117-118 (in Japanese).
- Mitomi, H., Yamazaki, F. & Matsuoka, M. 2000. Automated detection of building damage due to recent earthquakes using aerial television images. Proceedings of the 21st Asian Conference on Remote Sensing: 401-406.
- Mitomi, H., Yamazaki, F. & Matsuoka, M. 2001a. Development of automated extraction method for building damage area based on maximum likelihood classifier: Proceedings of the 8th International Conference on Structural Safety and Reliability: 8p. CD-ROM.
- Mitomi, H., Matsuoka, M., Yamazaki, F. & Saita, J. 2001b. Automated damage detection of buildings from aerial television images of the 2001 Gujarat, India earthquake: Proceedings of the IEEE 2001 International Geoscience and Remote Sensing Symposium 3p. CD-ROM: IEEE.
- Ogawa, N. & Yamazaki, F. 2000. Photo-Interpretation of building damage due to earthquakes using aerial photographs. Proceedings of the 12th World Conference on Earthquake Engineering: 8p. CD-ROM.
- O'Rourke, T.D., Roth, B.L. & Hamada, M. 1992. Large ground deformations and their effects on lifelines facilities: 1971 San Fernando Earthquake. Case Studies of Liquefaction and Lifeline Performance During Past Earthquakes 2: Technical Report NCEER-92-0002: 3:1-85.
- Sano, Y., O'Rourke, T.D. & Hamada, M. 1999. Permanent ground deformation due to Northridge Earthquake in the vicinity of Van Norman Complex. Proceeding of the 7th U.S.-Japan Workshop on Earthquake Resistant Design of Lifeline Facilities and Countermeasures Against Soil Liquefaction: Technical Report MCEER-99-0019: 115-130.
- Shimizu, Y., Watanabe, A., Koganemaru, K., Nakayama, W. & Yamazaki, F. 2000. Super high-density realtime disaster mitigation system. Proceedings of the 12th World Conference on Earthquake Engineering: 8. 7p. CD-ROM.

- Shinozuka, M., Ghanem, R., Houshmand, B. & Mansouri, B. 2000. Damage detection in urban areas by SAR imagery. *Journal of Engineering Mechanics* 127 (7): 769-777, ASCE.
- Shinozuka, M. & Rejaie, A. 2000. Correlational analysis of remotely sensed pre- and post-disaster images. SPIE's 7th Annual International Symposium on Smart Structures and Materials.
- Van Zyl, J.J., Zebker, H.A. & Elachi, C. 1987. Imaging Radar Polarization Signatures: Theory and Observation: *Radio Science*: 22(4): 529-543.
- Whitman, R.V., Anagnos, T, Kircher, C.A., Lagorio, H.J., Lawson, R.S. & Schneider, P. 1997. Development of a national earthquake loss estimation methodology: *Earthquake Spectra* 13(4): 643-661.
- Yamazaki, F., Katayama, T. & Yoshikawa, Y. 1994. On-line damage assessment of city gas networks based on dense earthquake monitoring. *Proceedings of 5th U.S. National Conference on Earthquake Engineering* 4: 829-837.
- Yamaguchi, N. & Yamazaki, F. 2001. Estimation of strong motion distribution in the 1995 Kobe earthquake based on building damage data: *Earthquake Engineering and Structural Dynamics* 30: 787-801.
- Yamazaki, F, Noda, S & Meguro, K. 1998. Developments of early earthquake damage assessment systems in Japan. *Structural Safety and Reliability: Proceedings of the 7th International Conference on Structural Safety and Reliability*: 1573-1580.
- Yamazaki, F. & Matsuoka, M. 1999. Remote sensing: Assessing the built environment by remote sensing technologies. *Second International Workshop on Earthquakes and Megacities*: 27-34.
- Yamazaki, F. & Murao, O. 2000. Vulnerability functions for Japanese buildings based on damage data due to the 1995 Kobe Earthquake: Implications of Recent Earthquakes on Seismic Risk. *Series of Innovation in Structures and Construction* 2: 91-102. Imperial College Press.
- Zebker, H.A., Van Zyl, J.J. & Held, D.N. 1987. Imaging radar polarimeter from wave synthesis: *Journal of Geophysical Research*: 92 (B1): 638-701.



*Prof. Fumio Yamazaki*

# **OVERVIEW OF RESEARCH ACTIVITIES RELATED TO URBAN SAFETY AT THE DEPARTMENT OF CIVIL ENGINEERING, CHULALONGKORN UNIVERSITY**

THANYAWAT POTHISIRI and BOONCHAI STITMANNAITHUM  
International Graduate Program in Civil Engineering,  
Chulalongkorn University, Bangkok, Thailand

## **1. INTRODUCTION**

The importance of the issue of public safety in the highly populated areas has recently been recognized by the modern society. The rapid increase in demand for public infrastructures in the urban areas has prompted for the construction of new civil engineering facilities (e.g., buildings, bridges, foundations, dams, etc.) to alleviate the overwhelming use of the existing ones. These public infrastructures essentially function on the daily basis and hence, consideration of the public safety is of extreme significance.

The complexity of the management system for a modern society requires that the strategy of the urban safety planning be carefully established. One of the key components of the urban safety plan is the area of research and development in the subjects related to public safety. This can be done through the educational system within the academic institutions by conducting research and arranging educational seminar to the public. Generally, the information obtained from research findings can be adopted by responsible authorities to establish rules and regulations on urban safety.

The Department of Civil Engineering, Chulalongkorn University has long been considered one of the leading academic institutions in the area of civil engineering technology in Thailand. The institution has an important role of providing information, training, as well as education in the subject of urban safety to the general public. In addition, the primary activities of the institution include research works that are related to the area of urban safety. These research works cover a vast array of subjects based on the four academic areas offered at the institution, which include construction engineering and management, geotechnical engineering, structural engineering, and transportation engineering. The overview of these researches will be described in the next section based on the specific area of specialization.

## **2. RESEARCH ACTIVITIES RELATED TO URBAN SAFETY**

The objective of this section is to present an overview of the current research works at the Department of Civil Engineering, Chulalongkorn



University that are directly related to the subject of urban safety. The research activities described as follows are based on the four academic areas discussed in the previous section.

Construction engineering and management focuses on the management of total construction operations. The study areas are project management, planning and control, the utilization of construction methods and equipment, modern techniques for decision-making in construction, quality and safety assurance for construction work as well as construction specification and legal aspects. In general, the main areas of research related to urban safety in the field of construction engineering and management are those related to construction works such as assessment, planning, and regulation of public safety during the construction projects.

Geotechnical engineering engages in the area of soil and rock research, especially Bangkok subsoil conditions. Bangkok subsoil profile and the problems of deep well pumping for water usage require considerations of safety in the design and construction process. Several laboratories were established to support both fundamental tests for practical usage and advanced tests for advanced research and development purposes at the Department of Civil Engineering, Chulalongkorn University. The research on soft clay includes conventional limit equilibrium analysis in the problems of stability of sand embankment and sheetpile, study of failure of preload embankment using normalized parameters, and ground improvement and soil modeling for predicting the stability and movement of case studies. The research on stiff clay and sand includes the study of pile capacity in Bangkok subsoils, having the tip depth of 50 to 60 meters, prediction of settlement of high-rise building, and development of soil models to predict the ground movement for the underground subway tunnels, which is under construction. Moreover, the research on the environmental impact of using landfills as foundation material is currently conducted, which includes the study of performance of sanitary landfills and the study of water quality around on-nut area.

Structural engineering primarily involves the analysis, design, and construction of civil engineering structures. The research activities in the area of structural engineering related to urban safety can be divided into three main categories. The first category is the study of wind and seismic evaluation and design of buildings at the Earthquake Engineering and Vibration Research Laboratory, Chulalongkorn University (CU-EVR). The second category is the study of fire safety of buildings at the Fire Endurance and Fire Safety Research Laboratory. The last category is the study of nondestructive assessment, repair, and rehabilitation of structural systems at the Full-Scale Structure Laboratory.

CU-EVR was established in 1986 with an aim at conducting research related to seismic hazard and seismic resistant design of buildings in Thailand as well as vibration problems due to other sources such as wind and traffic. In 1991, a cooperative program was set up between Chulalongkorn University and the Boundary Layer Wind Tunnel Laboratory



(BLWTL) of the University of Western Ontario, Canada to establish a proposed design wind map for Thailand and new design guidelines for wind loading on transmission line towers. Moreover, since 1992 the Earthquake Engineering and Vibration Research Laboratory, in joint collaboration with the Department of Public Works, Interior Ministry, has been operating a seismic monitoring program in which three buildings in Bangkok are monitored for seismic induced motion. The ultimate goal of the joint endeavor is to incorporate research findings in subsequent improvement of seismic code values in the earthquake resistant design of buildings. In addition to the structural engineering area, CU-EVR is also responsible for research on soil dynamics which currently focuses on cyclic behavior of soft Bangkok clays.

The Fire Endurance and Fire Safety Research Laboratory was established in 1994. The main objectives of this research laboratory are: 1) to study fire ratings of different construction materials and structural components; 2) to study ways to evaluate strength and safety of structures and to repair structures after fires; 3) to study ways to develop new construction materials that are suitable for fireproofing; 4) to improve construction methods for better fire safety; and 5) to promote fire safety awareness among Thai people. Because of several recent big fires in department stores and buildings, fire safety has received much more attention in Thailand. The research laboratory conducted fire rating tests for several construction materials, such as fire clay bricks, Autoclaved Aerated Concrete (AAC), and reinforced concrete, and for several structural components, including fire doors and different types of partitions. Examples of the current research projects at the laboratory are: 1) fire resistance of different types of partition, including clay bricks wall, reinforced concrete wall, AAC wall and precast panel wall; 2) fire resistance of fire doors and methods for improving fire safety performances: insulation and integrity of fire doors; and 3) the use of Perlite as fire proofing material for steel structures in Thailand. The funding for this research laboratory comes from the university research funds and from the research grants supported by private companies.

The Full-Scale Structure Laboratory comprises a 12 meters x 25 meters test floor and a 6.4 meters x 7.0 meters reaction wall. It is equipped with a 300-ton and two 150-ton actuators together with a high precision system for conducting static, dynamic or pseudo-dynamic tests. This facility greatly enhances the potential for testing large, full-scale structural components such as bridge girders or a whole story of a building frame. Current research activities include nondestructive evaluation of structural systems, development of repair and rehabilitation techniques using carbon fiber sheets, and assessment of damage in the structural systems.

Transportation engineering covers a wide spectrum of subjects from planning to operation and management of all means of transport. The research related to urban safety involves mainly in the area of urban transportation safety such as public safety research on accidents, traffic safety, and highway safety. The research projects are carried out through the

Center of Excellence on Traffic Engineering. The center is equipped with software and equipment sufficient for conducting research on road safety.

The research projects related to urban safety at the Department of Civil Engineering, Chulalongkorn University discussed above can be summarized in Table 1 in which the research topics are listed with respect to the four areas of specialization.

*Table 1: Research activities based on the specific area of specialization*

<b>Area of Specialization</b>	<b>Research Activities</b>
Construction Engineering and Management	<ul style="list-style-type: none"> <li>• A study of the relationship between accident prevention measures and accident losses in building construction sites</li> <li>• Safety system studies in construction and operation of Tanayong skytrain project</li> <li>• Safety assessment of construction sites in Bangkok</li> <li>• Safety management planning of construction firms in Thailand</li> <li>• The relationship between safety measure indicators and safety-related costs in high-rise building construction</li> </ul>
Geotechnical Engineering	<ul style="list-style-type: none"> <li>• Properties of soft marine clay and first stiff clay</li> <li>• Evaluation of available soil models for the problems of embankment stability and movements, including the problems of sheet piles stability and its movements and pile foundation problems</li> <li>• Ground improvement performance and methods of stability and settlement</li> <li>• Behavior of tunneling and methods for predicting the movement and stability</li> <li>• Soil dynamics and earthquake engineering</li> <li>• Performance of sanitary landfills in Thailand</li> <li>• Study of water quality around on-nut area</li> </ul>
Structural Engineering	<ul style="list-style-type: none"> <li>• Development of cementitious fire proofing for steel members using Perlite</li> <li>• Behavior of steel sections with large section factors (<math>H_p/A</math>) under fire</li> <li>• Post-fire behavior of reinforced concrete beams</li> <li>• Improvement of fire endurance for post-tensioned slabs</li> <li>• Seismic analysis and design of reinforced concrete structures</li> <li>• Vulnerability study of buildings in low to moderate seismic zones</li> <li>• Cyclic behavior of reinforced concrete components such as columns and shear walls</li> <li>• Improvement of ductility of reinforced concrete tied columns</li> <li>• Passive and semi-active control of building vibrations under major distant earthquakes</li> <li>• Structural assessment, repair, and rehabilitation</li> </ul>

*Table 1(continued): Research activities based on the specific area of specialization*

Transportation Engineering	<ul style="list-style-type: none"> <li>• The analysis of etiology and priority improvement of traffic accident</li> <li>• Evaluation of some remedy measures of roadway traffic accidents</li> <li>• The use of dynamic programming with roadway traffic accident improvement program</li> <li>• Patterns and traffic impact of incidents on expressways: a case study of the first and second stage expressing systems</li> </ul>
----------------------------	--

### 3. COLLABORATION OF ACADEMIC DEPARTMENTS ON RESEARCH PROJECTS

The Department of Civil of Engineering has established a strong collaboration on research activities related to urban safety with other academic departments at the Faculty of Engineering, Chulalongkorn University. The joint research projects include the study of flood control, ground water contamination, and coastal engineering with the Department of Water Resources Engineering, and the development of GIS remote sensing with the Department of Survey Engineering.

### 4. CONCLUSIONS

The overview of the research activities related to urban safety at the Department of Civil Engineering, Chulalongkorn University was presented. In addition, it was shown that the Department of Civil Engineering houses a number of research facilities to accommodate the research projects that are directly related to urban safety. Based on the specific areas of specialization offered at the department, the research area related to urban safety was divided into four main categories, i.e., construction engineering and management, geotechnical engineering, structural engineering, and transportation engineering. The research topics related to urban safety are summarized with respect to these areas of specialization. It is the authors' expectation that with the continuing support from the university research funds and research grants from private companies, the Department of Civil Engineering, Chulalongkorn University will continue to conduct research that will become tremendously beneficial to the public in the area of urban safety for a sustainable development of the nation.



***Dr. Boonchai Stitmannathum***

# **ASSESSMENT OF URBAN SAFETY AND ENVIRONMENT BY USE OF REMOTE SENSING**

YOSHIFUMI YASUOKA  
International Center for Urban Safety Engineering (ICUS/INCEDE),  
IIS, The University of Tokyo, Japan

## **1. INTRODUCTION**

Degradation of infrastructure and environment in Asian mega-cities has become critical social problems during the past decade. In Japan, for example, we have suffered from serious floods in urban areas due to unexpected heavy rain and due to insufficient urban infrastructure. We have also experienced risky concrete block falls in railway tunnels or under highway bridges due to concrete degradation. Rapid urbanization has provided with the increased convenience and benefit for people living there, however, on the other hand it has caused serious urban problems and has sometimes sacrificed urban sustainability and safety.

Monitoring of urban infrastructures or environment is essential to the proper management of urban safety or sustainability. However, it requires the measurement of wide variety of parameters covering physical, chemical, biological, or geographical aspects. Furthermore it needs to monitor spatial distribution of parameters covering from local to regional scale and from short to long time scale. It is, therefore, not easy to monitor parameters and to establish database system for urban safety and sustainability only with conventional ground survey methods. Remote sensing from space is expected to provide a new tool for observing wide range of variables over extensive areas regularly.

Development of remote sensing technology has been very rapid, and today various types of remotely sensed data are available ranging from high spatial resolution sensor data to coarse but wide coverage sensor data, and they are covering land, ocean and atmosphere. It is, however, not easy to extract effective information for urban safety from enormous amount of data. In this presentation new technologies in remote sensing are surveyed, and their application to urban safety assessment is introduced.

## **2. NEW TECHNICAL DEVELOPMENT OF REMOTE SENSING**

### **2.1 Hyper-spatial Observation**

Spatial resolution is one of the most important observation performances in remote sensing, and it has been drastically improved these twenty years. One meter spatial resolution is now realized in IKONOS and

ORVVIEW, and from these images we can identify buildings, roads or tree canopies in urban areas. High spatial resolution observation will enable us to retrieve more detail information on urban infrastructures, land surface characteristics or land topography from remotely sensed data.

## **2.2 Hyper-spectral Observation**

Number of spectral channels in conventional remote sensors has been limited to ten or at most to several tens in satellite and airborne systems. New hyper-spectral sensors have the capability of observing land surface in a couple of hundreds channels. For example, the Hyperion on EO-1 launched last year has 256 channels. Airborne sensor systems such as CASI and AVIRIS have also around two hundreds channels or more, and their spectral wavelength resolution is as narrow as several nanometers. Data from the hyper-spectral sensors has indicated the possibility of observing new parameters including detail vegetation categories, stress conditions of vegetations or materials of constructions, or stress condition in vegetation or detail vegetation categories, which could not be observed by the conventional sensors.

## **2.3 Microwave Range Observation**

With optical remote sensing ground conditions may not be observed through cloud or haze. Microwave remote sensing has an advantage of cloud and haze free (all weather) observation due to its longer wavelength characteristics. This observation capability enables us to monitor land surface conditions regularly even in heavily clouded regions including tropical regions or high latitude regions. Also microwave remote sensing has a possibility of monitoring land surface relief or soil moisture which may not be obtained by optical remote sensing.

## **2.4 Sensor Fusion and Data Integration**

Integration of data from multiple different sensor systems may provide us with more detail information that may not be retrieved from the data obtained by one single sensor. For example, combination between microwave sensor data (SAR) and optical sensor data provides new information on land surface characteristics. Also integration of data from an old sensor and the latest sensor enables us to monitor long-term land surface changes. It plays important role for assessing urban history.

## **2.5 Scaling between low resolution and high resolution sensor data**

High spatial resolution data (e.g. LANDSAT TM or SPOT HRV data) does not cover the whole continent or globe because of its narrow coverage. Combination between high spatial resolution data with low resolution but wide coverage data (e.g. NOAA AVHRR data) enables to extrapolate local information from high spatial resolution data to global scale by introducing the scaling model between them. Scaling is a way to link local with regional,

and one of the most important concepts in applying remote sensing to environment and disaster monitoring.

## 2.6 Coupling remote sensing with modeling

Physical or mathematical models play a vital role in predicting the future environment. Precipitation and weather conditions in the future are, for example, key parameters to manage urban sustainability. However it has been difficult to obtain various parameters or boundary condition data for models in two or three dimensions. Remote sensing is expected to provide boundary conditions or parameters to climate models or environmental models.

## 3. APPLICATION EXAMPLES OF REMOTE SENSING TO URBAN SUSTAINABILITY ASSESSMENT

Development of remote sensing technologies has been very rapid, and huge amount of data is now available for us. Then, how can we utilize these data for urban monitoring? In the following sections, two examples of remote sensing application to urban safety and sustainability assessment are introduced.

### 3.1 Monitoring of Urban Expansion with Satellite Images

History of urban expansion is one of the most important parameters in assessing urban safety and sustainability. However long-term monitoring of land surface condition in urban areas is not easy only with ground survey since it requires monitoring of complicated spatial structures of buildings, vegetations or roads.

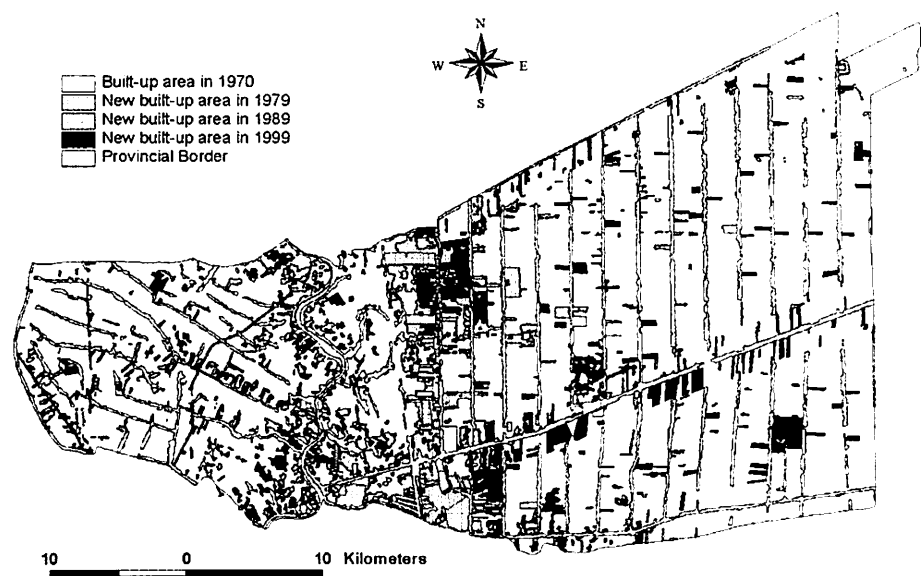


Figure 1: Urban Expansion in Pathum Thani area in Bangkok (1970-1999)

In this study spatial data analysis methods were investigated to assess spatial distribution of urban expansion by combining remote sensing and geographic information system (GIS). An example in Fig.1 demonstrates the assessment of urban growth around Pathum Thani area near Bangkok, Thailand from satellite data <sup>(1)</sup>. It shows the rapid expansion of built-up areas around Bangkok, and indicates the changes in population, environment and other social factors. Spatial analysis with remote sensing and GIS enables us to measure changes in spatial and temporal structures of urban areas, and further to integrate different characteristics including environment, disaster or socio-economic factors to assess urban sustainability and safety.

### **3.2 Monitoring of Concrete Degradation with Hyper-spectral measurement**

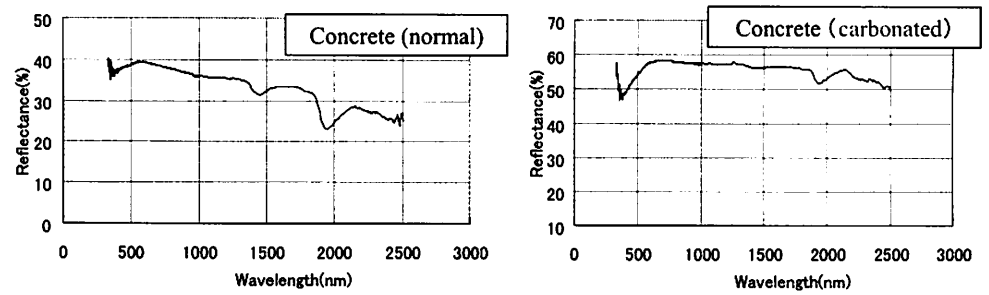
Concrete is one of the basic materials supporting our life, and therefore its proper management is of high priority for the maintenance of urban infrastructure. As shown in the accidents of concrete block falls in tunnels or under bridges in Japan, degradation of artificial constructions will be increased in most of urban areas, and therefore, it is highly urgent to develop an efficient inspection method for concrete degradation of buildings, bridges or highways.

In this study a non-destructive inspection method was investigated to assess concrete degradation due to carbonization, salt injury and sulfate degradation with hyper-spectral remote sensing on the ground. Figure 2 shows examples of spectral characteristics of normal concrete and the degraded concrete due to carbonization, and it shows the clear difference in spectral signatures in mid-infrared spectral range. This spectral signature difference may enable us to assess concrete degradation. The statistical analysis shows very high correlation between the spectral reflectance at specific wavelengths and the degradation depth of concrete (Fig.2 (c)), and the result indicates the possibility of concrete degradation assessment with hyper-spectral measurement. Hyper-spectral measurement is one of the most advanced remote sensing methods, and it may provide us with an efficient monitoring method of urban infrastructure including buildings, roads or tunnels by using vehicles, aircrafts or satellites.

## **4. CONCLUSIONS**

Application of remote sensing to urban safety and sustainability assessment was introduced. Most of the Asian mega-cities have been suffering from various kinds of infrastructure degradation and environmental degradation due to rapid urbanization. It may lead to more serious physical and social disasters in the near future. Establishing efficient monitoring system and database system for urban safety and sustainability is now urgent tasks.



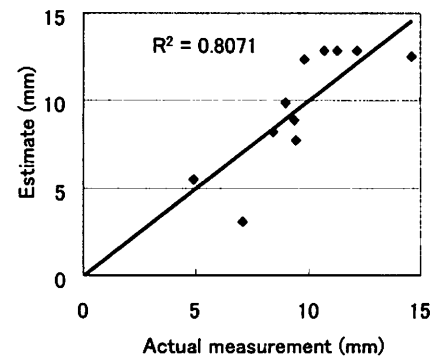


(a)

(b)

Upper: Spectral characteristics of normal and neutralized concrete. At the two specific wavelengths differences are clear.

Right: Comparison between the estimated and the observed neutralized depth.



$$H = 275.3X'_{440} + 531.0X'_{1500} + 506.9X'_{2341} + 4.4 \quad (c)$$

Figure 2: Spectral characteristics of concrete degradation by hyper-spectral measurement. (a) Spectral characteristics of normal concrete. (b) Spectral characteristics of carbonated concrete. (c) Comparison of the observed and the estimated degradation depth from spectral characteristics. The degradation depth  $H$  is estimated from the first derivative values of spectral reflectance at three wavelengths.

**REFERENCES**

1. Tran Hung, Y. Yasuoka (1999): Integration and Application of Socio-economic and Environmental Data within GIS for Development Study in Thailand, Proc. of the 20th Asian Conference on Remote Sensing.
2. Jun Arita, K. Sasaki, T. Endo, Y. Yasuoka (2001): Assessment of Concrete Degradation with Hyper-spectral Remote Sensing, Proc. of the 22<sup>nd</sup> Asian Conference on Remote Sensing.



*Prof. Yoshifumi Yasuoka*

# WAVELET AND SCALE-SPACE THEORY IN SEGMENTATION OF AIRBORNE LASER SCANNER DATA

T.THUY VU and MITSUHARU TOKUNAGA  
Space Technology Applications and Research  
Asian Institute of Technology, Thailand

## ABSTRACT

*An important property of any object in the world is that it only appears over a certain ranges of scales. Therefore, the scales should be considered in describing or analyzing of an object. Scale-space theory has been well developed in computer vision. Recent years, wavelet, a new and impressive mathematical tool, which can be said as an evolution of scale-space theory, has raised the consideration of the scientists in many fields including geoinformatics. Based on the idea well developed in pattern recognition, this paper is aimed to introduce the application of wavelet in segmentation algorithms of airborne laser scanner. In this paper, a segmentation wavelet based framework was set up. Afterwards, several experiments applied in testing site were done to prove the feasibility of proposed method in segmentation of airborne laser scanner data. This work is only a part of author's doctoral dissertation. As a consequence, this paper only presents the preliminary results of this work and the further developments will be pointed out.*

*Keywords: Wavelet, Airborne Laser Scanner, Segmentation*

## 1. INTRODUCTION

Airborne laser scanner was introduced as a high accurate tool for topographic mapping. There have been several attempts in both research and application to utilize this useful tool. However, the algorithm for segmentation of this kind of data, i.e. distinguish between ground surface and objects on the surface, is still on going researched. Several recent researches can be listed as Haala et al. 1998 derive parameters for 3-D CAD models of basic building primitives by least-squares adjustment minimizing the distance between a laser scanning digital surface model and corresponding points on a building primitive; Axelsson, 1999 introduced the classification algorithm based on the Minimum Description Length criterion; Maas and Vosselman, 1999 proposed two algorithms for extracting building from raw laser data; Haala et al. 1999 integrated multi-spectral imagery and laser scanner data to extract buildings and trees in urban environment. This research is aim to follow these attempts with a new approach, i.e. usage of scale information.

As been known, an important property of any object in the world is that it exists as a meaningful entity in the certain ranges of scale. Therefore, object appears in different ways depending on the scales of observation. Consequently, the analysis must depend on the scale of observation called multi-scale representation. Especially, the need of multi-scale representation is increasing when automatically deriving information from the acquired signals of objects in the worlds, like feature classification, feature extraction. Then, a very important question is opened; with a specific object, what the proper scale for information extraction is. In normal case, it is not obvious to determine in advance this proper scale. Therefore, the analysis of object should take over the whole scale space and then the proper scale is selected. Scale-space theory is a general framework that is generated by the computer vision theory for representing image data and the multi-scale nature of it at the very earliest stages in the chain of visual processing that is aims at understanding (perception) (Lindeberg, 1994).

Wavelet, which can be called an evolution of scale space theory, is linear scale space representation, which developed by many scientists from different fields and based on a solid mathematical background. The first idea of wavelet system was introduced by Alfred Haar in 1910. However, it has been mostly developed since last fifteen years in connection with many older ideas from other fields. The fundamental idea of wavelet is to analyze the signal according to scale or resolution. In this paper, a wavelet-based feature extraction method that is based on the algorithm introduced by Mallat and Zhong, 1992 was utilized in airborne laser scanner data. By utilizing the scale information, the difficulty in segmentation of airborne laser scanner was decreased.

## 2. METHODOLOGY

Airborne laser scanner data (see Table 1) provided by Kokusai Kogyo Co., Ltd. Geomatics Department with the acquired site in Japan was used in this research. The summarized flow chart of processing is illustrated in Figure 1.

*Table 1: Airborne Laser Data characteristics*

Operation Altitude	10,000 feet AGL max
Scan Swath Width	200m - 2000m
FOV	45 degrees max
Pulse Rate	15Khz max
Returns	5 @ 15Khz
Cross Track Spacing	1-8 meters
Along Track Spacing	2.5 - ? Meters (aircraft speed dependent)
X, Y Positional Accuracy	0.3 meters RMSE absolute
Z Positional Accuracy	0.15 meters RMSE absolute

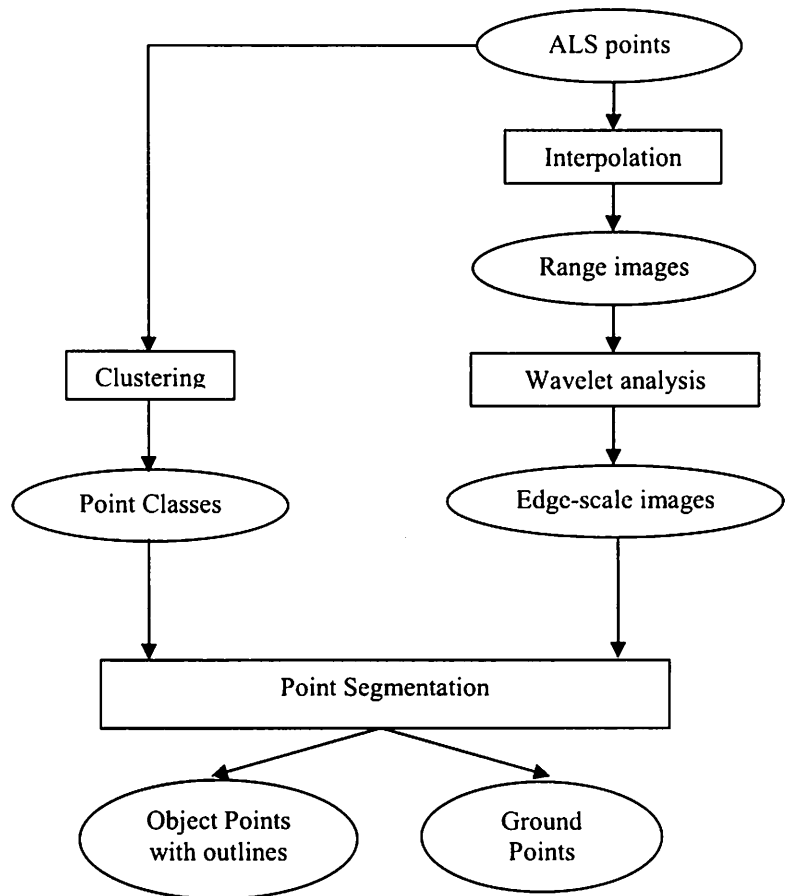


Figure 1: Flowchart of processing

### 3. RESULT AND DISCUSSION

After flying, a set of points with X, Y, Z value was acquired. In this paper, the study area with high density of building was considered; it is Roppongi region of Tokyo City, Japan. As mentioned, full information of object in 3-dimension space was considered in this paper in which the height information was analyzed through Z value of airborne laser points and the size of objects in horizontal plane through scale analysis, i.e. wavelet analysis.

To segment airborne laser scanner points in height, K-mean clustering was applied in Z value. Depending on the knowledge about study area, the number of class was given for driving the clustering. The result of K-mean clustering of our testing is illustrated in Figure 2 below. Being separated well by K-mean clustering of Z value, the airborne laser points presents three classes: high building, ground and others. There is an ambiguity in the third class, i.e. low building, highway and tree. However, these kinds of objects have different sizes in horizontal plane that might be distinguished by scale analysis.

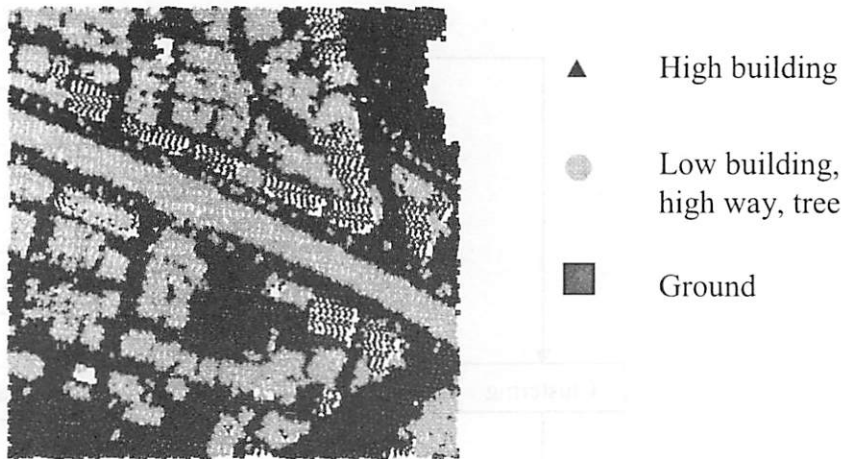


Figure 2: Cluster points using K-mean algorithm

Before utilizing of wavelet analysis, airborne laser points were interpolated to grid in which the laser data points have been triangulated, and then from irregular to regular grid. As a consequence, the range image is shown in Figure 3 with the grid size of 0.5 meter.

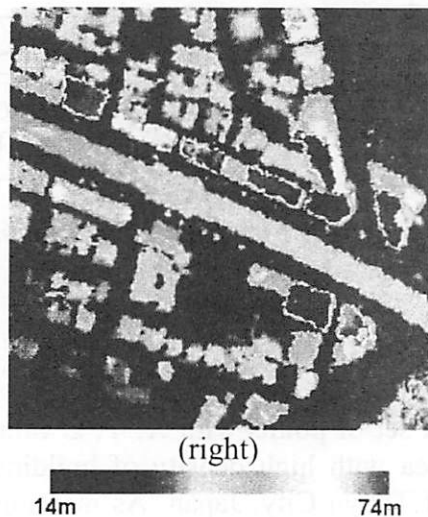


Figure 3: Range image of Roppongi area, Tokyo, Japan generated by rasterizing laser points – size 512x512; 0.5 meter grid size

The wavelet-based method proposed by Mallat and Zhong, 1992, which illustrated the equivalence of multi-scale Canny edge detector and detecting modulus maxima in two-dimensional dyadic wavelet transform, was implemented in this research for airborne laser scanner data. The general idea can be expressed as follow. The dyadic wavelet transform generated the smooth version of range images at several scales depending on the given number of maximum scale. Let  $S_1$  and  $S_2$  are two successive scales. The edges of objects with size in the range of  $S_1$  and  $S_2$  appeared in the differences between smooth version at scale  $S_1$  and one at  $S_2$ . These results are presented in Figure 4 below in which the different smooth versions of range images are shown along with edge images. Due to the limitation of paper length, only two examples of smooth images are

illustrated here. As can be seen easily in Figure 4, some details were disappeared when moving to the coarser scale. The remained task is how to select the proper scale of each kind of objects on the Earth surface.

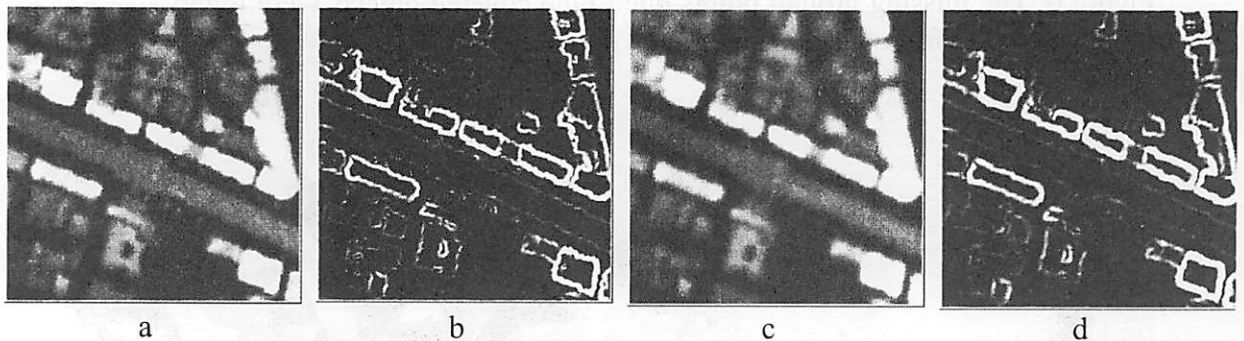


Figure 4: Smooth image at 2m (a) and modulus edge image 1m-2m (b) Smooth image at 4m (c) and modulus edge image 2m-4m (d)

Based on the signature of edge in scale space, the selection of proper scales for each kind of objects was done. As a consequence, there were three kinds of objects that could be distinguished, say high way, building and tree. This segmentation (see Figure 5) was converted to vector format in order to use for the combined segmentation later with laser points. Due to the complicated scene in the urban area, i.e. high density of building, the segmentation based on the edge introduced some ambiguity, especially when the building is a block of some others. This problem can be adjusted by using paper map. With the purpose to illustrate the capability of wavelet-based method, this paper did not validate with paper map as mentioned. The result shown in Figure 5, then, was used for combined segmentation with laser point clusters.

## Segmentation Scene

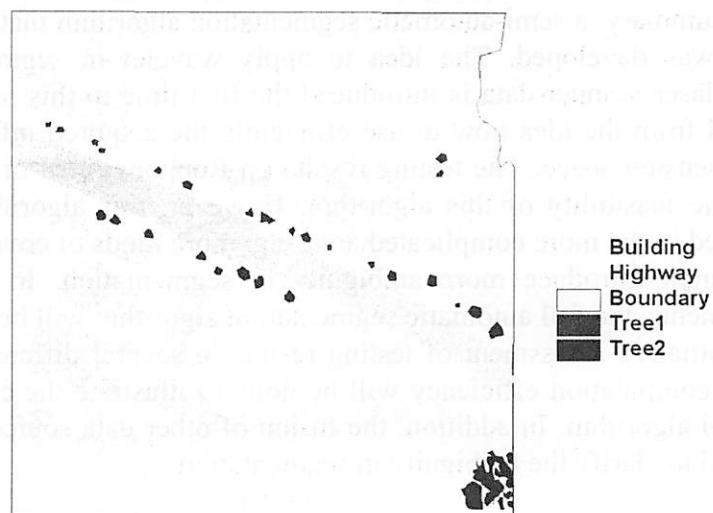


Figure 5: Scale space segmentation result

The combined segmentation was based on a developed vector-based algorithm, i.e. point in polygon. As a result, the points were classified as

ground points and object points. These two sets of point, afterwards, were triangulated to generate the Digital Terrain Model - DTM (bare Earth surface) and Digital Surface Model – DSM (with objects) as can be seen in Figure 6. The missing ground points due to the covered objects were found by interpolation from the existing ground points.

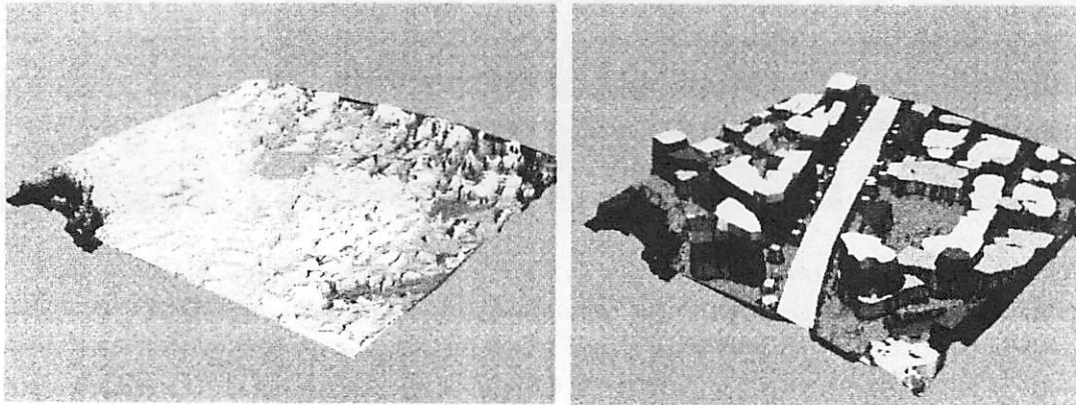


Figure 6: DTM (left) and DSM (right)

This paper is just a part of author's doctoral dissertation in which a full automatic segmentation framework will be developed. Therefore, only some preliminary results were presented in this paper. The validation of results as well as the assessment of algorithm capability should be done and will be presented in the next papers. In addition, this developed algorithm should be tested in several kinds of sites, which cannot be done due to the limitation of time and data.

#### 4. CONCLUSION

In summary, a semi-automatic segmentation algorithm that is based on wavelet was developed. The idea to apply wavelet in segmentation of airborne laser scanner data is introduced the first time in this paper. It was generated from the idea how to use efficiently the acquired information in three-dimension space. The testing results on Roppongi area of Tokyo city proved the feasibility of this algorithm. However, this algorithm has not been tested in the more complicated area, e.g. more kinds of covered objects, which might introduce more ambiguity in segmentation. In the further improvements, the full automatic segmentation algorithm will be developed. The quantitative assessment of testing results in several different kinds of area and computation efficiency will be done to illustrate the capability of developed algorithm. In addition, the fusion of other data sources might be performed to clarify the ambiguity in segmentation.

#### ACKNOWLEDGEMENT

The authors would acknowledge Kokusai Kogyo Co., Ltd. Geomatics Department for providing the necessary data for this research.



## REFERENCES

- Axelsson, P., 1999. Processing of laser scanner data – algorithms and applications. *ISPRS Journal of Photogrammetry & Remote Sensing*, 54, pp. 138-147.
- Haala, N. and Brenner, C., 1999. Extraction of buildings and trees in urban environment. *ISPRS Journal of Photogrammetry & Remote Sensing*, 54, pp. 130-137.
- Lindeberg, T., 1994. Scale-space theory: a basic tool for analyzing structures at different scales. *Journal of Applied Statistics*, 21(2), pp. 225-270.
- Maas, H. G. and Vosselman, G., 1999. Two algorithms for extracting building models from raw laser altimetry data. *ISPRS Journal of Photogrammetry & Remote Sensing*, 54, pp. 153-163.
- Mallat, S., 1998. *A Wavelet tour of signal processing*. Academic Press, UK.
- Prasad, L., and Iyengar, S. S., 1997. *Wavelet Analysis with application to image processing*. CRC Press LLC, Florida, USA.



*Dr. Mitsuharu Tokunaga*



# **REMOTE SENSING AND GIS ACTIVITIES IN ASIAN INSTITUTE OF TECHNOLOGY: EDUCATION, TRAINING AND RESEARCH**

KIYOSHI HONDA  
Space Technology Applications and Research (STAR) Program,  
Asian Institute of Technology, Thailand

## **ABSTRACT**

*Asian Institute of Technology (AIT) is an international academic institute that was established in 1959. Remote Sensing was introduced as a subject in 1979 with the establishment of the Asian Regional Remote Sensing Training Center (ARRSTC)". Since then Remote Sensing gained importance and finally a full educational program named Space Technology Applications and Research (STAR) was established in 1995. The STAR program confers Master and Doctor degrees to its students. The GIS Application Center (GAC) and the Asian Center for Research on Remote Sensing (ACRoRS) were established in 1995 and 1997 respectively, to promote training and research beyond the existing academic opportunities. The STAR program, GAC and ACRoRS work closely for the development and dissemination of GIS and Remote Sensing technology.*

## **1. INTRODUCTION**

Asian Institute of Technology (AIT) is an international graduate school located 42 km to the north of Bangkok, Thailand. The institute was founded in 1959 as a Southeast Asian Treaty Organization (SEATO) Graduate School of Engineering, which in turn became the Asian Institute of Technology (AIT) in 1967, an international graduate school, empowered to confer Doctor, Master and Diploma degrees to its graduates. Fully donor supported, the institute has continued to grow since its beginning with a multi-national environment of 1,400 students from more than 40 countries and a present faculty body of 148 from 29 countries. AIT has more than 10,000 alumni in Asia and all over the world.

Remote Sensing was introduced as a subject in 1979 with the establishment of the "Asian Regional Remote Sensing Training Center (ARRSTC)". Since then the importance of the field of Remote Sensing to development in Asia has increased, and led to the establishment of the Space Technology Applications and Research (STAR) Program in 1995. To promote training and research activities beyond traditional academic offerings, two more centers the GIS Application Center (GAC) and Asian Center for Research on Remote Sensing (ACRoRS) came into existence in 1995 and 1997 respectively.

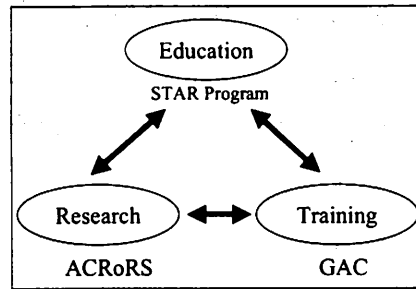


Figure 1: Structure of the three components

AIT has adopted an integrated approach to develop all three components, namely, Education, Training and Research in the field of Remote Sensing and GIS. These three components share resources such as human resources, equipments, data, Internet, research opportunities and etc. to maximize efficiency and productivity. Research experiences in ACRoRS are transferred to the education component, which in turn develop the human resources. Training materials are prepared from the research work carried out in ACRoRS.

Experiencing the expansion of applications of Remote Sensing and GIS, role of these three components are defined as technology partner and technology developer as shown in Table 1. As a technology partner, an institute-wide GIS and Remote Sensing Laboratory has been established to provide education and research opportunities to the entire AIT community. Short-term training courses on Remote Sensing and GIS are organized by GAC for users from all across the Asia-Pacific region. Training materials for various application fields are prepared by GAC from various research projects carried out in ACRoRS. Technical assistance and consulting services are provided by ACRoRS according to user needs. As a technology developer, student's expertise is used for developing new technologies through their Master and Doctor thesis work. ACRoRS has been involved in research projects through which in-house and applicable technologies in RS and GIS have been developed.

Table 1: Focus of three components

<b>Components</b>	<b>Technology Partner</b>	<b>Technology Developer</b>
Education	1) Institute-wide GIS course 2) Operation of Institute Wide GIS and RS Laboratory	Student and faculties in technology development
Training	Training course on Remote Sensing & GIS Material for applications development based on research	
Research	Technical assistance Consultancy	Research project for technology development

ACRoRS and GAC are housed in newly constructed Geoinformatics Center as shown in Figure 2. HRH Princess Maha Chakri Sirindhorn of the Thai Royal family graciously inaugurated this center in February 1999.



Figure 2: Geoinformatics Center in AIT

## 2. EDUCATION (STAR PROGRAM)

At AIT, the STAR program offers Diploma, Master and Doctor degrees with a focus on formal graduate training. The Master degree is comprised of 5 terms that runs for a total of 20 months with intake in May and graduation in the December of the following year. Students complete a minimum course work of 30 credits within 12 months for the Master degree. After successful completion of the course work, each of the students performs research work for another period of 8 months with 20 credits. The thesis topic is based on personal interest of the student, their specialization and extensive discussions with their thesis advisors. Subjects have traditionally been application based. Recently however, theses, which are more tools and technique development oriented, have been encouraged in order to complement applications experience and build in-house capabilities as a technology developer. The Doctor program typically lasts a minimum of three years, with a classroom requirement of 18 credits within the first 12 months. During their course work, students consult with their advisors and develop a proposal for their topic of interest for the Doctor thesis. After defending the thesis research proposal at the end of the first year, students concentrate on research work for the remaining period of time, with periodic progress reports that have to be passed if candidacy for the degree is to be maintained. Entry into the Doctor program occurs three times in a year, typically with the start of term in January, May or September.

STAR students are working in a wide range of fields for Master and Doctor theses. Most recently accomplished Master theses are:

- 1) Dynamic Spatial Modeling for Tourism Carrying Capacity in Thailand
- 2) A Model for Estimating Tea Yield by Combining Remote Sensing Parameters and GIS in Tea Plantations in Sri Lanka
- 3) Effect of Coherence of DEMs Derived from SAR Interferometry in Mayon Volcano in the Philippines
- 4) Real Time Volcano Activity Mapping System with Ground Fixed Single Digital Camera.
- 5) Oil Spill Detection Using JERS-1 L-band SAR Data for Oil Discharge from Ships in the East China Sea

- 6) Agricultural Drought Monitoring and Assessment using Remote Sensing and GIS
- 7) Rice Crop Yield Estimation Using RS and GIS: Acas Study in Subang, West Java, Inodensia.
- 8) Automatic Recognition and Location of Road Signs from Terrestrial Color Imagery
- 9) Estimation of Methane Emission from Deep-Water Rice Field Using RS: A Case Study of the Central Plain of Thailand

Being a part of AIT, the STAR Program also maintains a multi-national environment. Since its establishment in 1995, the STAR Program has enrolled 127 Master degree and 24 Doctor degree students. A detailed list student with nationalities is given in Table 2.

Table 2: Students in STAR Program since 1995

<i>Country</i>	<i>Master</i>	<i>Doctor</i>	<i>Total</i>
Thailand	18	10	28
Nepal	13	2	15
Vietnam	12	2	14
Laos	11	1	12
China	8	3	11
Philippines	9	1	10
Indonesia	9	-	9
Bangladesh	8	-	8
India	6	1	7
Sri Lanka	6	1	7
Cambodia	6	-	6
Pakistan	4	-	4
USA	3	1	4
Azerbaijan	3	-	3
Bhutan	3		3
Myanmar	1	1	2
Ethiopia	0	1	1
France	1	-	1
Japan	1	-	1
Korea	1	-	1
Malaysia	1	-	1
Mongolia	1	-	1
Netherlands	1	-	1
Papua New Guinea	1	-	1
Total	127	24	151

STAR students enjoy extensive modern facilities within the program. In recent times there has been a shift from analog to digital system in the field of geoinformatics. Spatial data handling requires high-end computing resources because spatial data is huge. The STAR Program has the most advanced commercially available computing resources. The list of hardware and software are given in the following page.

- 1) Server System
  - NT Server System (2)
  - UNIX Workstations (3)
- 2) Digital Image Processing Laboratory
  - with high end PC (15)
  - Remote Sensing and GIS Software
  - Development Environment
- 3) Institute Wide GIS and RS Laboratory
  - Pentium-III PC (15)
  - Remote Sensing and GIS Software

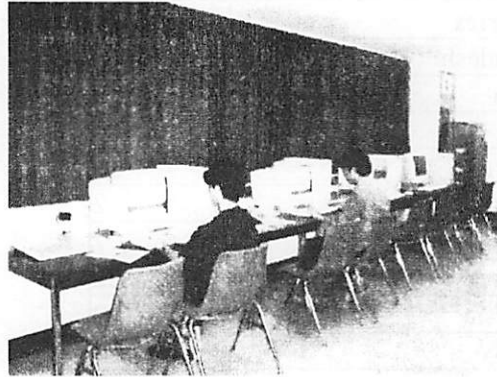


Figure 3: Institute Wide GIS and RS Laboratory

### 3. TRAINING (GAC)

Training programs on RS and GIS in AIT are conducted by the GIS Application Center (GAC). GAC was established in 1995 with initial financial support from United Nations Environment Program (UNEP) as a non-profit training center in the field of Remote Sensing and GIS. GAC offers training particularly to the scientists, engineers, planners and managers of the development agencies of the Asia-Pacific region. The training courses are carefully designed to meet the requirements of the region and are updated from time to time on basis of the research experience gained. The training programs conducted by GAC are applications of Remote Sensing and GIS in the issues that need urgent attention with an emphasis on its integration such as implementation of water run-off model, soil erosion estimation model and so on. Three types of training programs are conducted by GAC every year. Those training programs are classified as regular, sponsored and tailored. Regular training programs are offered at the basic or advanced level on general topics of GIS and Remote Sensing. Sponsored courses are offered with financial support from donor agencies. Tailored courses are designed as per specific requirements of an organization to train their staff in a particular application of Remote Sensing and GIS technology.

GAC has been organizing in various countries by sending its teaching team, which is so called caravan type training course. This type of training course is efficient to reach to many people in a country. GAC training has been sponsored by the National Space Development Agency of Japan

(NASDA), Remote Sensing Technology Center of Japan (RESTEC). United Nations Development Program (UNDP), Food and Agriculture Organization (FAO), Japanese International Cooperation Agency (JICA), World Health Organization (WHO) and Deutsche Gesellschaft für Technische Zusammenarbeit (GTZ).

GAC has trained 732 professionals from all over the Asia-Pacific region and representatives from various countries are shown in Table 3.

*Table 3: Trainees in GAC since 1996-2001 March*

<b>Countries</b>	<b>Trainees</b>
Bangladesh	69
Bhutan	5
Brunei	6
Cambodia	53
Ethiopia	2
Fiji	7
India	22
Indonesia	89
Korea	2
Laos	19
Malaysia	46
Mongolia	9
Myanmar	33
Nepal	62
Pakistan	17
Peoples's Republic of China	4
Philippines	45
Singapore	5
Sri Lanka	55
Taiwan	19
Thailand	107
United Kingdom	2
Vietnam	54
Total	732

The major training courses for the year 2002-2003 are as follows:

- Watershed Management
- SAR data potential
- Coastal zone monitoring and management
- Open GIS for Spatial Information Sharing
- GIS and RS for Disaster Mitigation
- Low-Moderate Resolution Remote Sensing





*Figure 4: Participants in GAC training*

#### **4. RESEARCH (ACRoRS)**

The research component is primarily carried out by the Asian Center for Research on Remote Sensing, a research laboratory dedicated to the development of geoinformatics science comprising Remote Sensing, GIS and GPS. ACRoRS is a self-funded, non-profit research center under AIT having the privilege of being a research center of the Asian Association on Remote Sensing (AARS). ACRoRS has the mandate of monitoring the environmental trends in the region, both in spatial and temporal basis. This often involves the collection and analysis of Remote Sensing data along with conceptual and numerical models providing comprehensive understanding of the trends of prevalent environmental phenomenon. In recent years, there has been an increased demand for resources in the Asia-Pacific region due to an explosion of population. As a result, a number of environmental problems have arisen. Keeping the importance of such problems in view, ACRoRS is carrying out various research projects to address these problems using Remote Sensing and GIS technologies. Through research activities, the Center is aiming at developing applicable in-house technologies. These technologies and research experiences are transferred to region through education and training activities. Currently four programs are being implemented in the Center, namely, Co-operative Research Program, Training Support Program, Research Promotion Program and Consultant Service Program. Through Co-operative Research Program, several research programs have been jointly organized with various institutions and in some of the cases researchers stay in the Center during the program. Under the Training Support Program, training materials have been prepared by the Center. Research Promotion Program includes processing and distribution of TERRA/MODIS, NOAA/AVHRR data, distribution of Japanese Satellite data with necessary technical support, contract research as well as own research. Consultant Service Program is basically aimed at providing technical help to the users. The center is also aiming at growing up young researchers and engineers, which is still only a thin layer in the region. Many of STAR graduates have obtained a chance to be involved in research projects, practical consulting

projects, based on which, some staffs have already graduated the center for further study or carrier.

## 5. FACILITIES IN ACRoRS

ACRoRS has been operating a NOAA AVHRR data receiving station since 1997, which marked the beginning of ACRoRS activities to serve data to the Remote Sensing community of the Asia-Pacific region. Also it started to operate MODIS receiving station in May 2001. All data are received and archived in ACRoRS and made available for distribution at a marginal cost.

There is a kinematic GPS base station. Within a radius of 40 km of AIT, this station provides a measurement accuracy of 20 cm for GPS users. A roving field station is connected by mobile telephone.

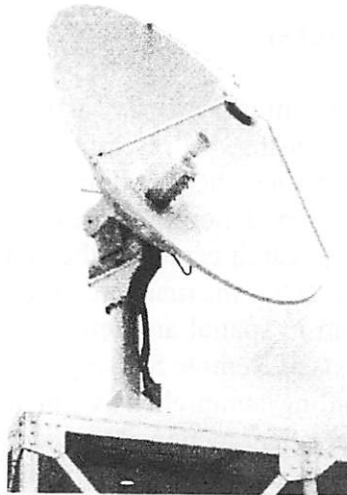


*Figure 5: 2.8m X-band antenna for MODIS Receiving*

ACRoRS has the state of art technology and equipment to cater the need of handling huge amount of data. The lists of hardware and software are given below.

### **Hardware:**

- NOAA/AVHRR data receiving station
- MODIS receiving station
- Real Time Kinematic Differential GPS
- NT Server System (2)
- UNIX Workstations (3)
- Pentium-III and Pentium-II PC (15)
- Plotter, colour printer, scanner etc.

### **Software:**

- ER Mapper, Erdas Imagine (RS)
- ARC Info, Arc View and Map Info (GIS)
- Application Development software

## Remote Sensing Data Processing and Distribution

ACRoRS is receiving NOAA-AVHRR imagery and produces 10-day composites operationally, which are distributed over a network and used to promote near real time applications. ACRoRS has been analyzing NOAA-AVHRR data for forest classification, forest fire monitoring, flood monitoring and sea surface temperature estimation. Geometric and radiometric correction of NOAA data are done using PaNDA software, developed with the collaboration of 7 Japanese Universities.

ACRoRS has established a MODIS data receiving station on 25<sup>th</sup> May 2002 by obtaining a support from University of Tokyo. It is archiving all Level 0 data. ACRoRS is also intensively developing MODIS data processing system to produce cloud free composite products. NDVI composite at 250m resolution will contribute to environmental monitoring in SE Asia. It is also pursuing a research on utilization of MODIS for disaster management, forest fire and etc.

These data is being distributed over the Internet for near real time monitoring. The Internet line between Bangkok city and AIT was upgraded for the purpose. Currently the data is being sent to a buffer server in NII ( National Institute of Informatics ) of Japan, from which the data is re-distributed to University of Tokyo, MAFFIN( Computer Center of Ministry of Agriculture, Forestry and Fisheries).

### Projects in ACRoRS

ACRoRS is implementing a number of research projects in the Asia-Pacific region. Having the MODIS, AVHRR data receiving station, ACRoRS is in a position to conduct research or provide value-added data to researchers of the region.

With its commitment to stimulate the application of Remote Sensing and GIS within the region, ACRoRS has been involved in a number of research projects as listed below:

- 1) *Mapping of Bangkok-Ayutthaya area*: Over the last decade, development in and around Bangkok City has been very rapid. Updated maps showing new infrastructure development activities during this period are not available for public use. Satellite data has been used to prepare an updated map using existing topographic maps as ancillary information. Information like major roads has been digitized from topographic maps. Digitized information has been overlaid on to the geometrically corrected satellite image followed by the necessary corrections and editions. Information like newly constructed roads, expressways, golf courses and industrial areas were interpreted on the image and checked from field visit and then incorporated in the updated map database.
- 2) *Flood monitoring in central Thailand*: This project is aimed at collecting reliable and consistent information on flood in the central plain of

Thailand. Microwave remote sensing data is used as it can provide images during day or night and in presence of cloud or rain. Flood map was prepared by using 33 scenes of JERS-1 SAR data. Multi-temporal data of NOAA AVHRR was used to examine the flood extent and its duration. To identify the land use category, a detailed analysis of Landsat TM data along with JERS-SAR data was carried out. Flood affected areas are identified by overlaying land use map and flood map.

- 3) *Study of Bangkok heat island phenomena*: The objective of this project is to study the heat island phenomenon, which is resulted from increased energy consumption in the densely populated cities. Heat island phenomenon creates undesirable changes in an urban environment, for example, rise in ambient temperature.
- 4) *Comprehensive disaster prevention around Mayon volcano in the Philippines*: Mayon is a highly active volcano in the Republic of the Philippines. Remote Sensing and GIS techniques are the promising tools for monitoring the volcanic activities in synoptic scale before or after an eruption. Soil erosion and the volume of pyroclastic deposition as a result of 1993 eruption was estimated using Remote Sensing data. These two parameters can be used to determine the disaster prone areas and for implementing a disaster prevention plan around Mayon volcano.
- 5) *Application of Remote Sensing for road planning*: Asian Highway project, connecting most of the Asian countries was initiated by the United Nations Economic and Social Commission for Asia and the Pacific (UN-ESCAP) to promote and co-ordinate the development of international road transport in the Asian region and stimulate economic growth. The major part of Asian Highway is the existing roads and a considerable portion of these roads needs to be upgraded to meet the Asian highway standard. A database on these roads is required and remote sensing satellites with their synoptic view and repetitive coverage offer a possibility for obtaining such information. Result shows that in most of the cases, remote sensing data has the capability to estimate the width with an accuracy of half of the spatial resolution or at least the accuracy better than its resolution.
- 6) *Assessment of environmental and socio-economic impacts of shrimp farming in the East Coast of Thailand*: A phenomenal growth of Intensive shrimp farming has been seen in the Chanthaburi province in the East Coast of Thailand since its inception in late 1988. Using Landsat TM data of 1987, status of shrimp farming before the beginning of full scale intensive shrimp farming in Chanthaburi province has been examined and it is found that only 299 hectare of land was under farming during that period of time. ADEOS-AVNIR image of 1997 provides a very clear picture of recent status and it found that 11,277 ha of land is under shrimp farming. Environmental impacts and its costs vary with the locations of the shrimp farms and it is dependent on specific environmental conditions of farm location.

- 7) *Japanese satellite data promotion project*: Under this project a number of tasks have been taken up where Japanese satellite data are used. The most important tasks are preparation of mosaic of Thailand, flood monitoring application development, coastal zone management application development and preparation ADEOS cloud free catalogue system.
- 8) *Pilot project in Thailand and Indonesia*: In order to examine the capability and use of Japanese Satellite data, a Pilot Project has been taken up involving four Thai and two Indonesian Government Departments. ACRoRS provides technical support for this project to ensure smooth implementation.
- 9) *Vegetation mapping in Ganges River Basin*: Objective of this project is to prepare spatial database for assisting in solving global environmental problems. This is a part of ambitious "Global Mapping Project" that targets to create a GIS database of the world with one-kilometer resolution. NOAA-AVHRR data along with climatic indices have been used to map the vegetation cover in the Ganges basin.
- 10) *Near Real Time Rice Growth Monitoring*: The center has been conducting RADARSAT synchronized rice field survey jointly with National Institute of Agro-Environmental Science of Japan. 5 corner reflectors are set around AIT to obtain sub-pixel geometric accuracy of images which will be overlaid with ground truth data. The data is being sent to AIT from Canada via Japan to AIT online.

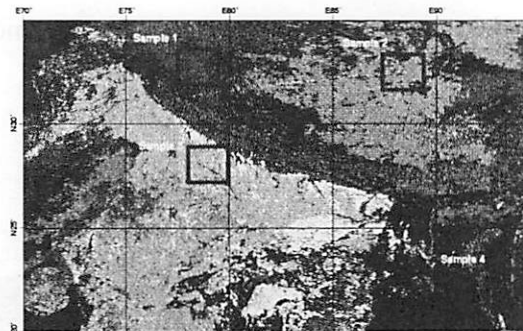


Figure 6: Land cover of Ganges basin

### Digital Asia

*Digital Asia*: ACRoRS is proposing Digital Asia concept and implementation plan. Digital ASIA is an initiative to provide people and community with easy access to geo-spatial information over the Internet by establishing a scheme to integrate and share the GIS and Remote Sensing data among all the countries of Asia. The Digital Asia consists of 4 components, namely Application Developer, Advisory Committee, Technical Support Team and Secretariat. Application Developers, who would like to open their data to contribute to the society, will work with the technical support team to open their data on a Internet Map Servers. Advisory committee will set policy and specification, give advises to technical support team. This initiative is planning to develop a series of demonstration map servers with various application developers in 3 years, which will be a base of operational systems

at larger scale. Several application developers have already worked with the technical support team and opened their data. ([http://www.acrors.ait.ac.th/digital\\_asia](http://www.acrors.ait.ac.th/digital_asia))

### Visiting Researcher

ACRoRS accepts visiting researchers from all over the world. The visiting researcher program allows the exchange of ideas among young scientists and exposes foreign researchers the issues of the Asia-Pacific region. Researchers from Finland, Germany, Japan, Sri Lanka and United States of America have worked in various research topics related to the region.

## 6. CONCLUDING REMARK

Being an international institute with excellent educational, training and research facilities, AIT will continue to play a major role in Remote Sensing and GIS activities in the Asia-Pacific region. AIT will continue to address the needs of the region in the field of geoinformatics and render its expertise. AIT is also keen on developing a network of people in the region for exchanging ideas and sharing experiences aimed at solving problems. Through Digital Asia, it would like to establish a mechanism for more direct contribution of geo-spatial information to the society.

The detail descriptions for education, training and research activities can be found in the following websites:

- STAR <http://www.star.ait.ac.th>
- GAC <http://www.acrors.ait.ac.th/gac>
- ACRoRS <http://www.acrors.ait.ac.th>
- ASRIN <http://www.star.ait.ac.th/~arsrin>



*Dr. Kiyoshi Honda*



# **OPTIMAL CAPACITY OF RIVER FLOOD CONTROL SYSTEM OF BANGKOK BASED ON FLOOD RISK AND ECONOMIC ANALYSIS**

TAWATCHAI TINGSANCHALI and TUANTAN KITPAISALSAKUL  
Water Engineering and Management Program, School of Civil Engineering,  
Asian Institute of Technology, Thailand

## **ABSTRACT**

*The Chao Phraya river flood level at Bangkok is strongly influenced by the upstream flood inflow at Bangsai and the downstream high tide at Fort Chula. A flood control system of Chao Phraya river for Bangkok is designed by a concept of optimal risk-based design. The concept involves the use of flood flow simulation, risk analysis, and optimization for maximum net benefit. The probability of flood protection failure of the flood control system and the expected annual damage cost are calculated for various river flood elevation, dike crest elevation and the components of flood control structures. It is found that without the flood control system the return period of flood protection failure is about 2.5 years. Optimization shows that for a flood control system with the existing river dikes, a flood diversion dam at Pak Kret, a 52 km long flood diversion channel of 40m base width, a sea barrier at the river mouth without pumping station, the return period of flood protection failure of the proposed flood control system is 270 years with a maximum net benefit of US Dollars 8 billion per year.*

## **1. INTRODUCTION**

A flood control system for Bangkok is proposed by the Asian Institute of Technology (AIT, 1986) as shown in figure 1. It consists of a diversion dam at Pak Kret, a flood diversion channel of 52 km long from the diversion dam to the gulf of Thailand, the embankments along the east and west perimeters of Bangkok, a sea barrier with a pumping station at the Chao Phraya river mouth. However, the original design of the flood control system did not consider various probabilities of coincidence of flood inflow and high tide.

The present study presents the development and applications of an optimal design of a flood control system for Bangkok taking into consideration flood flow simulation, risk analysis and design optimization based on maximum net benefit.

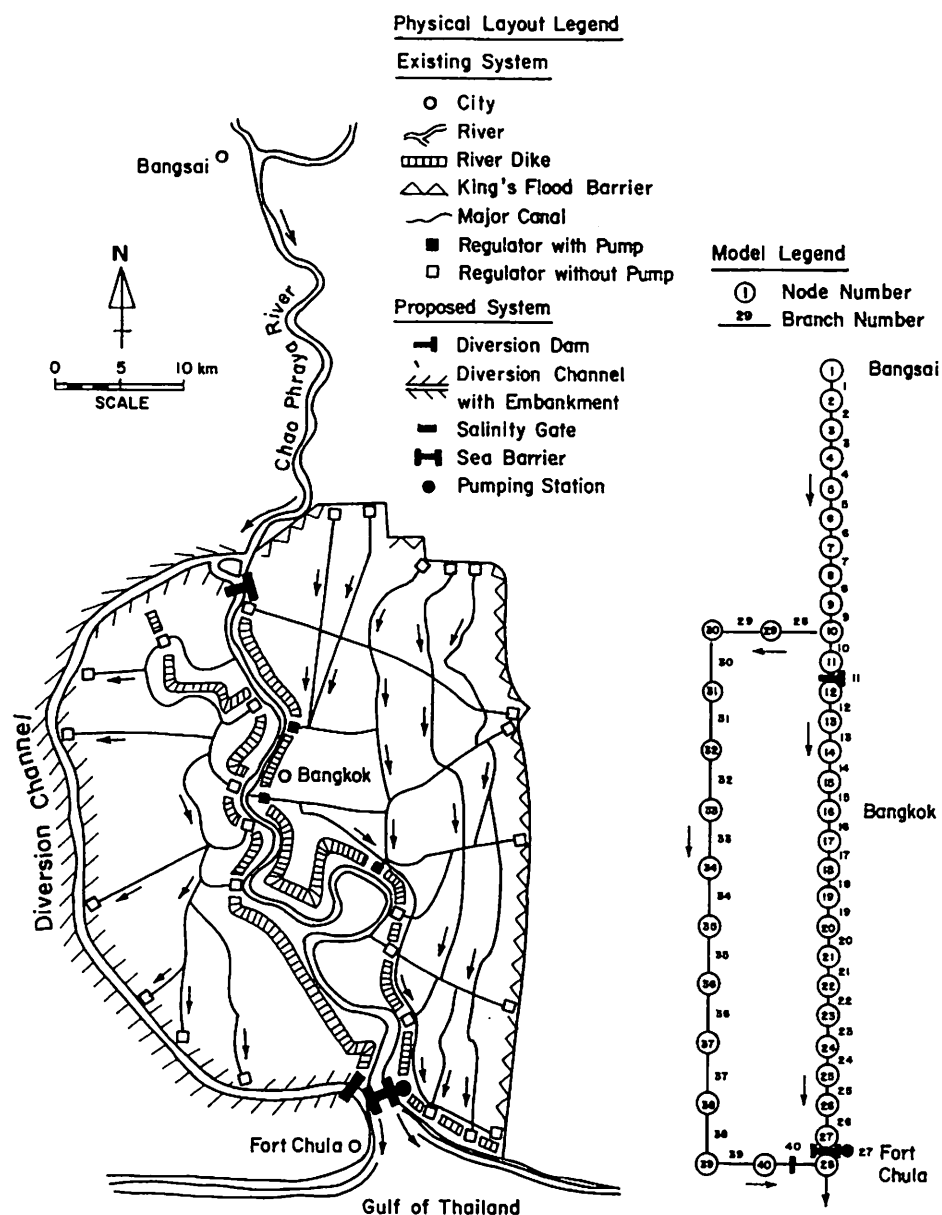


Figure 1: Proposed flood control system of Chao Phraya River at Bangkok and mathematical model configuration

## 2. THEORETICAL CONSIDERATIONS

### 2.1 Flood flow simulation

The flood flow simulation is done for the river flow from Bangsai to the river mouth. A one-dimensional flow model using a finite difference implicit scheme together with a node and branch schematization ( Tingsanchali and Ackermann, 1976) is applied. The governing equations and the finite different implicit scheme are described as in the next page.



**Governing Equations:**

Continuity equation for a node:

$$F \frac{dH}{dt} = \sum_{i=1}^m Q_{in,i} - \sum_{j=1}^n Q_{out,j} + Q_1 \quad (1)$$

Momentum equation for a branch

$$\frac{\partial Q}{\partial t} + \frac{2Q}{A} \frac{\partial Q}{\partial x} - \frac{Q^2}{A^2} \frac{\partial A}{\partial x} + gA \frac{\partial H}{\partial x} + \frac{gn^2 Q |Q|}{A^2 R^{4/3}} = 0 \quad (2)$$

where A = flow cross-sectional area of a branch, F = water surface area of a node, g = gravitational acceleration, H = water level of the node, n = Manning's roughness coefficient, Q = discharge of the branch,  $Q_{in,i}$  = i<sup>th</sup> inflow to a node,  $Q_{out,j}$  = j<sup>th</sup> outflow from the node,  $Q_1$  = lateral inflow to the node, R = hydraulic radius of the branch, t = time, x = distance

**2.2 Risk analysis**

The analysis applies a probabilistic approach to quantify risk of flood protection failure and expected annual damage cost of a flood control system subject to variations of load and capacity of flood control system (Ang and Tang, 1975). The expected annual damage cost of flooding will be evaluated by a damage cost function in relation to flood level.

The risk or probability of a flood to exceed the capacity of a flood control system can be expressed as (Tingsanchali and Kitpaisalsakul, 2000)

$$\alpha' = \int_0^\infty \int_0^{r-1} P_{L,R}(l,r) dr dl \quad (1)$$

where  $P_{L,R}(l, r)$  is the joint probability density function of flood magnitude l and capacity of the flood control system r. Considering that the flood magnitude and the capacity of the flood control system are independent, one can write

$$\alpha' = \int_0^\infty P_L(l) \left[ \int_0^{r-1} P_R(r) dr \right] dl = \int_0^\infty P_L(l) P_R(l) dl \quad (2)$$

where  $P_L(l)$  = probability density function of a flood magnitude l. Flood damages occur when the flood level exceeds the dike crest level, i.e.  $l > r$ . The expected annual damage cost E(D) can be expressed as

$$E(D) = \int_0^\infty K(l) \left( \int_0^{r-1} P_{L,R}(l,r) dr \right) dl = \int_0^\infty K(l) P_L(l) P_R(l) dl \quad (3)$$

where K(l) is the damage cost function which depends on flood level.

### 2.3 Design optimization

Let  $X_1$  and  $X_2$  are the design or decision parameters namely the base width of the diversion channel and the pumping capacity at the sea barrier respectively. It is required to maximize the net benefit by searching for the optimal values of the design parameters  $X_1$  and  $X_2$  considering the cost and benefit functions. The objective function can be expressed as

$$\text{Max}\{Z = B - C\} \quad (4)$$

where  $Z$  = net benefit,  $B$  = benefit,  $C$  = cost. The constraints are as followed:

$$T \geq T_d$$

$$B = f_1(X_1, X_2) \quad (5)$$

$$C = f_2(X_1, X_2) \quad (6)$$

$$T = f_3(X_1, X_2) \quad (7)$$

where  $T$  = expected design return period,  $T_d$  = minimum return period of flood protection failure in which in this case is 100 years. The other constraints are  $0 \text{ m} \leq X_1 \leq 80 \text{ m}$  and  $0 \leq X_2 \leq 2000 \text{ m}^3/\text{s}$ .

## 3. METHOD OF COMPUTATION

### 3.1 Flood flow simulation

The Chao Phraya river from Bangsai to the river mouth at Fort Chula is schematized into 40 nodes and 40 branches with distance interval about 4 km (see Figure. 1). The time step of 1,200 sec is used in the computation. The Manning's roughness coefficients of the Chao Phraya river and the diversion channel obtained from calibration are about 0.028 and 0.018 respectively (AIT, 1985). The capacity of the flood control system depends on the diversion channel base width from 20 to 80 m and the sea barrier pumping capacity from 0 to 2,000  $\text{m}^3/\text{s}$ .

The model boundary conditions for this design study are observed hourly river water level hydrographs at Bangsai and Fort Chula from October 1 to December 31 for the period 1971-1993. The lateral inflow to the river is neglected in the computation since the river water level is greatly influenced by the river flood inflow and the high tide relatively much more than the lateral inflow due to local rainfall. The initial condition of water levels and discharges along the river from Bangsai to Pak Kret diversion dam and along the diversion channel is specified based on a steady flow condition.

### 3.2 Risk computation

Failure of flood protection dike occurs when flow overtopping occurs. Probability of flood protection failure due to dike leakage and gate operation

failure in Bangkok are considered to be small and negligible compared to flow overtopping. The dike crest level can be variable due to various factors such as geological variations or human causes. The probability density function of the dike crest level is considered to have a normal distribution (Plate and Duckstein, 1987) with a mean equal to 1.5 m MSL. The standard deviation is assumed to have a value of 10 % of the dike height of 1 m. The probability density function of the flood magnitude is determined from the actual flood data from field measurements and from the flood simulation model. It is found that the shape of the probability density function has a shape of nearly a normal distribution but the peak is slightly skewed towards higher flood levels.

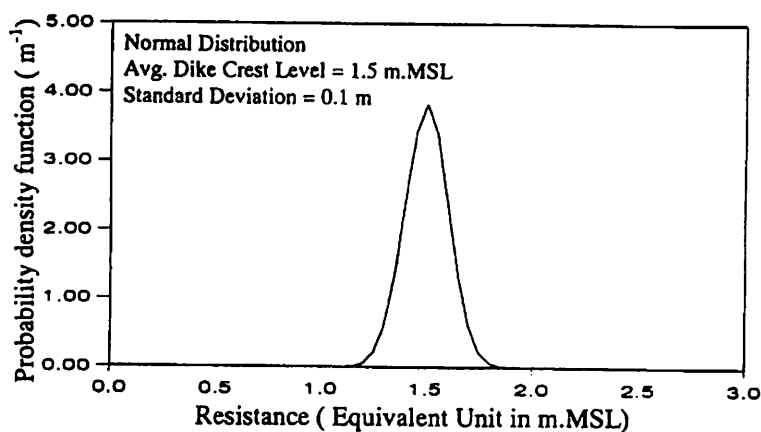


Figure 5: Probability density function of river dike resistance against flooding due to dike overtopping at Bangkok.

### 3.3 Design optimization

In the optimization the project life of the proposed flood control system is considered to be 50 years. The cost of the project includes the cost of construction, operation and maintenance. The project benefit is computed from the reduction of the cumulative expected annual damage costs throughout the project life. The damage cost is a function of flood level.

## 4. RESULTS AND DISCUSSIONS

From the flood simulation results, it is found that a diversion dam and a diversion channel can significantly divert the excessive flood inflow to the sea while a sea barrier can effectively reduce the backwater effect of high tide on the river water level. This flow regulation effectively lowers the river water level at Bangkok despite coincidence of large flood inflow from Bangsai and high tide at Fort Chula. When the diversion channel base width is larger, the river water level at Bangkok is more lowered. However, the pumping station can only slightly reduce the river flood level at Bangkok.

Under the existing condition (without the flood control scheme), the risk of flooding is determined from the integration of the joint probability density function of flood magnitude and the capacity of the flood control

system over the region where the flood level exceeds the existing river dike crest level.  $m$  (See Figure 5). It is found that under the existing condition the risk of flood due to flow overtopping the river dikes is 0.46 as shown in Figure 6. The corresponding return period of the flood protection failure is about 2.2 years. Compared to the case of constant dike crest level which is 1.5 m MSL, the risk or the probability of flood level exceeding 1.5 m MSL is 0.4 or a return period of 2.5 years. The difference in the risk is due to the effect of considering the variation of the dike crest level. The expected annual damage cost due to flood overtopping the river dikes for the case without the flood control scheme is shown in Figure 6.

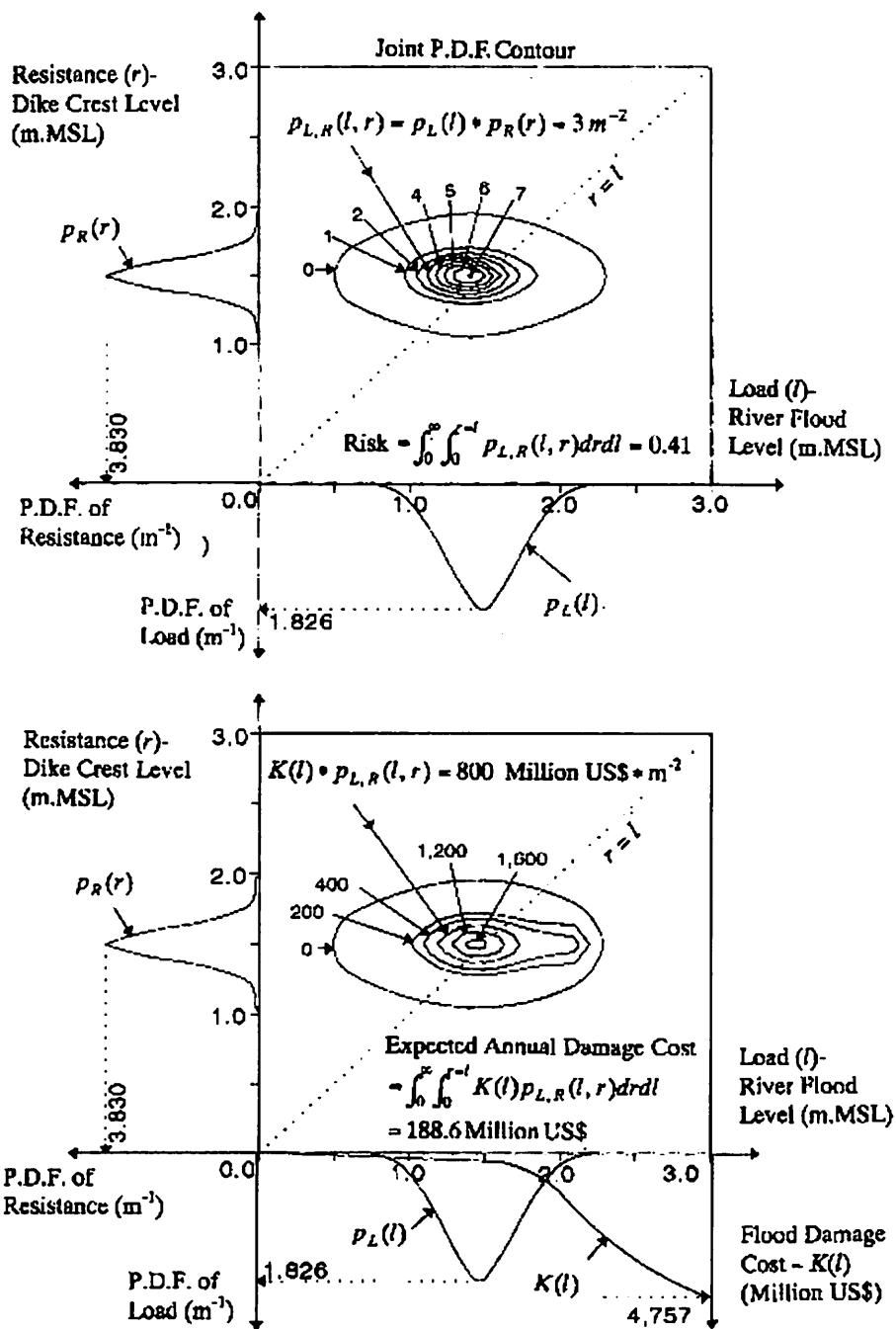


Figure 6: Risk of flooding at Bangkok due to dike overtopping and expected annual damage cost without flood control system

With the proposed flood control system, the joint probability density function of the flood magnitude and the flood control capacity changes significantly. It is found that the risk of flood protection failure is reduced drastically. The risk of flood overtopping the river dikes when the flood control scheme has a flood diversion channel of basewidth of 40 m and a sea barrier without pumping station is shown in Figure 7. The expected annual damage cost decreases significantly compared to the case without the flood control scheme. The project benefit is equivalent to the reduction in the annual damage costs for the case with and without the flood control scheme. The net benefit is the difference between the project benefit and the project cost. A diagram is developed for the relationship the capacity of the flood control system and the net benefit within the range of the design or decision parameters namely the base width of the diversion channel from 0

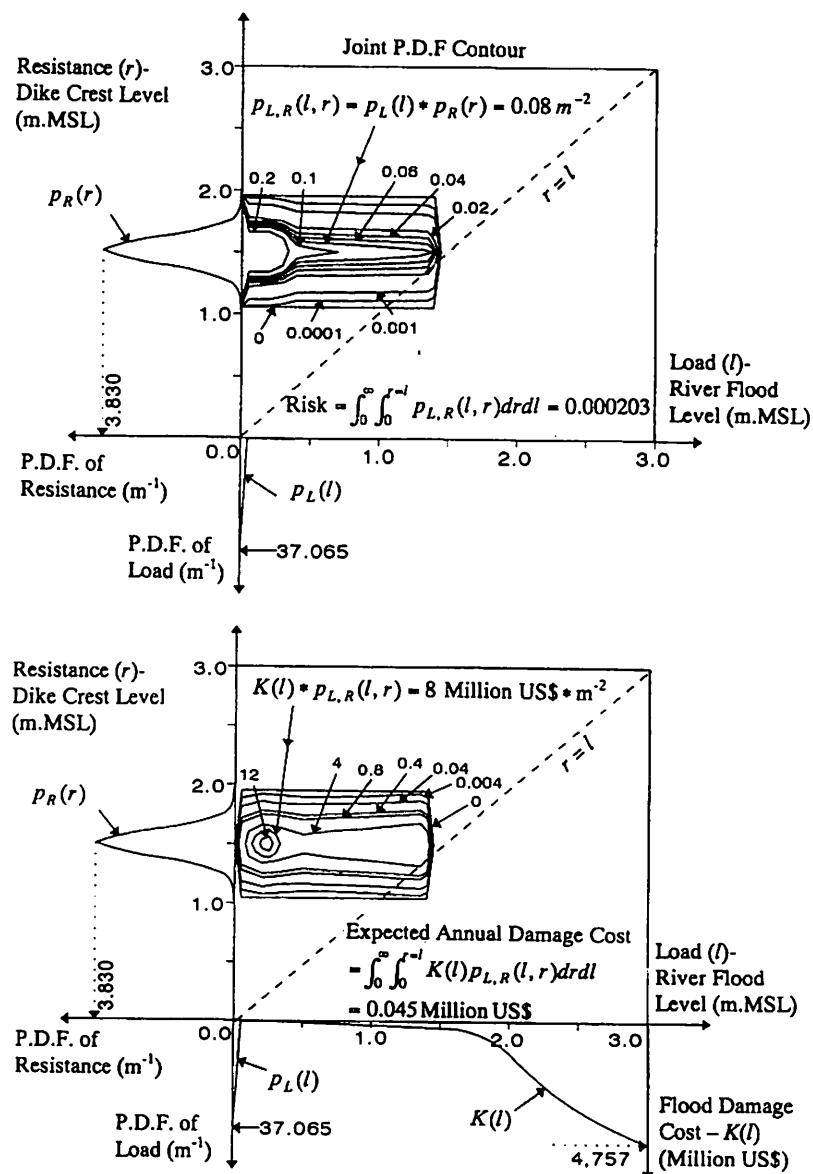


Figure 7: Risk of flooding at Bangkok due to dike overtopping and expected annual damage cost under flood control system with 40 m base width diversion channel and without pumping station

to 80 m and the size of the pumping station from 0 to 2000 m<sup>3</sup>/s. In the same diagram the relationship of the return period of the flood protection failure with the values of the design parameters is also shown. From the diagram, it is found that the maximum net benefit occurs when the flood control system has a flood diversion channel of trapezoidal section of 40m base width and a sea barrier without pumping station. From the results of analysis, the corresponding optimal return period of flood protection failure of the proposed flood control system of Bangkok is 270 years.

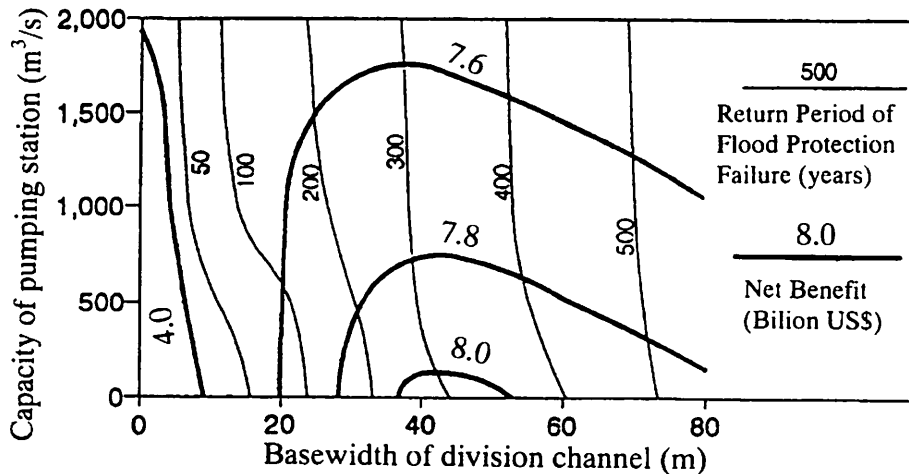


Figure 8: Optimal capacity of flood control system and maximum net benefit for Bangkok

## 5. CONCLUSIONS

Large floodings in Bangkok are usually caused by coincidence of high tides at the river mouth and high upstream discharge resulting in overtopping of flood water over the existing river dikes. To protect flooding in Bangkok for a given limitation in height of the existing river dikes, a flood control system is proposed consisting of an upstream diversion dam at Pak Kret, a flood diversion channel on the west of the Chao Phraya river from the diversion dam to the Gulf of Thailand, a sea barrier at the river mouth with a pumping station and the flood embankments around Bangkok.

The proposed flood control system is found to be very effective in lowering river water level at Bangkok. The diversion dam can divert a significant portion of incoming flood through a diversion. The sea barrier can significantly reduce the backwater effect of high tide on the river water level and consequently provide more river storage to accommodate the flood. The pumping station at the sea barrier can help in lowering the river flood level at Bangkok.

The reduction in flood level of the Chao Phraya river in Bangkok as a result of the flood control system is determined by using a flood simulation

model. The corresponding reduction in risk and annual damage cost due to flooding are estimated for different sizes of the proposed flood control system. The base width of the diversion channel is varied from 0 to 80 m and the capacity of the pumping station at the sea barrier is varied from 0 to 2,000 m<sup>3</sup> /s. From the simulation model it is found that the flood control system can significantly reduce the flood level in the Chao Phraya river at Bangkok.

By flood flow simulation, flood frequency and risk analysis and corresponding flood damage costs, an optimal design of the capacity of the flood control system for Bangkok is determined based on maximum net benefit. The project benefit is calculated from the reduction in expected annual damage costs of flooding for a project life of 50 years. Risk analysis is considered in the estimation of the expected flood damage cost considering the variation of flood level at Bangkok and the crest elevation of flood dike along the river banks. It is found that the optimal capacity of the flood control system is derived from a diversion channel with a base width of 40 m and without pumping at the sea barrier. This optimal flood control system can protect Bangkok from flooding with a return period of 270 years.

## REFERENCES

- Ang, A.H-S. and Tang, W.H., 1975. Probability concepts in engineering planning and design. John Wiley & Sons, New York.
- AIT - Asian Institute of Technology, 1985. Flood routing and control alternatives of Chao Phraya River for Bangkok, Research report, AIT, prepared for National Economic and Social Development Board, Thailand.
- AIT-Asian Institute of Technology and Thai Austrian Consortium (TAC), 1986. Bangkok flood protection, Chao Phraya 2 project, Research report, AIT, Prepared for Bangkok Metropolitan Administration, Thailand.
- Dyhouse, G.R. (1985), Stage-frequency analysis at a major river junction. *Journal of Hydraulic Engineering*, ASCE 111 (4), April, 565-583.
- Kitpaisalsakul, T. (1996), Optimal risk-based design of a flood control system. Doctoral dissertation WM-96-2, Asian Institute of Technology, Bangkok, Thailand.
- Plate, E.J. and Duckstein, L. (1987) Engineering reliability and risk in water resources. Series E, Applied Sciences 124, NATO Advanced Science Institute, Martinus Nijhoff Publishers, Dordrecht, Netherlands.
- Tingsanchali, T. and Ackermann, N.L., 1976. Effects of overbank flow in flood computation, *Journal of Hydraulics Division*, ASCE 102 (HY7), July, 1013-1025.



***Prof. Tawatchai Tingsanchali***



# **DIRECT FLOOD DAMAGE MODELING TOWARDS URBAN FLOOD RISK MANAGEMENT**

DUSHMANTA DUTTA, SRIKANTHA HERATH and KATUMI MUSIAKE  
International Center for Urban Safety Engineering (ICUS/INCEDE),  
IIS, The University of Tokyo, Japan

## **ABSTRACT**

*An estimate of losses from future floods is essential to prepare for a disaster and facilitating good decision making at the local, regional, state, and national levels of government. Flood loss estimates provide public and private sector agencies with a basis for planning, zoning, and development regulations, and policy that would reduce the risk posed by hazards. Flood loss estimates can also be used to evaluate the cost effectiveness of alternative approaches to strengthening disaster-mitigating measures. A standardised flood loss estimation methodology is essential for the hazard prone countries to manage the limited resources for disaster risk management.*

*In this paper, we give an overview of the currently available flood loss estimation methods in practice in several countries around the world. Looking at the currently available flood loss estimation methodologies in most of these countries, it can be observed that there is no standardisation of such methodology and various methods are used by different organisations without any national consensus.*

*A new GIS Based Flood Loss Estimation Modeling approach is introduced here, which can be used for loss estimation of post and future floods as well as for real-time loss estimation. This modeling approach is an integrated approach combing a flood inundation model and loss estimation model such that for any given condition, flood inundation and flood induced losses can be estimation. In the loss estimation modeling, direct flood damages are categorised into three main groups, namely urban, rural and infrastructure damages. GIS is an integral component of this modeling approach for pre and post-processing of the spatial input and outputs. An application of the model in Japan is presented. The simulation results were verified with the observations. The agreement between simulated results and observation was satisfactory. Further, the potential of using this loss estimation modeling approach in other Asia-Pacific countries is discussed.*

## **1. INTRODUCTION**

Despite the decade-long effort of United Nations towards natural disaster reduction through its program IDNDR (International Decade Natural

Disaster Reduction), no reduction in losses due to natural disasters has been observed. With the increase of population and urbanizations, natural hazards are becoming increasingly catastrophic. According to Munich Re, in year 2000, number of loss events rose to new record levels. With increasing frequency and expenses of natural disasters, a standardized loss estimation methodology for consistently compiling information about their economic impacts has become essential for all the concerned authorities for natural disaster reduction processes (NRC, 1999). An estimate of losses from future natural hazards is essential to preparing for a disaster and facilitating good decision making at the local, regional, state, and national levels of government. Hazard loss estimates provide public and private sector agencies with a basis for planning, zoning, and development regulations, and policy that would reduce the risk posed by floods. Hazard loss estimates can also be used to evaluate the cost effectiveness of alternative approaches to strengthening flood control measures.

However, most of the countries around the world do not have any standard methodology for loss estimation due to natural disaster with the exception of a few developed countries. Even in USA, only a few years ago, through concerted effort of leading research organizations, Federal Emergency Management Agency (FEMA) developed with a standard methodology earthquake loss estimation known as HAZUS.

In this study, we focus only flood loss estimation. At the beginning of this paper, we give an overview of the currently available flood loss estimation methods in practice in several countries around the world. The existing limited modelling approaches were introduced. Finally, a newly developed GIS based flood loss model is presented with a real world application.

## 2. FLOOD LOSS ESTIMATION

### 2.1 Losses due to floods:

Damages caused by any natural disasters are broadly classified into two categories, they are tangible damage and intangible damage. Tangible damages are those which can be evaluated quantitatively in economic terms such as, damage to lifelines, buildings, etc., and intangible damages are ones that are difficult to express in economic value, for example anxiety, mental tremor to victims, inconvenience and disruption of social activities, etc. In case of flood damage, both tangible and intangible damages can of two types, direct and indirect damages. (UNSW, 1981; Green et al.; 1983, Parker et al., 1987). Direct damages are caused by physical contact of floodwater. Indirect flood damages are those caused through interruption and disruption of economic and social activities as a consequence of direct flood damages. Direct and indirect damages can be subdivided into primary and secondary categories. In this study, scope of damage analyses is limited to tangible damages.

Generally, primary direct damages, secondary direct damages and primary indirect damages are measurable in monetary values in two-ways, one is using carefully applied survey procedures and second is based on the stage-damage functions. Secondary indirect damages are generally estimated in bulk form by regional multipliers or by the application of reasonable adjustment factors. In survey procedure, post flood questionnaire surveys are conducted among affected population to estimate losses to properties. In the second method, stage-damage functions relate damage extent to different types of property with flood parameters such as inundation depth and duration. Using such stage-damage functions, economic damage to different property categories are estimated and the summation provides the total flood damage. Stage-damage functions are derived either from past flood data analysis, or through analytical descriptions of flood damage to various properties considering the possible damage ratio to a given flood depth and duration. A number of studies are reported in literature that describes stage-damage functions derived from post flood damage analysis. The second way is more useful as with less time, effort and resources, damage caused by floods can be estimated.

## 2.2 Existing Damage Estimation Methodologies

Several countries around the world have damage assessment methodologies developed by responsible organizations. Mainly, these methodologies are developed for cost-benefit analysis of flood control measurements. However, looking at the flood damage assessment of various countries, some interesting differences can be observed. The following sections summarize existing flood damage estimation methodologies in Japan, United Kingdom, United States and Australia.

**Japan:** In Japan, the Ministry of Construction (MOC) issues an economic damage estimate for each flood. The estimate is carried out based on a standard procedure described in the 'Outline of River Improvement Economic Research Investigation' (MOC, 1996). An accompanying flood survey manual outlines how flood damage assessment surveys conducted in developing these guidelines. In carrying out damage assessment, either a direct survey specific to the particular flood may be carried out, or it can be estimated using previous depth-damage statistics for specific property categories, as well as empirical formulae based on past flood damage data. In this methodology, systematic procedures are available to assess only direct primary damages. The indirect primary damages are estimated based on statistics of direct primary damages. Damages considered in the Japanese methodology are classified into three groups.

1. Damage to General assets: which includes damage to residential and non-residential building; For assessment of damage to general assets, methodologies are developed based on post-flood surveys of previous floods for selected areas and damage functions are established for residential and non-residential buildings.

2. Damage to Crops: it includes damage to crops and vegetables of different types.
3. Damage to Public infrastructure: this category includes damage to rivers, streets (roads), bridges, farmland infrastructure, transportation, telecommunications, and electric power supply. Damage estimation methodology for public infrastructure is statistical, which provides percentage of damages for different public infrastructure in relationship with total general asset damage.

Business loss is considered as lump sum 6% of total general asset damage.

**United Kingdom:** For many years United Kingdom (UK) has employed a standard approach to flood damage assessment. Procedures developed in the mid 1970s, and continually refined since, are mandatory for agencies and local authorities wanting central government assistance with flood mitigation measures. Middlesex Polytechnic Flood Hazard Research Center (MPFHRC) has been to the forefront in developing flood damage estimation methodology in UK. Their main results are contained in three manuals, which explains detailed methodology for estimating damage for different categories. The manuals are known as 'Blue Manual', 'Red Manual' and 'Yellow Manual'. In 1979, MPFHRC produced the 'blue Manual' (The Benefits of Flood Alleviation: A Manual of Assessment Techniques) (*Penning-Rowse et al., 1979*). This volume provides assessment techniques and a range of depth-damage data for a wide range of common urban buildings and their contents. The Red Manual (Urban Flood Protection Benefits: A Project Appraisal Guide) was published in 1987 (*Parker et al., 1987*). This provides depth-damage data and assessment methods for most common types of indirect flood loss including those associated with manufacturing, retail, road traffic, utilities and services, households and emergency services. Direct losses for all but residential properties are also considered. The 'Yellow Manual' (The Economics of Coastal Management - A Manual of Benefit Assessment Techniques) was produced in 1992 (*Penning-Rowse, 1992*). This manual discusses assessment of coastal erosion and expands upon the other manuals, particularly with regard to assessment of environmental effects. The flood damage assessment methodologies described in these three manuals had two basic purposes. The first purpose was to facilitate the reliable assessment of the benefits of urban flood protection through providing new methods for assessing flood loss potential. The second purpose was to explain the principles of benefit-cost analysis, which were fundamental to the assessment of flood protection benefits, especially the indirect benefits.

**United States:** In United States, U.S. Army Corps of Engineers (USACE) has nationwide responsibilities in water resources planning and management. One of the important tasks of USACE is to evaluate damage potential due to flooding with and without proposed plans of improvement. For this purpose, USACE has produced its own guidelines for urban flood damage measurement, the National Economic Development Procedures Manual (*USCE, 1988*). The manual is based on the US Water Resources Council's

1983 publication on 'Principles and Guidelines for Water and Related Land Resources Implementation Studies'. The methodology adopted in the manual is very comprehensive for estimation of damage to urban buildings and to agriculture. However, no specific methods have been developed for estimation of damage to lifeline systems and indirect damages such as interruption losses. In the United States, as part of an attempt to develop standardized methodology of flood damage assessment for whole country, the US National Science Foundation (NSF) is developing a guidebook called 'Damage Handbook: A Uniform Framework and Measurement Guidelines for Damage from Natural and Related Man-made Hazards'. The NSF is also funding a major review of hazard research, which includes examination of economics.

**Australia:** In Australia, flood damage assessment methodologies have been developed by a number of organizations. These include the Center for Resource and Environmental Studies (CRES) at the Australian National University and University of New South Wales. However, a recent Australian report of flood damages suggests that in Australia, there is no standard approach and most authorities make little attempt to achieve standard approach, nor is there any set of standard methodologies and consequently, data sets are very diverse and case specific. There is, as a result, little comparability between studies (*Thompson, 1996*).

**Summary of the Existing Methodologies:** The flood damage assessment methodologies adopted in different countries have large variation; some countries like UK have established detailed methodologies for estimation of tangible losses. However, in case of Japan, USA, etc., detailed damage estimation methodology is limited to urban damage. It can be noted that most of the countries have adopted similar approach in damage estimation known as unit loss approach, which is based on a property-by-property assessment of potential damage (*Parker et al., 1987*). From the various available reports, it is found that countrywide standard methodologies of flood damage assessment are available in Japan and UK, that is, for assessment of damage caused by floods in any part of the country, same standard methodologies are used. United States is in the process of developing a standardized methodology for the whole country. However in Australia and many other countries, damage assessment methodologies vary in different regions within the country according to individual studies. Table 1 gives a comparative review of components of damage considered in damage assessment methodologies in these four countries.

### 2.3 Existing Flood Loss Estimation Models

Establishment of an adequate flood damage estimation model involves many issues due to nature of damage caused by floods. Some of the most important issues in flood damage estimation are estimation of flood parameters such as flow velocity, depth and duration at any given point, proper classification of damage categories considering nature of damage, establishment of relationship between flood parameters and damage for different damage categories. Fragility functions, also known as stage-damage

functions, define the relationship between flood parameters and possible damage, which are derived based on historical flood damage information, questionnaire survey, laboratory experiences, etc. This is the conventional way of damage estimation in different countries around the world. Only a handful of models are available for flood damage assessment at present. Out of that two well-known models are FDA (An Integrated Software Package for Flood Damage Analysis) and 'ANUFLOOD'. The FDA package, developed by US Army Corps of Engineers, utilizes the 'frequency method' for the expected annual damage calculation procedure (*Carl et al., 1989*). The package calculates damage potential for specific flood magnitudes and then weights the damage values with the probability that these events might be exceeded. 'ANUFLOOD' is an Australian model developed by Center for Resource and Environmental Studies (CRES), Australian National University for flood damage assessment based on synthetic stage damage curves for residential and commercial property, which is available as an interactive computer package (*Smith et al., 1988*). FDA considers only urban damage such as damage to residential and non-residential buildings. ANUFLOOD also deals with direct damages to residential property and small businesses only. These models use past data of flood parameters for estimation of damage. None of the two models can be used for real-time flood damage estimation.

Table 1: Summary of existing flood loss estimation methodology

Damage categories		Japan	Australia	UK	USA
Urban damage	Residential	detail	detail	detail	detail
	Non-residential	detail	detail	detail	detail
Rural damage	Crop damage	rough	detail	detail	detail
	Farmland damage	detail	none	detail	detail
	Fishery	none	detail	detail	none
Infra-structure	System damage	rough	rough	detail	none
	Service loss	rough	rough	detail	none
Business loss		rough	detail	detail	detail
Environmental damage		none	none	detail	none

Only a few research works have been conducted on real-time loss estimation modeling so far. In 1996, Delft Hydraulic Institute developed a flood hazard assessment model integrating GIS and hydraulic model in an attempt of real-time damage estimation modeling (*Jonge et al., 1996*). For a series of discharges, the model calculates the flooding depth in the flood plains and the damage estimated based on calculated flood depths. The model focuses on the socio-economic impacts of flooding. The flood model considered in this methodology is one-dimensional hydraulic model of river. For a given discharge curve at the upstream boundary, the hydraulic model calculates water levels at discrete points in the river for each defined time step. The flood model uses the maximum water level during the simulation time in each water level point as input. The flood model does not have a physically based model for surface flood inundation simulation, only GIS is used for spreading of floodwater based on river model simulation.

Although there has been a great need of real-time damage estimation model in various measures in flood disaster mitigation, it is realized from the review of previous research works on this subject that only a few research works have been done so far on damage estimation modeling by a handful of researchers or, research organizations. The main difficulty associated with such modeling is obtaining adequate flood inundation parameters, which are the most important inputs in damage estimation modeling. It shows a definite need of an integrated modeling approach, which combines flood inundation simulation model and a generalized flood damage estimation model such that simulated flood inundation parameters can be used in the damage estimation model for real-time flood damage estimation.

### 3. A NEW GIS BASED APPROACH OF FLOOD LOSS ESTIMATION

The GIS based methodology presented here is an integrated approach combining a physically based hydrologic model for flood inundation simulation and a loss estimation model. Figure 1 shows a schematic diagram of the integrated model. The flood simulation model consists of different hydrological components. Physically based governing equations for flow propagation in different hydrologic components are solved using finite difference schemes. The detailed description of the hydrologic model for flood inundation simulation was given elsewhere (*Dutta et al., 2000*) and not described in detail in this paper. The following section describes the formulation of the loss estimation model.

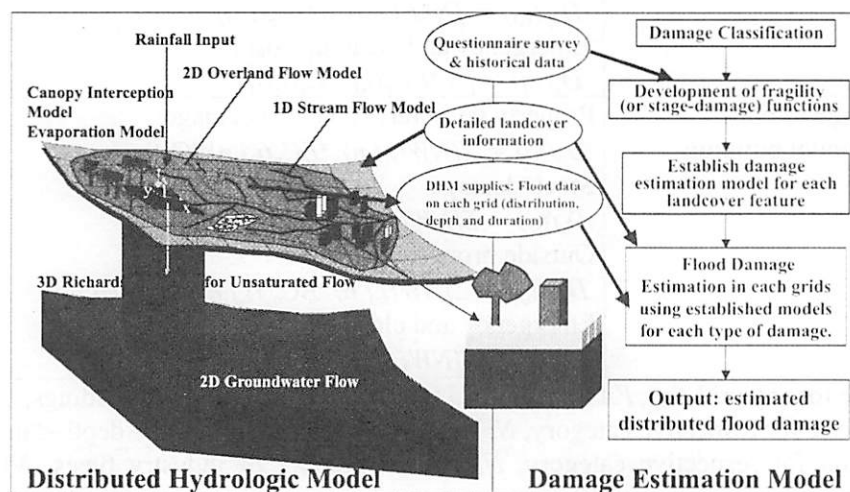


Figure 1: Schematic diagram of the integrated model

#### 3.1 Formulation of Loss Estimation Model

The loss estimation model consists of three kinds of direct tangible flood damages namely, urban, rural and infrastructure damages, which are further sub divided into several categories as shown in Table 2 to incorporate in the model. The model is constructed based on the similar grid network used

for the distributed hydrological model. In application process, the distributed hydrologic model simulates flood inundation parameters for each grid and supplied to damage estimation model for simulation of flood damage in each grid.

**Urban Damage:** The grid based mathematical models for estimation of urban flood damage are shown in Table 3.

Table 2: Detailed damage categorizations for modeling

Major categories	Sub-categories
Urban damage (residential and non-residential buildings)	- structure damage - content/stock damage - outside property damage - emergency and clean costs
Rural damage	- damage to crops and vegetables - damage to farm infrastructure
Infrastructure damage	- system damage - interruption loss

Table 3: Mathematical models for urban flood damage

Damage type	Mathematical model
Damage to residential buildings	Structure damage $D_s(i,j) = [FA(i,j) * EC_s(i,j) * C_s(i,j)]$ Content damage $D_c(i,j) = [NF(i,j) * EC_c(i,j) * C_c(i,j)]$ Outside property damage $D_{op}(i,j) = [N * EC_{op}(i,j) * C_{op}(i,j)]$ Emergency and clean up costs $D_e(i,j) = [N * EC_e(i,j) * C_e(i,j)]$
Damage to non-residential buildings	Property (structure+content) damage $D_p(i,j) = \Sigma[NW(i,j,n) * EC_p(i,j,n) * C_p(i,j)]$ Stock damage $D_s(i,j) = \Sigma[NW(i,j,n) * EC_s(i,j,n) * C_c(i,j)]$ Outside property damage $D_{op}(i,j) = \Sigma[NW(i,j,n) * EC_{op}(i,j,n) * C_{op}(i,j)]$ Emergency and clean up costs $D_e(i,j) = \Sigma[NW(i,j,n) * EC_e(i,j,n) * C_e(i,j)]$
Where for any grid (i,j), FA = residential floor area; N = number of buildings, EC = unit price for respective category, NF = number of households, C = depth-damage function for respective category, NI = total number of industry types, NW = number of workers for industry n.	

**Rural Damage:** Average damage to agriculture products in any grid (i,j) can be estimated as follows,

$$AD(i,j) = \sum_{k=1}^n [D_m(i,j,k) \times CRP_a(i,j,k) \times mn(k)]$$

$$D_m = CP_k \times Y_k \times DC_k(i,j)$$

Where, n = total number of crops; and AD = total agriculture damage. For any type of crop k at any grid (i,j); D<sub>m</sub> = damage to crop per unit area (damage as



a proportion of flood-free gross returns);  $CRP_a$  = total area of cultivation of crop type  $k$ ; and  $CP_k$  = estimated cost per unit weight of crop type  $k$ .

Property and stock damage to farmhouses can be estimated using similar models used for non-residential buildings. Damage to Farmland infrastructure can be estimated using the following model.

$$D_{fl}(i,j) = NH(i,j) * TA(i,j) * EC_{fl}(i,j) * C_{fl}(i,j)$$

Where in any grid  $(i,j)$ ,  $D_{fl}$  = total damage to infrastructure;  $TA$  = total farm area;  $EC$  = estimated cost of complete replacement of farm infrastructure;  $C$  = stage-damage function; and  $NH$  = amount of deposited debris.

**Infrastructure Damage:** Due to many uncertainties involve in flood damage to infrastructures, which are governed by many local factors in addition to flood parameters, there are no well-established methodologies. The adopted methodology in this study is based on the lifeline facilities damage estimation methods for earthquake (*NIBS, 1997*), which state that:

System damage to any component  $x$  of a lifeline system;

$$SD_x = \sum_{i=1}^{nc} [DR_c \times TC] \text{ where; } DR_c = \sum_{i=1}^n [DR_i \times P(ds_i)]$$

and, service disruption loss of any lifeline system due to damage of any component  $x$ ;

$$SL_x = \sum_{i=1}^{nc} [RF_c \times SC] \text{ where; } RF_c = \sum_{i=1}^n [RF_i \times P(ds_i)]$$

Where,  $nc$  = total numbers of lifeline component  $x$ ;  $TC$  = replacement costs of component  $x$ ;  $DR_c$  = total damage ratio in percentage;  $P(ds_i)$  = probability of being in damage state  $i$ ;  $DR_i$  = damage ratio for damage state  $i$ ;  $n$  = total number of damage states;  $SC$  = service loss per day due to disruption;  $RF_c$  = total restoration function; and  $RF_i$  = Restoration for damage state  $i$ . For both system damage and interruption of losses, damage states may vary with type of objects and according to the classification made by users.

Traffic interruption loss due to a flood event is the total of marginal costs and opportunity costs. The two important factors in traffic interruption loss estimation are duration of closer of any particular road due to floods and diversion routes and reallocation of traffic. In this study, using network model with OD information, possible diversion routes are estimated for given condition of flooding of a particular route. The Marginal and Delay costs can be estimated as follows.

Marginal costs;

$$MC = \sum_{i=1}^n \left[ \sum_{j=1}^m [E_i(i) \times \{a(j) + \frac{b(j)}{v(i,j)} + c(j) \times v(i,j)^2\} \times T_v(i,j) \times t \times d] \right]$$

Delay costs;

$$DC = \sum_{i=1}^n \left[ \sum_{j=1}^m [E_l(i) \times v(i, j) \times D_c(i) \times T_v(i, j) \times t \times d] \right]$$

Where,  $n$  = number of roads flooded;  $m$  = mode of transport in any road  $i$ ;  $E_l(i)$  = extra length to be covered due to floodwater in road  $i$ ;  $a(j)$ ,  $b(j)$ ,  $c(j)$  = fuel consumption related constants for mode of transport  $j$ ;  $T_v$  = total volume of traffic in road  $i$  per hour;  $t$  = total duration of flood in hours,  $d$  = factor to consider the variation of traffic volume in weekdays and week-ends; and  $D_c$  = delay cost per unit time for road  $i$ .

### 3.2 Establishment of Fragility Functions

Fragility functions (or stage-damage functions) are essential components of flood damage estimation methodology, which relate flood damage to flood inundation parameters for different classes of objects (*Smith, 1994*). In mathematical models for estimation of damage, stage-damage functions are used to calculate unit damage percentage to any object for given condition of flood. The fragility functions are usually derived two ways, one is based on damage data of past floods, and other is from hypothetical analysis based on land cover pattern, type of objects, information of questionnaire survey, etc., which are known as synthetic stage-damage functions. In this study, fragility functions for different objects are adopted from the data published by the Ministry of Construction, Japan (*MOC, 1996*).

As depth of floodwater is the governing flood parameter for damage to urban buildings, in development of fragility functions for urban damage, only flood depth is considered. Total five categories of fragility functions are used to describe urban flood damage; fragility functions for residential structures (for wooden and non-wooden structure), for residential contents, for non-residential property and for non-residential stocks. Due to lack of data, no fragility function could be established for outside properties and emergency and cleaning up costs due to floods for different urban buildings and for business interruption losses. Fragility functions for property and stocks of farmer houses can be expressed in polynomial functions, which are similar to the fragility functions of property and stocks of non-residential building.

For agriculture damage, both depth and duration factors are considered in fragility functions. For this purpose, depth is divided into several ranges and for each range of depth scale; fragility functions define the relationship between flood duration and damage. Crops and vegetables cultivated in different regions in Japan are grouped into a total of eight categories based on their nature of vulnerability due to floods. For each of these categories, fragility functions were different. Due to lack of enough information and data, no fragility functions could be established for lifeline facilities. Damage estimation procedure for transportation interruption loss is different from

other lifeline facilities and usually, they are estimated more conventional ways than using fragility functions.

#### 4. MODEL APPLICATION

The study area selected for the model application is Ichinomiya river basin, a moderate basin in size with an area of 220 sq. km, located in the Chiba prefecture, Japan between longitude 35°18'N to 35°30'N and latitude 140°10'E to 140°25'E (Figure 2). The mean annual rainfall is approximately 1,700 mm and rainfall distribution is uniform in the entire basin. Severe damage occurred to the urban areas many times in the past due to major floods. During September 22- 25, 1996, the basin suffered from a big flood disaster due to the heavy rainfall caused by Typhoon 17. Within 24 hours during September 21-22, the whole basin received about 360 mm rainfalls. In this study, this flood event of September 1996 in the Ichinomiya river basin was selected for application of flood inundation and damage estimation model.

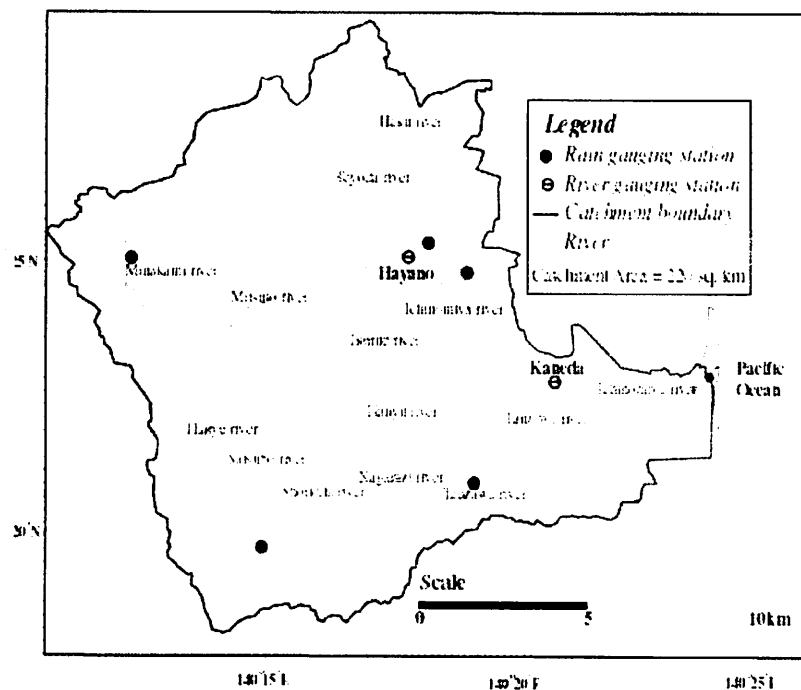


Figure 2: Study area: Ichinomiya river basin

##### 4.1 Data preparation

DEM of study area was generated from 50m grid elevation data that was obtained from Japan Map Center. As the river system generated from the original DEM did not follow the actual river path, it was modified with additional 1m interval contour data from 1:2,500 scale map for the lower flat area and river network was generated again. There were a total of six major landcover classes within the study area namely, forest, paddy, light grass,

vegetable, water body and urban, as classified from the SPOT satellite data of 20m resolution. Hourly rainfall data from 5 rainfall-gauging stations were available. Daily pan evaporation of one station was known. There were six major soil classes in the basin. Soil parameters for different soil classes were averaged from the soil field test data conducted in different locations within the basin.

Various data sets required for urban damage estimation were available at ward level from the local city office. The population data was available in ward level from the 1990 Population Census. The Housing Survey of Statistics Bureau of Management and Coordination Agency of the Ministry of Japan include detailed information of residential housing system of different wards of every prefecture in Japan. Industry statistics in the different wards within the study area were obtained from the existing Industrial Statistics. Land cover distribution map of the study area, obtained from LANDSAT satellite data, was used to derive residential floor area and spatial distribution of industries in each ward. As the ward level data did not contain information of their spatial distribution within the wards, GIS was used for spatial distribution of these datasets within the ward using estimated residential and non-residential floor areas from detailed landcover map.

Various agriculture data for Chiba prefecture were obtained from the census report of Ministry of Agriculture, Forestry and Fisheries of Japan (MAFF). About 30% of the total land cover pattern is agriculture area in the Chiba prefecture, 4.8% of the total households are farm household, compared to 7.9% nationwide average. Out of the various crops and vegetable cultivated in the Chiba prefecture, the main crops and vegetables are paddy, radish, carrot, taro, chinese cabbage, cabbage, spinach, welsh onion, onion, eggplant, tomato, cucumber, sweet pepper, lettuce, potato, pumpkin, green peas, soybeans, kidney beans, sweet corn, strawberry, water melon, cauliflower, chestnuts, and broccoli. Paddy is planted in average area of 69,500 ha. The flood event of 1996 considered for model application occurred in the month of September after the harvesting of paddy and therefore, paddy was not affected by this flood event.

Traffic data for the study area were collected from Traffic Census Report prepared by the Ministry of Transportation, Japan.

## **4.2 Result Analysis**

Figure 3 shows the simulated flood inundation map with floodwater depths and the boundaries of surveyed flooded areas. The simulated flood extent shown in the figure is the maximum flooded area with floodwater level above 40cm. By comparing the model results with the survey flood, in general it can be said that the simulated result is close to the actual situation. However, there are some differences between simulated and observed flood inundation. For example in the simulated results, floodwater can be seen in some surface areas along the upstream channel networks. One of the possible reasons of this may be the averaged topography data due to which estimated

slopes may be different from the actual ones in the upstream areas. In this

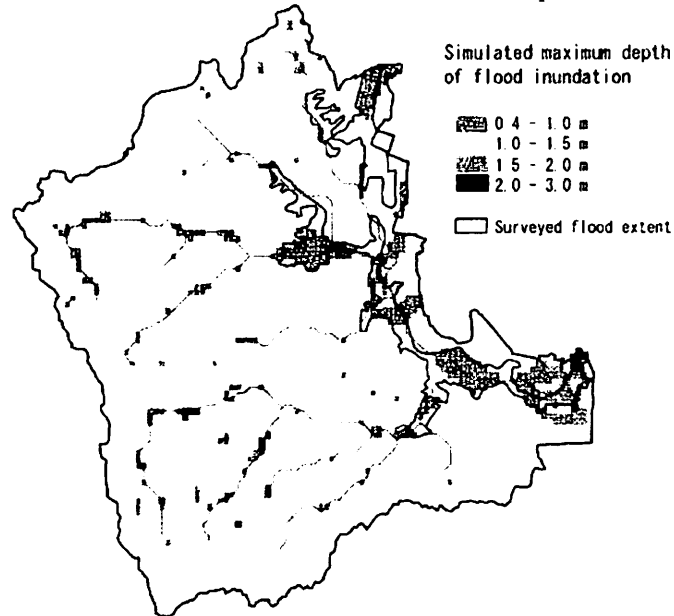


Figure 3: Simulated maximum flood extents and depth

study, topography data used for the upper part of the basin was the averaged dataset of 50m-grid size. A high resolution and accurate topography data is essential for getting higher accuracy in simulated inundation output. Due to lack of detailed information about hydrogeological properties of different soil types in the basin, several assumptions are made in estimation of soil characteristics. This may be another possible reason of less precised output. It can be noticed from the figure that there is shifting of simulated flood inundation area from the surveyed one. This is due to the difference between the actual and generated channel from the DEM, the latter was used in the simulation. As most of the flooded areas are along the rivers, simulated flooded areas also shifted from the original locations along with the generated river network. The larger extension of simulated flood inundation area in the lower part of the basin compared to the observation was most likely due to existing elevated highways. In actual situation, the elevated highways worked as embankments in many areas and that prevent the movement of floodwater from riversides, however in the model, the elevated road networks were not separately considered.

Figure 4 shows the comparison of simulated flood hydrographs with observed hydrographs at the Hayano and Kaneda gauging stations (refer to Figure 2). Except the peak, simulated flood hydrographs are matching quite well with the observed hydrographs.

The estimated urban damage of different categories for the simulated flood inundation parameters of 1996 flood are shown in Figure 5. Comparing urban damage of simulated floods with surveyed flood parameters, as shown in the figure, it can be observed that estimated structure damage from simulated flood inundation is higher than the estimated structure damage from surveyed flood inundation parameters. Structure damage for both residential and nonresidential buildings are estimated based on unit floor area

concept. The simulated flood extent is larger than surveyed flood extent, as can be seen from Figure 3. Due to this, estimated structure damage for residential and nonresidential buildings are higher in case of simulated flood inundation. Figure 6 shows spatial distribution of simulated damage to residential contents and nonresidential properties in the flood affected areas of the basin.

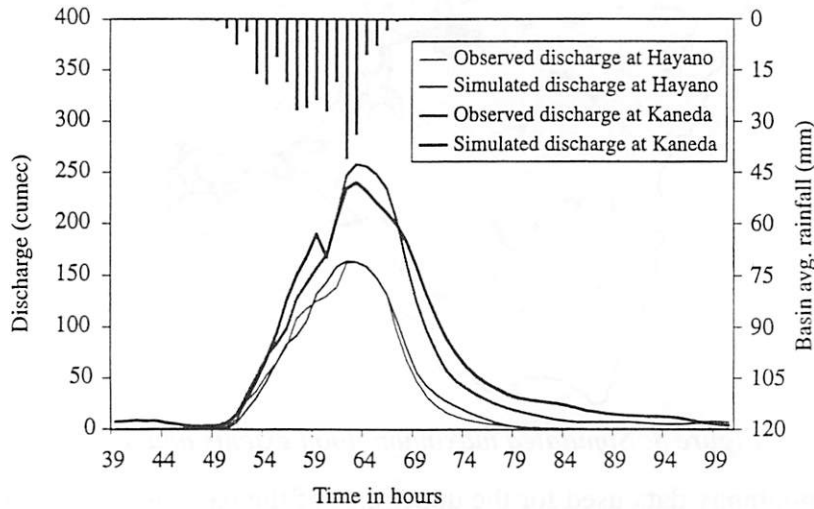


Figure 4: Simulated and observed hydrographs

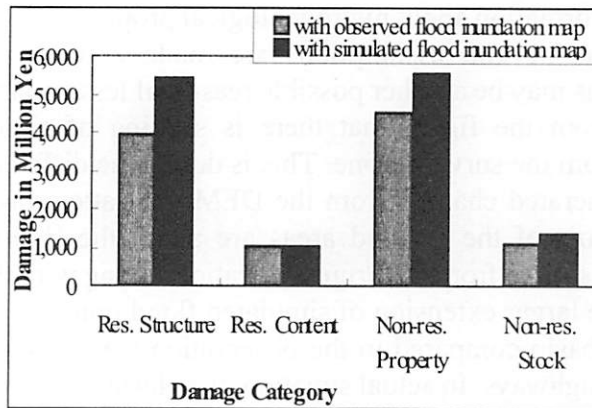


Figure 5: Simulated urban flood damage

Estimated different categories of rural damage by the model are shown in Table 3. The 1996 flood occurred during September 21-23 and rice paddy harvesting in the study area was over by that time. Also, floods inundated mainly the urban areas; inundated agriculture area was much small. Due to these reasons, agriculture damage was very less, only about 2% of the urban damage.

The estimated marginal and delay costs are shown in Table 4. From this table, it can be seen that delay costs is much higher than the marginal costs, which is due to the larger costs per unit time per vehicle. Overall traffic interruption loss was much less in this flood event compared to urban flood damage, only about 4 %, as the duration of flood was very short and only a few major roads were inundated.

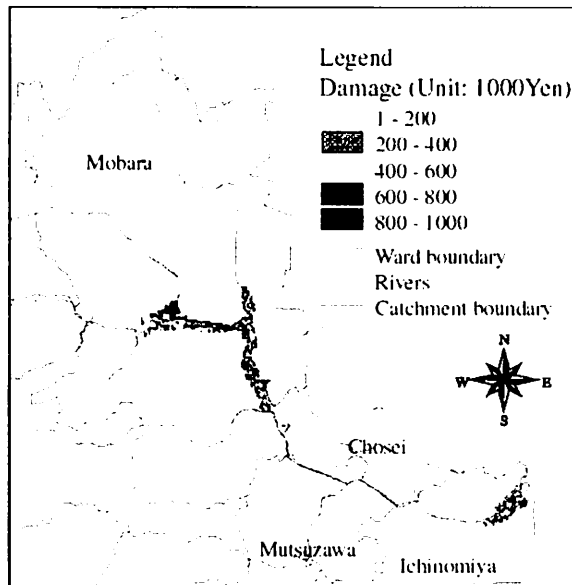


Figure 6(a): Damage for residential content

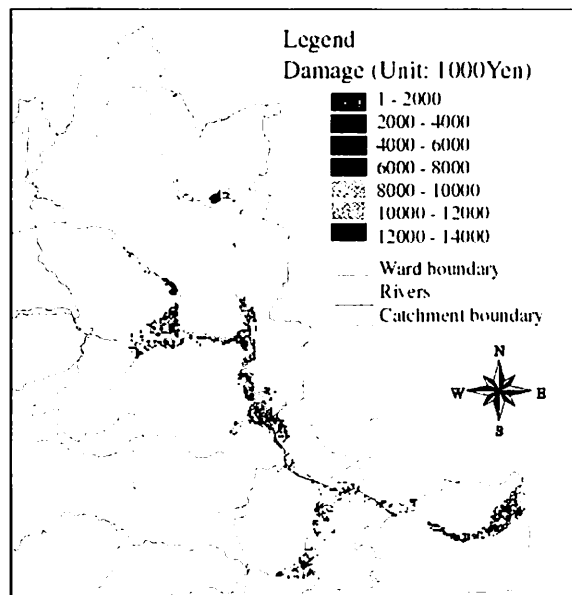


Figure 6(b): Damage for non-residential property

Table 3: Simulated rural flood damage

Damage category	Damage in 1000 yen
Farm house property	1,551
Farm house stock	1,310
Crops and vegetables	236,979

Table 4: Simulated traffic interruption loss

Damage category	Damage in 1000 yen
Marginal costs	1,046
Delay costs	552,106

Simulated rural damage and traffic losses could not be verified with actual damage as there was no observation of actual damage done for rural and infrastructure damages for this flood event.

## 5. CONCLUSIONS

In this paper, existing flood loss estimation methodologies in different countries were discussed. From overview of the existing methodologies, it can be observed that there is no standardisation of such methodology and various methods are used by different organisations without any national consensus except in UK and Japan. A standardized approach of flood loss estimation, a newly developed GIS based loss estimation model is presented with a case study of Japan. The model is an integration of physically based distributed hydrologic model and a flood damage estimation model. It considers all the physical processes in a river basin for flood inundation simulation and takes into account of stage-damage relations for different landcover features for economic loss estimation caused by floods.

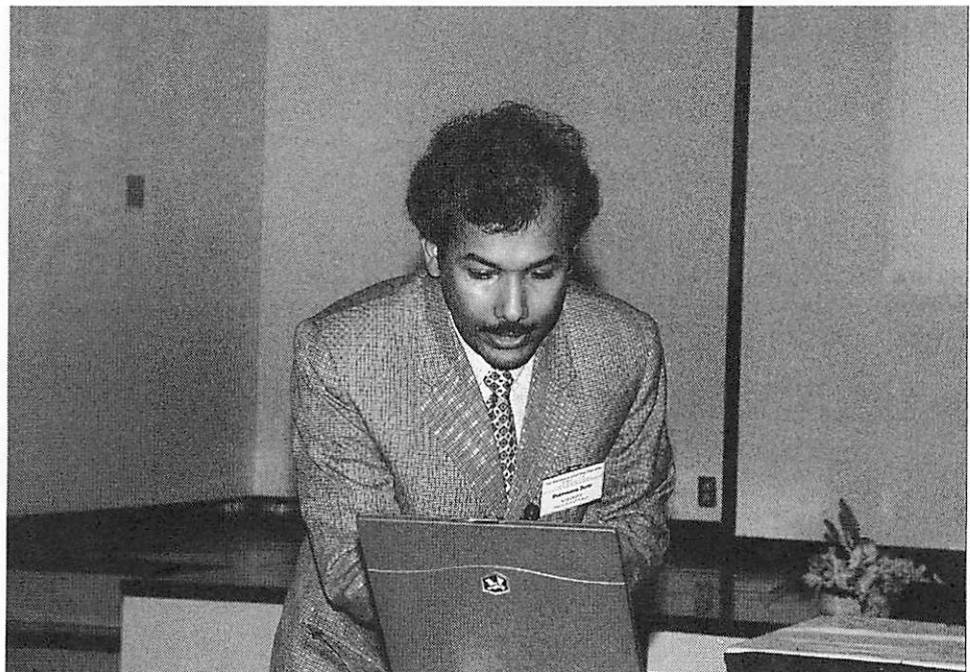
The integrated loss estimation model presented here is a new approach of its kind. The results of the model application in the Japanese river basin show that model can simulate flood inundation parameters well. The damage estimation model performs well in urban damage estimation, however, its applicability for rural and infrastructure damage estimation was not duly verified due to lack of observed data. Further study is required to carefully validate the model results for rural and infrastructure damage estimation.

## REFERENCES

- Carl, R.D. and D.W. Davis (1989). An Integrated Software Package for Flood Damage Analysis; Technical Report, Hydrologic Engineering Center, US Army Corps of Engineers, USA.
- Dutta, D., S. Herath and K. Musiak (2000). Flood Inundation Simulation in a River Basin Using a Physically Based Distributed Hydrologic Model, *Journal of Hydrological Processes*, John Wiley & Sons, Vol. 14 (3), pp. 497-520.
- Green, C. H., D.J. Parker, P.M. Thompson and E.C. Penning-Rowsell (1983). Indirect Losses from Urban Flooding: An Analytical Framework; Flood Hazard Research Center, Middlesex Polytechnic, UK.
- Jonge, T.D., K. Matthijs and M. Hogeweg (1996). Modeling of Floods and Damage Assessment using GIS; *HydroGIS 96*, IAHS Publication, No. 235, pp. 299-306.
- MOC (1996). Outline of River Improvement Economic Research Investigation, River Planning Section, River Department, Ministry of Construction, Japan, (in Japanese).
- NTIS (1996). Analysis of Non-residential Content Value and Depth-Damage Data for Flood Damage Reduction Studies; National Technical Information Service, U.S. Department of Commerce, USA.



- NIBS (1997). HAZUS: Earthquake Loss Estimation Methodology; National Institute of Building Sciences, 1090 Vermont Ave., Washington, D.C.
- NRC(1999). The Impacts of Natural Disasters – A Framework for Loss Estimation; ISBN 0-309-06394-9, National Research Council, National Academy Press, Washington D.C., USA.
- Penning-Rowsell, E.C. and J.B. Chatterton (1979). The Benefits of Flood Alleviation: A Manual of Assessment Techniques; Gower Technical Press, United Kingdom.
- Penning-Rowsell, E.C. (1992). The Economics of Coastal Management – A Manual of Benefit Assessment Techniques; Bethaven Press, United Kingdom.
- Parker, D. J., Green C. H. and Thompson P. M. (1987). Urban Flood Protection Benefits - A Project Appraisal Guide, Gower Technical Press, UK.
- Smith, D.I. and M. Greenaway (1988). The Computer Assessment of Urban Flood Damage: ANUFLOOD; Technical Report, Desktop Planning, Melbourne, Australia.
- Smith, D. I. (1994). Flood Damage Estimation: A Review of Urban Stage-Damage Curves and Loss Functions, Water SA, vol. 20, pp. 231-238.
- Thompson, P. and J. Handmer (1996). Economic Assessment of Disaster Mitigation: An Australian Guide; Technical Report, Center for Resource and Environmental Studies, Australian National University, Australia.
- UNSW (1981). Economic Evaluation Methodology of Flood Damage in Australia; University of New South Wales, Australia.
- USCE (1988). National Economic Development Procedures Manual; US Army Corps of Engineers, Fort Collins, USA.



*Dr. Dushmanta Dutta*



# APPENDIX I

## WORKSHOP PROGRAM

September 21, 2001 (Day 1)

### PLENARY SESSION

09:00-09:45	Opening remarks	W. Kanok-Nukulchai T. Uomoto
09:45-10:00	<i>Coffee break</i>	

### SESSION I (Chaired By Y. Yasuoka and P. Warnitchai)

10:00-12:15	Seismic Hazard in Bangkok due to Long-Distance Earthquakes	P. Warnitchai
	Urban Safety and Disaster Mitigation	K. Meguro
	Sustainable Urban Development	
	Reflecting Regional Urban Climate	R. Ooka
10:00-12:15	The Roles of Civil Engineers in Urban Safety	W. Kanok-Nukulchai
	Concrete Degradation and its Non-destructive Testing	T. Uomoto
	Durability Problems of Concrete Structures in Thailand and their Solutions	
12:15-13:30	<i>Lunch Break</i>	S. Tangtermsirikul

### SESSION II (Chaired by W. Kanok-Nukulchai and K. Meguro)

13:30-16:00	Use of Remote Sensing and GIS for Earthquake Disaster Mitigation	Fumio Yamazaki
	Overview of Research Activities Relating to Urban Safety at the Department of Civil Engineering, Chulalongkorn University	B. Stitmannaitum
	Assessment of Urban Sustainability and Environment with Remote Sensing and GIS	Y. Yasuoka
	Application of 3D Urban Modeling derived from Laser Scanning Data	M. Tokunaga
	Activity on Remote Sensing and GIS at AIT	K. Honda
	Optimal Risk Based Design of Flood Control Structures	T. Tingsanchali
	Distributed Hydrologic Modeling for Urban Flood Disaster Mitigation	D. Dutta

*CLOSING SESSION*

16:00 – 16:30	Closing remarks	W. Kanok-Nukulchai Y. Yasuoka
16:30 – 16:45	<i>Coffee break</i>	

**September 22, 2001 (Day 2)**

09:00-09:15	Summary of the Day 1	P. Warnitchai
09:15-09:30	Plans for future collaboration	T. Uomoto
09:30-10:00	Possible research field of ICUS for collaboration	T. Uomoto K. Meguro Y. Yasuoka
10:00-10:30	Possible research field of AIT for collaboration	P. Warnitchai W. Kanok-Nukulchai
10:30-11:00	<i>Coffee break</i>	
11:00-12:00	Free discussion	
12:00-12:30	Workshop Resolution	

## **APPENDIX II**

### **WORKSHOP RESOLUTIONS**

This workshop sponsored by the International Centre for Urban Safety (ICUS/INCEDE), Institute of Industrial Science, University of Tokyo, afforded an opportunity to researchers from ICUS/INCEDE and the Asian Institute of Technology, Bangkok, to exchange information about the current research work underway at their Institutes, and make an effort to identify areas of mutual interest where further work can be carried out jointly.

The research works in the areas of urban safety engineering; improvement of sustainability of urban structures; prediction, assessment and control of natural and artificial disasters; and information technologies and systems for urban safety, were discussed in detail during the workshop. The discussions focused on promoting collaborative research work and increase in exchange of information and technology. Participants agreed that the workshop was very successful and had led to a better understanding of the research work in participating Institutes.

The participants emphasized the need for increased cooperation between researchers at the ICUS-INCEDE and AIT. It was also felt that researchers from Universities like Thammasat University and Chulalongkorn University could also be encouraged to participate in developing research projects of mutual interest.

The following resolutions were approved during the workshop:

1. There are many areas of common interest to researchers at ICUS/INCEDE and AIT, in the field of Urban Safety Engineering. It is therefore resolved that continued cooperation between researchers and practitioners in these institutes be encouraged, and mechanisms for improved technology exchange and sharing be explored.
2. Participants agreed that products of the research work should not only target researchers, but also practitioners and policy makers. It was resolved to create a task force of researchers to spearhead the efforts to identify areas and projects, which could be taken up for further consideration. It is therefore resolved that research proposals should be developed keeping in mind both the above target users.
3. Based on the results of this workshop, opportunities for collaborative research and information sharing should be further explored, and potential funding sources for such collaborative research should be identified and contacted within Japan and the Thailand.

4. The participants recognized the need to closely monitor the work identifying joint projects and share information. To this end it was resolved that the next meeting of the research team may be held sometime in late 2002. The details of the venue and timing will be worked out at a later date.



***INTERNATIONAL CENTER FOR URBAN SAFETY ENGINEERING***

*Institute of Industrial Science, The University of Tokyo*

*4-6-1 Komaba, Meguro-ku,*

*Tokyo 153-8505, Japan*

*<http://icus-incede.iis.u-tokyo.ac.jp/>*

*E-mail: [icus@iis.u-tokyo.ac.jp](mailto:icus@iis.u-tokyo.ac.jp)*

***Tel: (+81-3)5452-6472***

***Fax: (+81-3)5452-6476***